

University of Cadiz



Department of Materials Science,
Metallurgy, and Inorganic Chemistry

al-Farabi Kazakh National University



Department of Thermal Physics and
Technical Physics

UDC 006:54(043)

Manuscript

BERGALIYEVA SALTANAT AMANGELDINOVNA

**Standardization of Recycled Plastic Materials
for Additive Manufacturing**

8215 - Energy and Sustainable Engineering
8D07502 – Standardization and Certification (by industry)

Dissertation submitted to qualify for
the degree of Philosophical Doctor (Ph.D.)

Scientific advisor:
Bolegenova Saltanat Alihanovna
Doctor of Physical and
Mathematical Sciences
Full Professor
Almaty, Kazakhstan

Foreign scientific adviser:
David Sales Lérica
Ph.D., Assistant Professor
University of Cádiz , Cadiz, Spain

The Republic of Kazakhstan
Almaty, 2023

CONTENT

LIST OF ABBREVIATIONS	4
ABSTRACT	5
RESUMEN	6
АБСТРАКТ	8
INTRODUCTION	10
1 CURRENT STATE OF THE ISSUE	15
1.1 Additive manufacturing and 3D printing	15
1.2 Material extrusion based additive manufacturing	18
1.3 Polylactide for fused filament fabrication and fused granular fabrication	22
1.4 Polymer recycling and additive manufacturing	23
1.5 Standardization in additive manufacturing	25
2 MATERIALS AND METHODS	31
2.1 Materials processing and manufacturing of samples for testing.....	31
2.1.1 Shredding of polylactide waste	31
2.1.2 Sieving of shredded polylactide waste.....	31
2.1.3 Filament making in single-screw extruder.....	31
2.1.4 Fused filament fabrication of samples for testing.....	31
2.1.5 Reprocessing of polylactide granules to receive an imitation of polylactide waste.....	32
2.1.6 Nanocomposites fabrication.....	33
2.1.7 Fused granular fabrication of samples from nanocomposites.....	34
2.2 Controlled degradation process.....	36
2.2.1 Thermal ageing according to ISO 188-2023.....	36
2.2.2 Hydrothermal ageing according to St JSC 002-2023	37
2.3 Characterization	38
2.3.1 Conditioning.....	38
2.3.2 Dimensional measurements	38
2.3.3 Structural analysis	38
2.3.4 Differential scanning calorimetry	39
2.3.5 Thermogravimetric analysis.....	40
2.3.6 Determination of mechanical properties	40
2.4 Standardization of nanocomposite from recycled polymer	42
Conclusions to chapter	42
3 EFFECT OF THERMAL AND HYDROTHERMAL ACCELERATED AGEING ON 3D PRINTED POLYLACTIDE	43
3.1 Materials used during the experiment.....	43
3.2 Results of experiment.....	43
3.2.1 Dimensional stability	43
3.2.2 Calorimetry.....	45
3.2.3 Thermogravimetry.....	47
3.2.4 Tensile testing	49

Conclusions to chapter	50
4 MANUFACTURE AND CHARACTERIZATION OF POLYLACTIDE FILAMENTS RECYCLED FROM REAL WASTE FOR 3D PRINTING	52
4.1 Materials used during the experiment	52
4.2 Results of experiment.....	52
4.2.1 Thermogravimetric analysis.....	52
4.2.2 Differential scanning calorimetry	54
4.2.3 Scanning electron microscopy	57
4.2.4 Mechanical properties	58
Conclusions to chapter	59
5 IMPROVING THE THERMAL AND MECHANICAL QUALITY INDICATORS OF RECYCLED POLYLACTIC ACID USING NANO ADDITIVES	61
5.1 Materials used during the experiment	61
5.2 Results of experiment.....	62
5.2.1 Scanning electron microscopy	62
5.2.2 Thermogravimetric analysis.....	66
5.2.3 Differential scanning calorimetry	67
5.2.4 Tensile testing	69
Conclusions to chapter	71
6 STANDARDIZATION OF RECYCLED POLYLACTIDE FOR ADDITIVE MANUFACTURING	72
Conclusions to chapter	75
CONCLUSIONS	76
REFERENCES	78
APPENDIX A Summary of officially published standards according to ISO/TC 261 official catalogue	89
APPENDIX B List of standards which are under development according to ISO/TC 261 official catalogue	92
APPENDIX C Standard of organization St JSC 002-2023 “Polylactide for additive manufacturing. Accelerated hydrothermal ageing test”.....	94
APPENDIX D Standard of organization St JSC 001-2023 “Nanocomposites based on virgin polylactide and its waste with titanium dioxide nanoparticles for additive manufacturing. Technical specifications”	100
APPENDIX E Certificate of Implementation.....	115

LIST OF ABBREVIATIONS

The following abbreviations are used in this thesis:

ISO	International Organization for Standardization
ASTM	American Society for Testing and Materials
AM, FA, AII	Additive manufacturing
FFF	Fused filament fabrication
FGF	Fused granular fabrication
CAD	Computer aid design
PLA, V	Polylactic acid, polylactide
rPLA, R	Recycled (secondary) polylactic acid (polylactide)
TiO ₂ , A	Titanium dioxide
PET	Polyethylene terephthalate
PP	Polypropylene
PEHD	High density polyethylene
PELD	Low density polyethylene
SEM	Scanning electron microscopy
EDX	Energy-dispersive X-ray spectroscopy
DSC	Differential scanning calorimetry
TGA	Thermogravimetric analysis
<i>R</i>	Shrinkage ratio
<i>L_o</i>	Length of the specimen before ageing
<i>L_a</i>	Length of the aged specimens
<i>T_g</i>	Glass transition temperature
<i>T_c</i>	Crystallization temperature
<i>T_m</i>	Melting temperature
ΔH_c	Enthalpy of crystallization
ΔH_m	Heat of melting
ΔH^*	Heat of melting for an infinitely large crystal
<i>X_c</i>	Degree of crystallinity
<i>T_{loss5%}</i>	Temperature at 5 % wt. mass loss
<i>T_i</i>	Initial polymer decomposition temperature
<i>T_f</i>	Final polymer decomposition temperature
<i>T_{i-T_f}</i>	Difference between initial and final decomposition temperatures
<i>T_{max}</i>	Maximum polymer decomposition temperature

ABSTRACT

Polymer extrusion-based additive manufacturing (AM) is a process that creates an object from a 3D model, a feedstock in form of polymeric filaments or pellets, and a 3D-printer. Recycled polymers can be used as feedstock for this technology. This thesis aims to enhance the quality of some plastic wastes to meet the standardized thermal and mechanical properties and make them suitable for 3D printing.

In the modern manufacturing revolution, AM plays a key role as an enabling technology, allowing objects with almost any geometry to be created in a more direct way. Material extrusion-based AM can be divided into fused filament fabrication (FFF) and fused granular fabrication (FGF). The FGF method is not so limited by the variety of materials, as all industrial polymers can be found as pellets. Moreover, the preparation of feedstock for FGF eliminates the second thermal processing for wire production, which always results in the reduction of the polymer's molar mass.

The most famous polymer for 3D printing is polylactide acid (PLA). The slow degradation rate in natural environments could lead to PLA accumulation. One way to utilize PLA waste is composting. But this method is used to degrade industrial waste, where a large amount of waste is collected every day. Also recycling the scraps for AM is interesting to save costs because PLA is an expensive polymer, and the construction of composting facilities currently involves large capital investments. In addition, an analysis of the normative base of AM in the polymer sphere revealed that ISO and ASTM organizations only developed seven standards for polymers in AM, without specifying the type of polymer.

To achieve the goal of the thesis study, a series of three interrelated experiments was performed. The first experiment on accelerated thermal and hydrothermal ageing of PLA was aimed at studying the temporal dynamics of polymer degradation. Thus, it was found that hydrothermal ageing for 1344 h, which corresponds to more than 1.5 years of operation under real conditions, leads to a significant decrease in the tensile strength of PLA samples. Based on these results, PLA waste from 3D printing up to 1.5 years old from the date of printing was collected for the second experiment. This debris was mixed with pure PLA in proportions of 25 %, 50 % and 75 %, respectively. The results of this experiment showed that a material based on pure and recycled PLA is a feasible material for FFF. In the last experiment, the properties of the mixtures received in the previous research were modified by adding titanium dioxide nanoparticles, and the samples were printed using FGF. The nanocomposite based on primary and secondary (recycled) PLA with the addition of 7 % titanium dioxide nanopowder has similar thermal and mechanical properties to the primary polymer, considering the standard deviation. Finally, to ensure the quality of the received nanocomposite and the reproducibility of the properties, the quality indicators have been documented in an organization standard.

Thus, in this work, it has been experimentally proved that using recycled PLA for extrusion-based AM is a realistic and achievable task, able to produce parts with improved comparable thermal and mechanical properties to those of primary PLA.

RESUMEN

La fabricación aditiva (FA) o impresión 3D basada en la extrusión de polímeros consiste en crear capa a capa un objeto a partir de un modelo 3D, un material polimérico de partida en forma de hilo o granza y una impresora 3D dotada con extrusora. Es posible alimentar impresoras 3D con materiales poliméricos reciclados. Esta tesis tiene como objetivo mejorar la calidad de algunos residuos plásticos para conseguir unas propiedades térmicas y mecánicas estandarizadas que permitan su adecuación como material de partida para la impresión 3D.

En la cuarta revolución industrial, o concepto de Industria 4.0, la FA tiene un papel fundamental como tecnología habilitadora, permitiendo crear objetos con casi cualquier geometría en un proceso más directo. La extrusión de material basada en FA se puede dividir en fabricación mediante fundido de filamentos (FFF) y fabricación mediante fundido de gránulos (FGF). FFF utiliza filamentos de alta calidad, ni demasiado frágiles ni demasiado flexibles con un diámetro específico y constante. Por lo tanto, solo ciertos materiales con las propiedades mecánicas apropiadas podrían ser procesados por FFF. En comparación, el método FGF no está tan limitado por la variedad de materiales, ya que todos los polímeros industriales se pueden encontrar en forma de gránulos o pellets. Además, la preparación de la materia prima para FGF excluye el segundo procesamiento térmico para la producción de hilo, que siempre resulta en una reducción del peso molecular del polímero.

El polímero más comúnmente usado para la impresión 3D es el ácido poliláctico (PLA). Es un poliéster termoplástico biodegradable y derivado de fuentes naturales (principalmente almidón y azúcar). No obstante, su degradación en ambientes naturales normales es lenta, lo que podría conducir a la acumulación de residuos de PLA en el medio ambiente. Una forma de utilizar los residuos de PLA es el compostaje, pero este método conlleva normalmente el uso de grandes instalaciones para degradar residuos que se generan en grandes cantidades, lo que no es el caso del PLA en la actualidad. Asimismo, reciclar residuos para su uso en AM es una opción que permitiría ahorrar costes, ya que el PLA es un polímero caro, y la construcción de instalaciones de compostaje implicaría afrontar grandes inversiones. Además, el análisis de la base de datos de normativas de estandarización resulta que, en el ámbito de la FA de polímeros, las organizaciones ISO y ASTM solo han desarrollado siete estándares para polímeros, sin especificar el tipo de polímero.

Para lograr el objetivo de la tesis, se realizó una serie de tres experimentos interrelacionados. El primer experimento sobre el envejecimiento térmico e hidrotérmico acelerado del PLA tuvo como objetivo estudiar la dinámica temporal de la degradación de este polímero una vez procesado en FFF. Por lo tanto, se encontró que el envejecimiento hidrotérmico durante 1344 h, que corresponde a más de 1,5 años de operación en condiciones reales, conduce a una disminución significativa en la resistencia a la tracción de las muestras de PLA. Sobre la base de estos resultados, se recogieron residuos de PLA de la impresión 3D de hasta 1,5 años de edad desde la

fecha de impresión para el segundo experimento. Estos desechos se mezclaron con PLA primario en proporciones de 25 %, 50 % y 75 %, respectivamente. Los resultados de este experimento mostraron que un material basado en PLA primario y reciclado es un material factible para FFF. En el último experimento, las propiedades de las mezclas recibidas en la investigación anterior se modificaron mediante la adición de nanopartículas de dióxido de titanio, y las muestras se imprimieron utilizando FGF. El nanocompuesto basado en PLA primario y secundario (reciclado) con la adición de nano-partículas de dióxido de titanio al 7 % tiene propiedades térmicas y mecánicas similares al polímero primario, considerando la desviación estándar. Finalmente, para garantizar la calidad del nanocompuesto recibido y la reproducibilidad de las propiedades, los indicadores de calidad se han documentado en una norma de estandarización.

Por lo tanto, en este trabajo, se ha demostrado experimentalmente que el uso de PLA reciclado para AM basado en extrusión de polímeros es técnicamente viable, siendo posible producir piezas con propiedades térmicas y mecánicas comparables o mejoradas a las del PLA primario.

АБСТРАКТ

Аддитивное производство (АП) или 3D-печать на основе экструзии полимеров - это процесс, в котором послойно создаются объекты из 3D-модели с помощью полимерного материала в виде нити или гранул и 3D-принтера, оснащенного экструдером. В 3D-принтерах можно использовать переработанные полимерные материалы. Данная диссертация направлена на улучшение качества некоторых пластиковых отходов для достижения стандартизированных термических и механических свойств, которые позволяют использовать их в качестве исходного материала для 3D-печати.

В современной промышленной революции, которая следует концепции Индустрия 4.0, АП играет фундаментальную роль в качестве вспомогательной технологии, позволяющей создавать объекты практически с любой геометрией. АП на основе экструзии материалов можно разделить на изготовление плавленными нитями (FFF) и изготовление плавленными гранулами (FGF). FFF использует высококачественные нити, не слишком хрупкие и не слишком гибкие, с определенным и постоянным диаметром. Таким образом, только определенные материалы с соответствующими механическими свойствами могут быть использованы в FFF. Для сравнения, метод FGF не так ограничен разнообразием материалов, поскольку все промышленные полимеры можно найти в виде гранул. Кроме того, подготовка сырья для FGF исключает вторую термическую обработку в ходе производства нитей, которая всегда приводит к снижению молекулярной массы полимера.

Наиболее часто используемым полимером для 3D-печати является полилактид (PLA). Это биоразлагаемый термопластичный полиэстер, полученный из натуральных источников (в основном крахмала и сахара). Однако, его деградация в нормальных природных условиях происходит медленно, что может привести к накоплению полилактидного мусора в окружающей среде. Одним из способов утилизации отходов PLA является компостирование. Но этот метод обычно используют для разложения промышленных отходов, где мусор собирается в больших количествах каждый день, чего нет в случае с PLA на сегодняшний день. Переработка отходов для использования в АП является интересной задачей, потому что позволит сэкономить затраты, поскольку PLA является дорогим полимером, а строительство установок по компостированию требует больших инвестиций. Кроме того, анализ нормативной базы в области полимерного АП показывает, что организации ISO и ASTM разработали только семь стандартов на полимеры в области АП, не указывая тип полимера.

Для достижения цели диссертационной работы была проведена серия из трех взаимосвязанных экспериментов. Первый эксперимент по ускоренному термическому и гидротермическому старению PLA был направлен на изучение временной динамики деградации этого полимера. Было установлено, что гидротермическое старение в течение 1344 ч, что соответствует более чем 1,5

годам эксплуатации в реальных условиях, приводит к значительному снижению предела прочности образцов PLA. На основании этих результатов для второго эксперимента были собраны PLA остатки от 3D-печати возрастом до 1,5 лет с даты печати. Эти отходы смешивались с первичным PLA в пропорциях 25 %, 50 % и 75 % соответственно. Результаты этого эксперимента показали, что материал на основе первичного и переработанного PLA является приемлемым материалом для FFF. В последнем эксперименте свойства смесей, полученных в предыдущих исследованиях, были модифицированы добавлением наночастиц диоксида титана, а образцы были напечатаны с использованием FGF. Нанокompозит на основе первичного и вторичного (переработанного) PLA с добавлением 7 % наночастиц диоксида титана имеет сходные с первичным полимером тепловые и механические свойства с учетом значений стандартного отклонения. Наконец, для обеспечения качества полученного нанокompозита и воспроизводимости свойств показатели качества были задокументированы в стандарте стандартизации.

Таким образом, в данной работе экспериментально продемонстрировано, что использование переработанного PLA для АП на основе экструзии полимеров технически осуществимо, что позволяет получать изделия с улучшенными термическими и механическими свойствами, сравнимыми с характеристиками первичного PLA.

INTRODUCTION

General description of the work

The thesis presents results on quality enhancement and standardization of recycled polylactide acid for additive manufacturing.

Relevance of the topic

Today, the accumulation of plastic waste is a huge threat of environmental pollution. To deal with plastic waste, i.e. slow-degrading petroleum-based polymers, in addition to the generally accepted methods of processing plastic waste, alternative biodegradable polymers are being developed. One of the most popular biodegradable polymers is polylactic acid ($(C_3H_4O_2)_n$) or PLA. Its tensile strength is comparable to that of polyethylene terephthalate, and also PLA has a relatively low melting point. Because of its properties, this polymer is widely used in the field of food packaging and in the production of surgical sutures and pins. In addition, PLA is one of the most popular polymers for additive manufacturing (or 3D printing) based on material extrusion.

Additive manufacturing, in the industrial revolution Industry 4.0, is a perspective direction in product manufacturing due to the speed of production changeover, which is problematic in the traditional plastic industry. Also, the ability to locate additive manufacturing closer to the consumer is an important advantage of this technology in the rapidly developing modern world. Due to the ease of use and relatively inexpensive price of 3D printers, additive manufacturing based on the extrusion of materials is suitable for small-scale production and domestic use.

However, despite the positive qualities of additive manufacturing, one must consider that 3D printing and prototyping generate polymer waste, including polylactide acid. To prevent the accumulation of polylactide acid waste in the environment from 3D printing, this waste must be placed in compost plants, as rapid biodegradation of polylactide can only be achieved under certain composting conditions. The construction of composts is economically justified only for industrial waste in large volumes and is unprofitable for small-scale production. To date, the market price of polylactide is higher than the price of petroleum-based polymers. Thus, to prevent the accumulation of polylactide waste in the environment and save resources, various methods of recycling polylactide waste from 3D printing are being explored.

Life cycle assessment studies of PLA have shown that mechanical recycling is the most environmentally friendly way to recycle PLA. However, during the mechanical processing of polylactide waste, the tensile strength of the received products becomes lower than that of the primary polymer. Taking into account the fact that when 3D printing products from recycled polylactide there are problems with interlayer adhesion of layers of products and clogging of the nozzle of a 3D printer, it is necessary to improve quality indicators and ensure the printability of recycled polymer, i.e. create a material with improved properties based on recycled polylactide.

Based on world practice, for sustainable development and ensuring competitiveness, quality and safety of the material, standardization is used, through which uniform requirements are set for the standardized object. Thus, improving a polymer based on recycled polylactide waste for additive manufacturing and standardizing its quality indicators is an urgent task.

Based on the above, the thesis work aims to improve and standardize the quality indicators of polylactide waste for its use in material extrusion-based additive manufacturing.

Connection of the thesis topic with the plan of scientific projects

The thesis work was conducted within the framework of the project “Improvement in resource efficiency and sustainability through the implementation of additive manufacturing methodologies for maintenance of facilities in the chemical industry”. Funding: Fundación Campus Tecnológico. Participating entities: Universidad de Cádiz and Indorama Ventures Química SLU. Period from 1 January 2020 to 31 June 2021. Granted amount: 6058,48 €. Coordinator: Sales Lérica, David

The thesis aims is the advanced standardization of the thermophysical properties of filaments and granules for 3D printing, obtained on the basis of polylactide waste.

To achieve these goals, it was necessary to solve the following tasks:

- to investigate the standardized accelerated hydrothermal ageing process of 3D-printed polylactide samples for subsequent recycling;
- to check the quality of polylactide filaments manufactured from real 3D printing waste with the addition of pure polylactide;
- improve the quality of filaments and granules for 3D printing made from recycled polylactide by adding pure polylactide and/or titanium dioxide nanoparticles;
- to develop an organization standard for nanocomposites based on pure and recycled polylactide with nano-TiO₂ for additive manufacturing based on material extrusion.

The object of study is polylactide waste from 3D printing.

The subject of study is the standardization of recycled polylactide with improved thermal and mechanical properties.

Research methods

The following methods were used to solve the tasks and achieve the goals:

To study the dynamics of thermal and hydrothermal ageing of 3D printed polylactide samples, the method of controlled accelerated laboratory ageing was used.

Polylactide waste was shredded, screened and extruded in a single screw extruder to manufacture filaments for FFF printed samples.

A twin-screw extruder was used to manufacture nanocomposites, from which samples were FGF printed.

The properties of the obtained samples were characterized by scanning electron microscopy, differential scanning calorimetry, thermogravimetric analysis and mechanical testing.

The methods of unification and advanced standardization, as well as the ordering of standardized objects were applied to standardize the recycled polylactide acid.

The scientific novelty of the work is that for the first time:

1. Accelerated laboratory ageing was used to experimentally determine the changes in the thermo-mechanical quality indicators of 3D-printed polylactide samples.

2. The quality of samples made from polylactide waste and mixtures of polylactide waste and primary polylactide in ratios of 25-75, 50-50, and 75-25 was checked.

3. Nanocomposites based on primary and secondary polylactide with the addition of titanium dioxide nanoparticles were made and their quality was checked.

4. The quality indicators of the improved material based on recycled polylactide were standardized and documented in the organization's standard.

Statements for defense

1. Standardized process of accelerated hydrothermal ageing in standard of organization St JSC 002-2023 “Polylactide for additive manufacturing. Accelerated hydrothermal ageing test” of 3D printed polylactide samples at 50 °C and 70 % humidity for 1344 hours results in a 33 % reduction in tensile strength;

2. Increasing the proportion of secondary polylactide from 0 to 75 % in a mixture with pure polylactide increases the tensile strength of FFF printed samples from 44.20 ± 2.18 MPa to 52.61 ± 2.28 MPa;

3. Adding 18 % of pure polymer and 7 % of titanium dioxide nanoparticles to secondary polylactide increases the tensile strength and fluidity of FGF samples to match those of a standard sample during 3D printing;

4. Standard of organization St JSC 001-2023 “Nanocomposites based on polylactide and its waste with titanium dioxide nanoparticles for additive manufacturing. Technical specifications” establishes the percentage of pure and recycled polylactide and titanium dioxide nanoparticles in proportions 25/75/0, 22/75/3, 18/75/7 for subsequent certification.

Theoretical and practical significance of the work

Accelerated thermal and hydrothermal ageing reveal the changes in the dimensional, thermal, and mechanical properties of polylactide samples over time. This theoretical knowledge is necessary to understand the period during which 3D-printed polylactide products maintain optimal quality.

The nanocomposite based on recycled polylactide with a primary polymer and titanium dioxide nanoparticles demonstrates the feasibility of mechanically recycling polylactide waste for additive manufacturing based on material extrusion with quality indicators matching a standard sample.

It were developed two standards of organization. The first standard St JSC 002-2023 “Polylactide for additive manufacturing. Accelerated hydrothermal ageing test” regulates the process of accelerated hydrothermal ageing of polylactide to identify the dynamics of its ageing. The second standard “Nanocomposites based on polylactide and its waste with titanium dioxide nanoparticles for additive manufacturing. Technical specifications” documents the thermal and mechanical quality indicators of nanocomposites based on recycled polylactide with the addition of virgin polymer and titanium dioxide nanoparticles. If the requirements of the second standard are met, the quality of products obtained from this nanocomposite through additive manufacturing based on the extrusion of materials can be guaranteed. These two standards were approved by the director of JSC “Ust-Kamenogorsk Machine-Building Plant of Industrial Fittings”. In the future, JSC “Ust-Kamenogorsk Machine-Building Plant of Industrial Fittings” plans to use the second standard of organization to certify nanocomposites based on pure and recycled polylactide with the addition of titanium dioxide nanoparticles, which will increase its competitiveness.

The practical significance of the obtained results is confirmed by publications in international peer-reviewed publications and participation in regular international conferences.

Publications in international peer-reviewed journals and participation in regular international conferences confirm the practical significance of the results obtained.

The author's contribution consists of conducting the entire thesis work, choosing the research method, solving problems, conducting research on the thermomechanical properties of polylactide samples for additive technologies, and developing regulatory and technical documentation independently. The author collaborated with the supervisors in setting tasks and discussing results.

Reliability and validity of the obtained results

The reliability and validity of the results obtained are confirmed by publications in high-ranking journals far abroad with a high impact factor and in publications recommended by the Committee for Quality Assurance in the Field of Science and Higher Education of the Ministry of Science and Higher Education of the Republic of Kazakhstan for the publication of the main results of scientific activity, and in the proceedings of international scientific conferences of the near and far abroad.

Approbation and publication of thesis work

Seven scientific publications, including three articles in journals indexed by Web of Science (Clarivate Analytics, USA) and Scopus (Elsevier, the Netherlands), one article in a journal recommended by the Committee for Quality Assurance in the Field of Science and Higher Education of the Ministry of Science and Higher Education of the Republic of Kazakhstan for obtaining a PhD degree, and three papers in abstracts of international conferences, published the main results of the thesis work.

Scientific publications with a high impact factor indexed by Scopus and Web of Science:

1. **Bergaliyeva S.A.**, Sales D.L., Delgado F., Bolegenova S., Molina S.I. Effect of Thermal and Hydrothermal Accelerated Aging on 3D Printed Polylactic Acid // Polymers (Basel). – 2022. – Vol. 14, №23. - P. 5256. <https://doi.org/10.3390/polym14235256> (IF=5.0, **Q1**, Percentile= 82 %)

2. **Bergaliyeva S.A.**, Sales D. L., Delgado F., Bolegenova S., Molina S.I. Manufacture and Characterization of Polylactic Acid Filaments Recycled from Real Waste for 3D Printing // Polymers (Basel). – 2023. – Vol. 15, №9. P. 2165. <https://doi.org/10.3390/polym15092165> (IF=5.0, **Q1**, Percentile= 82 %)

3. **Bergaliyeva S.A.**, Sales D.L., Cabello J.M.J., Pintos P.B., Delgado N.F., Gago P.M., Zammit A., Molina S.I. Thermal and mechanical properties of recycled-poly lactide acid/titanium dioxide nanocomposites for material extrusion additive manufacturing // Polymers (Basel). – 2023. – Vol. 15, №16. P. 3458. <https://doi.org/10.3390/polym15163458> (IF=5.0, **Q1**, Percentile=82 %)

Scientific publications recommended by the Committee for Quality Assurance in Education of the Ministry of Education of the Republic of Kazakhstan for publishing the main results of scientific activity:

1. **Bergaliyeva S.**, Bolegenova S., Sales D.L. Standardization of additive manufacturing // Bull. KBTU. - 2020. - Vol. 4, № 55. - P. 142–149.

Publications in books of abstracts of international scientific conferences:

1. **Bergaliyeva S.**, Bolegenova S. Prospects for the processing of polymer waste // International conference of students and young scientists “Farabi alemi”. - 2019. - P. 298.

2. **Bergaliyeva S.**, Bolegenova S. Determination of the thermal stability of polymeric materials obtained through additive manufacturing // International conference of students and young scientists “Farabi Alemi”. - 2020. - P. 119.

3. **Bergaliyeva S.**, Sales D.L., Bolegenova S., Molina S.I. Thermal analysis of 3D printed polylactic acid after accelerated thermal ageing // Alternative Energy Sources, Materials & Technologies (AESMT’20). – 2020. – Vol. .2. - P. 91-92

1 CURRENT STATE OF THE ISSUE

1.1 Additive manufacturing and 3D printing

In recent years, the upgrading and replacement of products have become increasingly rapid. New products with enhanced functions and/or more innovative designs supersede existing products in the market. The increased competition for manufactured products to reach the global market before any competitors has resulted in companies having to launch their new products in the shortest possible time. Conventional manufacturing technologies, in general, involve long production times, are prone to material wastage due to the subtractive nature of the processes and are labor intensive. Some examples include casting and machining. To keep up with this accelerated process of product change, new technologies must be developed. Time spent on the design, manufacture, test, and market phases have to be shortened [1].

Additive manufacturing (AM) technologies, also called 3D printing or rapid manufacturing, are among the enabling technologies in Industry 4.0. AM is a technology that manufactures products based on a 3D model by the addition of material in a layer-by-layer manner [2]. The application of this technology is widespread and due to its ease of use and large industrial applications, it has a high potential manufacturing prospect. Aerospace, medical, aeronautics and automation are the main sectors involved in the application of AM [3].

The fundamental concepts of AM were developed and demonstrated more than 150 years ago. The first computer-based AM systems were demonstrated about 55 years ago. Vat photopolymerization machines were introduced to the market in 1987 as beta test systems, with full commercialization a year later [4]. The first AM technologies were initially used to make prototypes of products as shown in Figure 1.1, this being the main purpose of these technologies also known as Rapid Prototyping [5].



Figure 1.1 - Prototype of an automotive distributor cap produced in 1987 using vat photopolymerization machine [4]

The aerospace industry was an early adopter of AM. Boeing and Bell Helicopter started using polymer AM parts for non-structural production applications in the mid-1990s. Airbus, GE Aviation, Honeywell Aerospace, Lockheed Martin, and Northrop Grumman are currently using AM extensively. The European Space

Agency, NASA, and the companies Relativity Space and SpaceX are using AM to produce igniters, injectors, combustion chambers, and fuel tanks for rockets. Most commercial aircraft contain 3D-printed parts, but they are not visible in the cabin. These include airducts, brackets, clips, and devices to secure wires and cables. The Boeing Company is flying more than 70,000 AM parts on commercial and military aircraft and satellites [4].

Regarding the healthcare sector, most orthopaedic implants used today are made in standard sizes. They are typically produced using traditional methods such as casting, machining, and moulding. However, a growing number of polymer and metal devices in serial production are being made using AM. As of February 2022, the Food and Drug Administration (FDA) had cleared more than 250 medical devices made by AM, according to a representative of the FDA’s Additive Manufacturing Working Group [4].

However, due to certain disadvantages of conventional manufacturing techniques, such as material waste, long manufacturing time, and limited versatility in manufacturing complex geometries, AM is increasingly being used for the creation of final parts with complex geometry and high added value [6]. Thus, the industrial exploitation of these techniques has grown to represent a market of billions of dollars annually, especially in the last decade [7]. The report Wohlers of 2023 [8] indicates that, in 2022, 3D printing services registered a growth of about 16.7 %, which represents a little bit less increase with respect to the previous year, which had increased by a 19.5 %, resulting in an investment of approximately 15 billion dollars in the global AM business, as shown in Figure 1.2. Additionally, AM is presented as a key element of manufacturing from the sustainability point of view. Various studies emphasize energy saving, emissions reduction and the incentive for consumer self-manufacturing [9], which demonstrates its current and future importance.



Figure 1.2 - Global revenue for AM products and services. From [8]

These technologies are associated with potentially strong stimuli for sustainable development to time- and cost-saving [10–13]. With benefits such as tool-less material processing, high geometric freedom, fast prototyping and cost-efficient small-scale production, additive manufacturing (AM) has the potential to revolutionize the manufacturing industry [14]. Wittbrodt et al. [15] showed that even making the extremely conservative assumption that a household would only use the 3D printer to make a selected 20 products a year, the avoided purchase cost savings would range from about 300 to 2000 USD/year.

The size of the modern AM market was more than 18×10^9 \$ in 2022 with a growth rate of about 15-25 % [16]. Thus, world industrial leaders and experts predict that by 2030 two thirds of all manufactured products in the world will be produced with printed components, and by 2030-2050 in a number of manufacturing sectors, 3D printing will allow printing of fully finished products. [17] The global increase of AM in production can be explained by the following main advantages:

- a reduced amount of raw material required in the supply chain;
- a reduced need for energy-intensive, wasteful, and polluting manufacturing processes. Estimated primary energy savings in a rapid adoption scenario reached 70–174 PJ per year in 2050 fleet-wide, with cumulative savings of 1.2-2.8 EJ [18];
- more efficient, flexible and generative product design with better functional and operational performance and biomimicry;
- reduced weight of transport-related products and improved carbon footprint. The cumulative greenhouse gas emissions reduction was estimated at 92.8–217.4 Mt [18];
- decentralized production, closer to the point of consumption, simplify logistics, transportation, storage, and supply chain;
- reduced time to market, so products are obtained and start to commercialize faster thanks to the agile and rapid creation of prototypes and the ability to make immediate design adjustments as well as carry out pre-commercialization test of products, providing the companies that use these techniques of greater competitiveness. In addition, due to the continuous growth of these techniques, each time more final parts are produced instead of prototypes
- reduction of tooling;
- reduced inventory and part consolidation;
- reduced lead time and on-demand manufacturing;
- sustainability and waste reduction. The implementation of AM promotes the development sustainability that the planet requires to fight against change climate. Energy consumption is reduced and so are costs derived from transport, since the raw material occupies less space. In addition, some specific technologies of 3D manufacturing allow the recycling and reuse of primary materials, for which makes the most of the matter and generates the least amount of waste;
- custom product manufacturing.

There are different types of AM processes, which have been improving and innovating to offer better profitability in production, as well as a greater number of

practical applications in different sectors. With the intention of classifying all these technologies, in 2013 the American Society for Testing and Materials F42 (ASTM F42) committee classified the different AM techniques into seven primary categories [19], as shown in the Table 1.1.

Table 1.1 - The seven AM process categories by ASTM F42 [20]

Process type	Definition	Material	Example of Technology
Vat Polymerization	Liquid photopolymer in a vat is selectively cured by light-activated polymerization	Photopolymers	Stereolithography (SLA), digital light processing (DLP)
Material Jetting	Droplets of build material are selectively deposited	Polymers, waxes	Multi-jet modelling (MJM)
Binder Jetting	A liquid bonding agent is selectively deposited to join powder materials	Polymers, Metals, Ceramics	Powder bed and inkjet head (PBIH), plaster-based 3D printing (PP)
Material Extrusion	Material is selectively dispensed through a Nozzle or orifice	Polymers	Fused deposition modelling (FDM), Fused filament fabrication (FFF), Fused granulated fabrication (FGF)
Powder Bed Fusion	Thermal energy selectively fuses regions of a powder bed	Polymers, Metals, Ceramics	Electron beam melting (EBM), selective laser sintering (SLS), selective heat sintering (SHS), and direct metal laser sintering (DMLS)
Sheet Lamination	Sheets of material are bonded to form an object	Paper, Metals	Laminated object manufacturing (LOM), ultrasonic consolidation (UC)
Directed Energy Deposition	Focused thermal energy is used to fuse materials by melting as the material is being deposited	Metals	Laser metal deposition (LMD)

1.2 Material extrusion based additive manufacturing

According to ISO/ASTM 52900:2015 standard [21], the material extrusion is one of the seven approaches to the processing of materials using 3D printing. In this technique, the material is melted, pushed through a nozzle and deposited layer by layer to reproduce the previously designed model of the object. Depending on the form of material and the type of the extruder extrusion-based AM can be divided into fused granulated fabrication (FGF) and filament fused fabrication (FFF) presented in Figure 1.3a and 1.3b, respectively.

The most widely used AM among extrusion based AM process is FFF due to its simplicity, low running, and material costs [22]. This is a layer AM process that uses a thermoplastic filament by fused depositing which transferred by the gears. This technique is also named as FDM, which is trademarked by *Stratasys Inc* in the late 1980s [23]. Its popularity is based on its relative simplicity and broad availability of the low-cost solutions in the market [24].

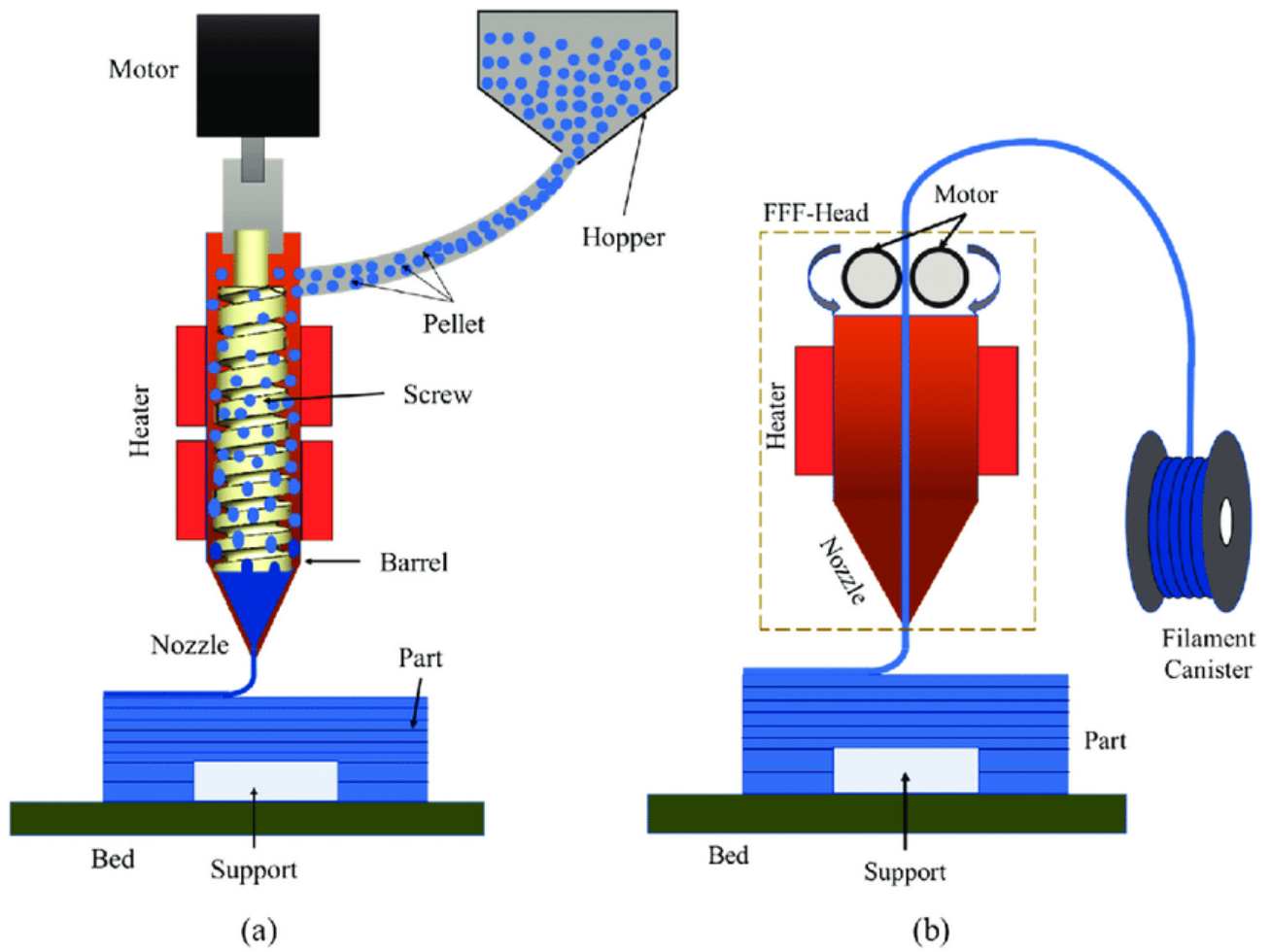
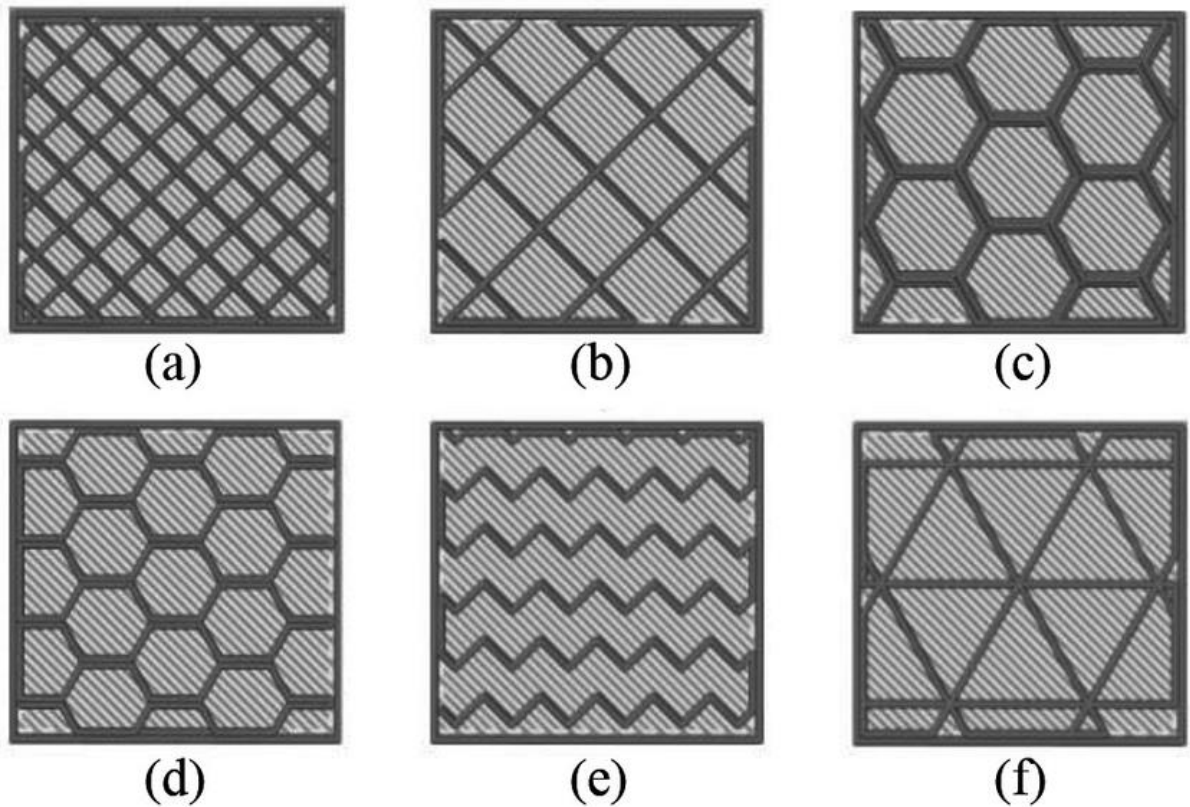


Figure 1.3 - Schematic diagram of fused granular fabrication (a) and fused filament fabrication (b) [25]

There is an ongoing necessity to enhance product quality in all production processes. Many factors influence the product's aesthetics and mechanical qualities. As a result, optimizing important parameters to reduce errors throughout the printing process is critical in obtaining excellent quality. Numerous mathematical and statistical studies have been carried out to produce specimens correctly and get high-quality results. Some parameters that influence the quality of printed components are described next [26]:

- the filling pattern. The shape of components could be hollow or solid, determined by the infill percentage. The infill percentage varies between 0 and 100 %. It is available in a variety of shapes and geometries: straight, grid, full honeycomb, partial honeycomb, wave, or triangle patterns are possible as shown in Figure 1.4. The filling pattern substantially influences the mechanical characteristics and stiffness of printed components;
- the temperature of the nozzle is another critical parameter, which depends on the polymer's melting point (typically varies from 170 to 220 °C). The inappropriate nozzle temperature affects the process of printing and layer bonding;



(a) straight, (b) grid, (c) full honeycomb, (d) partial honeycomb, (e) wave, and (f) triangle

Figure 1.4 – Examples of filling patterns [27]

- the temperature of the printing bed is another important factor in controlling the 3D-printed product quality. Based on the material characteristics, the range of temperature varies from 0 to 80 °C;
- the diameter of the nozzle impacts the product's surface quality and mechanical capabilities. The nozzle diameter typically ranges in size from 0.2 to 0.8 mm. Printing with a narrower nozzle diameter produces better surface roughness and tolerance, but it takes a longer printing time [28];
- the importance of build orientation in material extrusion AM cannot be understated. This parameter impacts mechanical characteristics and surface texturing [29]. Objects can be deposited from any angle (0°–180°) and in any direction (x, y, and z);
- the air gap is the distance between successive rasters in a layer as shown in Figure 1.5. For the 3D-printed components, tensile strength is affected by the air gap and the orientation. For the components fabricated by 3D printing, stiffness and strength were improved by an air gap of (- 0.003) [30];
- the material bead width and the angle of the x-direction raster pattern are referred to as raster width and raster angles, and these variables cause warping and shrinkage. Experiments revealed that as road width, layer thickness, contours, and air gap decrease, the percentage change in part width reduces accordingly [30];

- layer thickness is the separation between the nozzle and the platform, which determines the height of every layer. This factor significantly impacts the surface roughness of components and the time required for printing [31]. The thickness of the layer ranges from 0.06 to 0.6 mm. Product quality is improved, whereas the time of printing is extended by reducing the layer thickness.

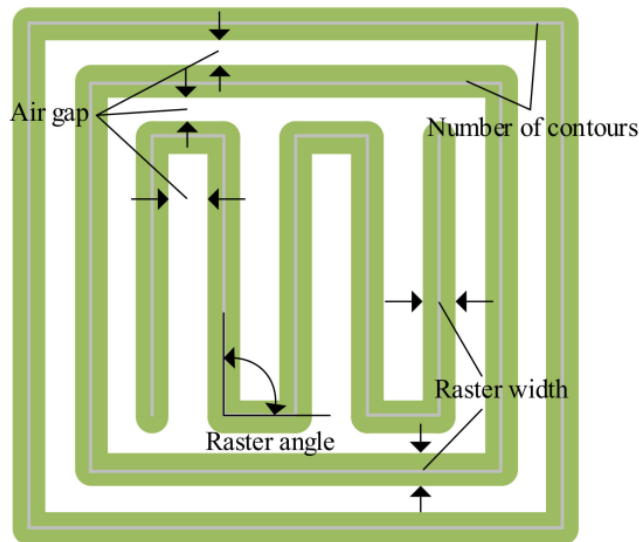


Figure 1.5 – Extrusion based AM process parameters related to toolpath [32]

From the economical point of view, FFF prices can go as down as 0.2 €/part, thus making it an attractive technology [6]. Also, FFF uses non-toxic thermoplastic materials such demanding less heating energy for the nozzle and worktable [18]. FFF uses high-quality, not too brittle or too flexible filament with a specific and constant diameter. So, only certain materials with the appropriate mechanical properties could be processed by FFF. In comparison, FGF method is not so limited by the variety of material [24], while all industrial polymers could be found as pellets [33]. The use of polymeric pellets as feedstock material can improve production times by up to 200 times [34] and reduce costs by a factor of 10, as a prior additional filament-extruding step is not required during the pellet-based AM process [35]. In addition, one-step preparation of feedstock for FGF excludes second thermal processing of the polymers which always results in the reduction of their molar mass [24].

The quality of components produced by this technology depends mainly upon process parameters adopted for printing. The most critical process parameters in pellet-based material extrusion are screw speed and barrel temperature. Barrel temperature is the surface temperature of the barrel. The screw speed determines how long the material is exposed to heating systems. Kumar et al. studied the impact of screw rotational speed and barrel temperature on melt flow speed and cross section of deposited filaments [36]. It was observed that as screw rotation speed and barrel temperature were increased, melt flow speed increased. This occurred because the pressure gradient increased as the screw speed increased, resulting in increased flow

speed. Also, chains of polymer move and glide quickly on one other as barrel temperature rises, causing increased material melt speed.

When considering the statistical data, it should be noted that the research sector related to AM has grown from 10 % to 50 % since 2015 to 2019, which indicates that 3D printing is a rapidly growing manufacturing method.

1.3 Polylactide for fused filament fabrication and fused granular fabrication

A broad range and successively increasing variety of plastics suitable for AM are available in the market. These materials vary in transparencies, thermal or mechanical properties. Depending on the application of the printed plastic product, a suitable material should be selected. Currently, materials exhibit properties mimicking those used in traditional manufacturing and have since replaced poor performing brittle materials used in the early 1990s [1].

The most famous polymers for 3D printing is polylactide acid (PLA). It is a biodegradable and renewable thermoplastic polyester [37] derived from renewable sources (mainly starch and sugar) [38]. It replaces conventional petrochemical-based polymers, such as acrylonitrile butadiene styrene, and reduces oil consumption by 30–50 % [39–42]. Its relatively high tensile strength and modulus compared to other thermoplastics such as polyethylene terephthalate and polypropylene, the low impact strength, less heat tolerance, brittleness with less than 10 % elongation at break [40], low crystallization rate, poor ductility make it inadequate for more demanding applications [40,41]. Otherwise, PLA has a relatively low melting point (150-160°C) and is a safer alternative to acrylonitrile butadiene styrene, another popular AM polymer [43].

The global production of PLA was around 0.2 million tons in 2017 [44] and around 0.19 million tons in 2019 [45]. In addition, the annual output of PLA is expected to reach 0.56 million tons by 2025, an increase of 53.8 % over 2020 [46]. PLA is a three carbon membered thermoplastic with a hydroxyl and carbonyl at the end, has a very slow biodegradation rate, and it is brittle despite its low degree of crystallinity [47]. However, the role of biodegradable plastics in solid waste management is somewhat controversial because of their slow degradation rate and their possible interference with plastic-recycling efforts [48]. Therefore, increasing the production of PLA might cause some problems, mainly related to the management of the waste generated after its use [49].

PLA is supposed to finish its life in compost [39]. It degrades slowly in nature, taking between 2 and 10 months in dry conditions [50]. Jeffrey *et al* [51] estimated that biodegradation in landfills at 20°C will take 100+ years. To be decomposed in natural environments it needs microorganisms [41,52,53]. The slow degradation rate could lead to PLA accumulation in the environment [40,49,54–57]. One way to utilize PLA waste is composting. But this method is used to degrade industrial waste, where a large amount of waste is collected every day [58]. Considering also the fact

that PLA and construction of composting facility have quite high price currently [59,60], this is why to reprocess the scraps could be interesting in order to save costs [61]. Also, it must be mentioned, that the cost of PLA production is currently high relative to conventional petroleum-derived plastic products [62]. The ratio between the price of virgin PLA and the price of PLA recyclate from post-industrial waste is 46 % and 51 % for post-consumer [56].

1.4 Polymer recycling and additive manufacturing

Despite many benefits of 3D printing technologies, it still creates a significant amount of waste [38]. Filament material is widely thrown out during the fabrication process due to printing failures, broken parts, filament replacement, discarded support structures, and nozzle tests [22]. Moreover, some printed products are used as prototypes that could be discarded at the end of the product development process [63,64]. Hence, a certain increase in the amount of plastic waste associated with the development of the polymer AM market could be predicted. Previous studies have shown that over 40 % of material related waste can be avoided using AM and 95 % of unused material can be reused [43]. Costs could also be reduced by recycling locally, where individuals, groups, or small businesses could procure recycling equipment in the range of 3000 USD [38].

So, it is necessary to develop effective recycling methods for PLA 3D printed waste [65]. Furthermore, limited research in the area of recycling plastics from 3D printing has been conducted [38]. Additionally, in a new transformation industry 4.0 there is a need in developing cost-effective recycling processes. AM Technologies is one way to utilize plastic waste economizing natural resources and time. Through design, material preparation, manufacturing, usage, and end-of-life treatment AM gives opportunities to reduce energy and material consumption [18].

Some works tried to solve recycling through AM problem. For example, Baechler et al. developed an extruder to produce filament from polymer waste [66]. Filabot, a plastic filament maker that utilizes post-consumer plastic [63]. Woern et al. designed the open source recycling system which costs less than 700 \$ in materials and can be fabricated in about 24 h. [67]. Dongoh Lee et al. designed a recycling system for making post-consumer filaments for 3-D printers [63].

Actually, recycling PLA filaments for 3D printing is a feasible option, as it offers environmental benefits, such as reducing landfill and CO₂ emissions from waste transportation [68]. In this sense, a comparative life cycle assessment conducted on meat trays showed that PLA production (in the form of granulates) contributes 63 % to its overall greenhouse gas emissions, with this rate being greater than that for amorphous polyethylene terephthalate (PET, 53 %) and polypropylene (PP, 44 %) [69]. Additionally, over 80 % of the embodied energy used in transportation and collection could be saved [70], distributed recycling and manufacturing methods could reduce energy consumption by a factor of two compared with traditional manufacturing ones [71], and making 3D printing filament

at home from recycled filament saves about 40 times more energy than commercial production [66].

There are not many previous research works on the topic about recycling plastics in 3D printing. The most relevant are summarized next.

Zander et al. showed that FFF filament from 100 % recycled bottles and packaging PET without any chemical modifications or additives is a viable new feedstock for FFF, with the mechanical properties of the printed parts comparable to the parts made from commercial filament [72]. In work [73], Zander et al. processed blends of PET, PP, and polystyrene waste into filaments for 3D printing with tensile strengths comparable to some lower-end common commercial filaments, such as high-impact polystyrene. Fabio et al. recycled PLA in an open-source additive manufacturing context [74]. As shown in [75], low-density polyethylene (LDPE)/linear LDPE is a soft, low-modulus, high-toughness polymer, which leads to a variety of additive manufacturing complications. In [66] and [76], filament made of recycled high-density polyethylene (HDPE) pellets had favourable water rejection, with an extrusion rate and thermal stability comparable to those of the filament made of acrylonitrile butadiene styrene pellets. According to data from studies, polymers could only be recycled to a lower material level (downcycling), so they could be used in less critical applications because of worse mechanical properties [38,63,64,74]. To improve the quality of recycled polymers, composites were created from polymer waste by adding natural/synthesis particles and/or fibres of a micro- or nanoscale size. For instance, in [77] and [78], the authors manufactured 3D printable composites based on the waste of PP by adding glass fibre in the first work and basalt fibre in the second one. The produced filament with 5 % wt. of basalt had the highest tensile strength among all the produced samples [78]. It must be mentioned that the quality and processability of fabricated filaments mainly depend on extrusion parameters, such as the rpm/speed of the screw, extrusion temperature, and load. These extruder settings are optimized experimentally and can vary. According to the above-mentioned studies, PET filament was extruded at a temperature that is equal to the melting point. To fabricate filament from PP, LDPE, and HDPE, the extrusion temperature was set up much higher than the melting temperature. The opposite is true for PLA.

Some studies revealed the coupling of open-source 3D printers with polymer processing could potentially offer the basis for a new paradigm of distributed recycling process. Anderson [38] produced filament for FFF recycled from 3D printed parts, Cruz Sanchez et al. [74] reprocessed PLA filament 5 times in open-source AM, Sasse et al. [14] investigated filaments with different contents of recycled PLA, Babagowda et al. [79] optimized the parameters such as layer thickness and PLA build material which is mixed with recycled PLA material. The main conclusion that can be drawn from the listed researches is that 3D printing with recycled PLA is a viable option. Some of the listed authors wrote that there was some nozzle clogging during reprinting of recycled materials. This drawback is common in filament-fed printers, used in the works mentioned above. On the other hand, these studies showed

the decreasing tendency of mechanical properties. This problem can be solved by adding of nanofillers which could also add functionalities to the produced nanocomposites [80]. The physical, chemical, and mechanical improvements in nanocomposites have been found to be significantly greater than the more traditional polymer-composites with micron sized fillers. [81]

Regarding the cost of post-consumed plastics that can be processed by FFF, PET, for instance, has a cost of 0.10 \$/kg while polystyrene, HDPE and LDPE, and PP have an even lower cost, 0,03- 0,06 \$/kg, which is more than a thousand times the commercial filament costs [82].

Manufacturing materials mainly affect the quality and performance of parts made of FFF. The mechanical effects of recycled PLA content on PLA filaments should, therefore, be studied to attain the desired quality characteristics in the parts developed by the FFF process. Studying the effect of the parameters on the response characteristics of the FFF parts helps to adjust the level of the process variable that improves the parts' quality [83].

All in all, previous works have shown that 3D printing is a cost-effective recycling process that economizes natural resources and time. However, the physical and chemical properties of recycled plastics should be studied to make them effective and standardized to make them widespread and reliable.

1.5 Standardization in additive manufacturing

While many companies have explored the potential of AM for new business opportunities through novel designs that were previously impossible and will alter the makeup of supply chains, several hurdles prevent its wider adoption. One of the most critical barriers is the qualification of AM parts. Many manufacturers and users do not have full confidence and certainty that AM parts would exhibit consistent quality and reliability within and across different printers and geographies [1].

Developing AM specifications and standards that are accepted by the industry is especially essential in this rapidly evolving environment and can facilitate faster and more robust qualification, which, in turn, could expedite device/product certification by regulatory agencies [84].

It must be mentioned that existing standards for the polymer-based material are very general, and there are no open standards developed for resin-based and filament-based AM [1]. Without such standards in place, it would not be possible to conduct a proper comparison across and within different AM processes [1]. It is widely recognized that the lack of AM standards has slowed down the adoption of AM systems in industrial processes [85].

The literature review in the Scopus Web of Science Core Collection database from 1948 to 2023 showed that there are only 277 papers using the combination of keywords: “additive manufacturing and standardization”. Compared to the search using the keywords “additive manufacturing”, which gave 425,239 results, indicating a lack of information from this difference in the field of standardization of additive

manufacturing. Similar results were obtained in the Web of Science (Clarivate) database, as shown in Figure 1.6. The main achievements in the field of AM standardization are summarized next.

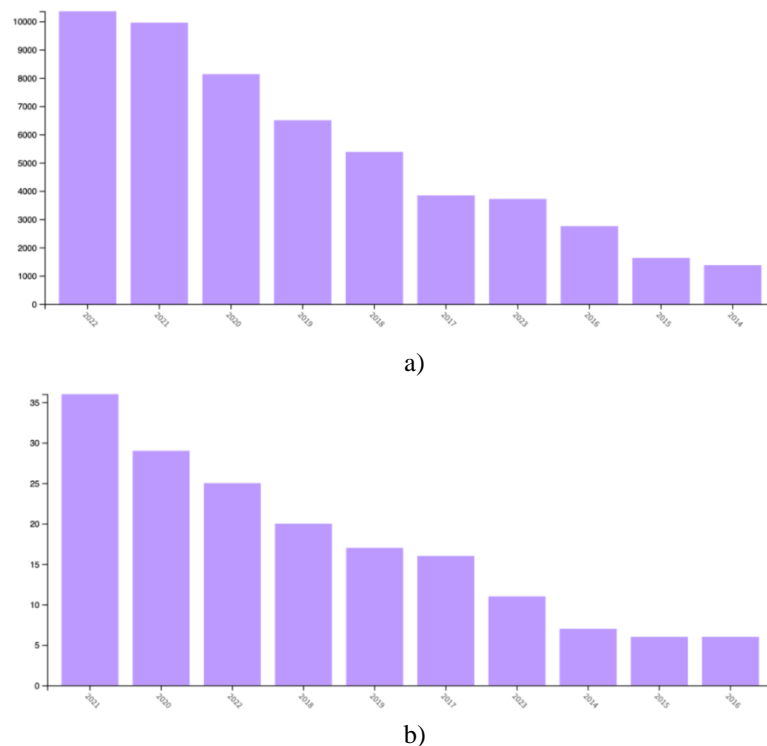


Figure 1.6 - Number of published articles per year as registered in the Web of Science (Clarivate) for the search “additive manufacturing” (a), and “additive manufacturing AND standardization” (b)

Monzon et al. [85] and Kawalkar et al. [86] emphasized the importance for standardization for all sectors, starting from industrial manufacturers to delivering it to the consumers. The lack of AM standards is always a barrier to the acceptance of AM in all aspects of manufacturing. Based in this prospective, Monzon et al. [85] drew the following conclusions:

- there is an urgent need for AM standards;
- it is crucial that the AM standards are global and internationally accepted;
- the customer requirements are the main driver for implementing standards and the basis for future AM standards;
- the priority topics for AM standardization are materials, processes/methods, and test methods;
- the development and application of standards are expected to improve the reliability of machines and processes;
- the main arguments for why standards are needed are related to quality or qualification (system qualification; material quality, part quality, quality control);
- future standards are directly linked to market opportunities.

From the initial workshops that stipulated the initial layout to modern day collaboration between ISO and ASTM, the AM industry has established standards for the emerging scientific community. These steps are helping to realize the potential of expanding AM industry, which brings larger market revenue worldwide and ensures quality and certified products in critical sectors such as aerospace and medical.

Pei has published a series of reports on the standardization efforts of ISO/TC 261 “Additive Manufacturing” during every plenary meeting of this technical committee [87]. Jinhua Xiao et al. [88], on the other hand, standardized AM machine tool representation according to four important ISO standards (ISO 10303, ISO 14649, ISO 15531 and ISO/CD 18828), to solve the problem of process planning and operation management.

Even though polymer AM is the most widespread one, most of the published works on AM standardization focuses on metal. For example, Seifi et al. [84] applied many sections of manuscript to a broad range of material systems produced by AM technology (both metallic and non-metallic), but the primary focus was on metal AM processes. Mohsen et al. state that the need for qualification standards covering all aspects of the technology is becoming more prevalent as the AM industry moves towards industrial production. While some standards and specifications for documenting the various aspects of AM processes and materials exist and continue to evolve, many such standards still need to be matured or are under consideration/development within standards development organizations. The authors says that for AM, as a relatively new manufacturing technology, the specific testing procedures still need to be developed to reflect the unique nature of AM material systems (including anisotropy, inherent material anomalies, location-specific properties, and residual stresses), focused on the characterization and understanding of fatigue and fracture properties of AM materials, and the corresponding testing methodologies. Besides the “conventional” crystallographic fatigue crack initiation mechanisms in homogeneous substrate materials, crack initiation due to the presence of inherent AM material anomalies such as porosity, lack of fusion defects, or inclusions also must be considered. This paper summarizes some of the important standardization activities and limitations associated with using currently available standards for metal AM with a focus on measuring mission-critical properties.

It must be mentioned that many different types of AM machines having a broad range of prices and sizes are currently available on the market. The AM processes and materials are often different from one machine to another, but ultimately, they are all designed to print complex 3D parts and components from 3D CAD drawings. AM system manufacturers typically provide their own system specifications such as minimum dimensional resolution and feature size. However, Jeong et al. [89] noticed that currently there is not a reliable method to evaluate and certify AM parts against the specifications claimed by the manufacture. Jeong et al. [89] offered to establish a reliable validation process like defining a standardized AM part that can be produced by any AM system from the same 3D CAD drawing. In their investigation [89] for standardization of FFF, an ultrasonic imaging system

originally developed for visualization of microstructures in sheet metals, with capabilities of generating plane two-dimensional images at spatial resolutions between 1 and 200 μm , was used to quantitatively evaluate a FFF processed 3D test part. Finally, a suggestion is made for adopting controlling process parameters to qualify or certify FFF based AM machines in the market by applying a reliable nondestructive evaluation validation method to a standardized part with various features of different shapes and physical dimensions. But the main problem to use this method is that it practically needs to be officially regulated.

García-Domínguez et al. [90] claimed that there is still no defined and homogeneous regulatory context for AM field, especially they emphasized that standards for mechanical test are very general and are not specific for materials nor for the corresponding manufacturing processes.

ASTM International has supported the development of AM for more than a decade [4]. The first reported standard development was carried out by E28.16 Rapid Prototyping Subcommittee of the ASTM E-28 Mechanical Testing Committee which develops tensile specimens for testing purposes which eventually led to the foundation of a new committee for additive manufacturing i.e. ASTM F42 in 2009, which governs all activities with respect to additive manufacturing till date [86].

Nowadays, the development of standards in the field of AM is carried out by International Organization of Standardization (ISO) and American Society for Testing and Materials (ASTM) [91]. These international organizations united and created technical committees at ISO/TC 261 “Additive Manufacturing” and ASTM Committee F42, “Additive Manufacturing Technologies”. The main objective of ISO/TC 261 is to standardise the processes of additive manufacturing, the process chains (data, materials, processes, hard- and software, applications), test procedures, quality parameters, supply agreements, environment, health and safety, fundamentals and vocabularies [87]. The working committees of ASTM F42 and ISO TC261 collaboratively are composed to work for betterment on below stated fronts [86]:

- qualification and method improvements for certification;
- design guidelines;
- testing methods carried out for determining characteristics of raw materials;
- testing methods carried out for determining mechanical properties of finished AM parts;
- guidelines for Material recycling (re-usage);
- standard guidelines for comparative testing methods;
- standards for test artifacts;
- requirements for purchasing AM parts;
- harmonization of existing ISO 17296-1 and ASTM 52,912 terminology standards.

To date, 27 published ISO standards and 33 standards are under development [92]. The standards define terminology, measure the performance of different production processes, ensure the quality of the end products, and specify procedures for the calibration of additive manufacturing machines [93]. All implemented

standards published on the official ISO and ASTM websites on 29.05.2023 were marked by materials to which they refer and classified into 4 groups according to standard classification:

- general standards;
- standards applied to terms and definitions;
- standards for processes (works), includes design standards and processes regulations;
- product standards;
- standards applied to test methods.

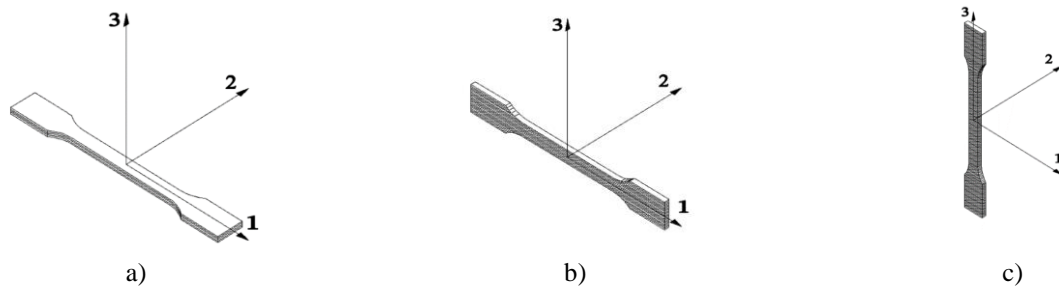
For example, ISO 17296-2:2015 [94] entitled “Additive manufacturing - General principles - Part 2: Overview of process categories and feedstock” related to the contextual and theoretical framework of AM, while ISO 17296-3:2014 [95] named “Additive manufacturing - General principles - Part 3: Main characteristics and corresponding test methods” related to the standardization of the tests to be performed for the characterization of the pieces obtained as a result of these processes. Result of this classification is presented in Table A.1 of appendix A.

Most of these standards have been developed for the metal 3D printed products, they are 45 standards from 52 officially published standards in AM field. In addition, 29 standards from 45 AM standards for metals are specified especially on metal or on definite type of metal, they are not general, for all bulk materials type. In contrast, only 7 standards are developed for polymers without specifying the type of polymer.

The ISO 17296-3:2014 should be highlighted because it identifies the test methods to be used for different materials. As can be seen when consulting the standards identified by ISO 17296-3:2014, all these mechanical test standards are characteristic of other productive and technological contexts, which are different from AM. In addition, for surface and geometric requirements the same standards are indicated for metallic materials, as plastics and ceramics [90].

The standard referred for tensile tests in both UNE 116005:2012 and ISO 17296-3:2014 is ISO 527. However, with regard to the description and identification of the specimens, UNE 116005:2012 includes some aspects that are considered noteworthy against the information provided in part 1 and part 2 of ISO 527. Thus, three test tube orientations are explicitly distinguished. First, from a general approach to any piece obtained by additive manufacturing, by identifying three axes associated with three possible orientations or positions of the specimen. Subsequently, representations of the three orientations for the tensile specimens are included in Figure 1.7 [96].

While some standards and specifications for documenting the various aspects of AM processes and materials exist and continue to evolve, many such standards still need to be matured or are under consideration/development within standards development organizations [84]. The standards under development of ISO/TC 261 are listed in Table B.1 of appendix B.



a) type 1A, horizontal position; b) type 1A, edgewise position; c) type 1AV, vertical position

Figure 1.7 - Representation of possible orientations in parts obtained by additive manufacturing based on UNE 116005:2012

Table B.1 of appendix B shows that no special standards for polymers was planned for developing for next several years. However, the world community of specialists working in the field of AM states that this base does not satisfy the needs of all types of AM. The application of conventional standards used in standard manufacturing for materials or technology may not be applicable in the case of additive manufacturing technology [86]. The review of all these normative developments also reveals a lack of specific references, similar to the ones developed for certain polymer. There is a need to create standards for individual industries. Moreover, analysis of normative and technical documentation shows that most of the standards are developed for AM metals, so there is a great need for standards for products made of plastic. The standards for polymer-based materials are very general, and there are no standards developed for AM based on polymers and threads.

The lack of standards in the field of AM leads to the fact that this technology cannot be applied in industries where mandatory certification is required. In Kazakhstan, these are such industries as the production of building materials, packaging products and the production of children's toys, in the medical industry. Also, the lack of standards leads to the fact that if there are no uniform requirements, the principle of interchangeability may not be observed. Therefore, standardization for such a new and rapidly developing AM industry is very important and necessary.

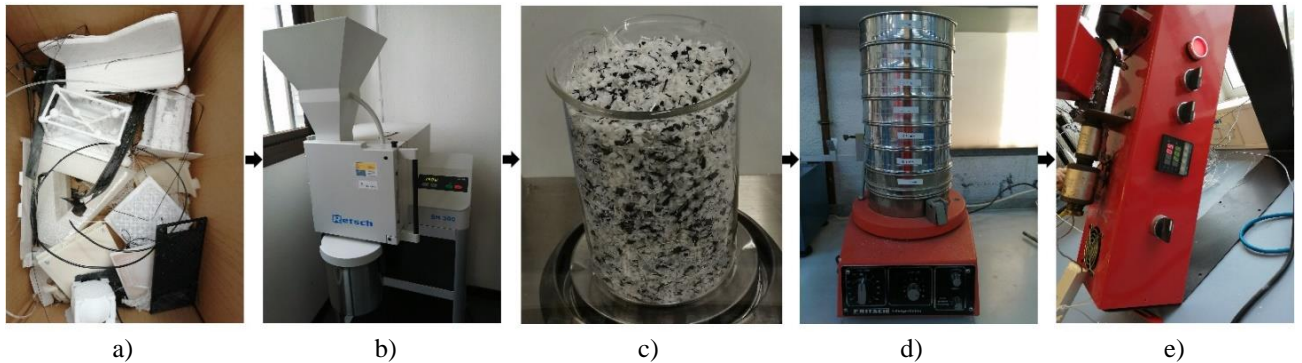
Thus, as general conclusions, the industry of polymeric waste using additive manufacturing is relevant, requires further research, causes less environmental impact, and may have great economic effect. Additionally, standardization in the field of AM is needed mainly for the integration of AM into production.

2 MATERIALS AND METHODS

2.1 Materials processing and manufacturing of samples for testing

2.1.1 Shredding of polylactide waste

Plastic waste was processed by different methods, but for FFF printed samples real waste after 3D printing was used. Figure 2.1 shows the first steps to making PLA pellets from 3D-printed post-consumer plastic and manufacturing the filament from them. Real debris was collected for about one year, so PLA waste had a different composition of PLA plastics with dissimilar life cycles. The recycled fraction of PLA was prepared by shredding PLA waste using a Retsch SM300 (Germany).



a) PLA debris collection; b) shredding; c) shredded PLA; d) sieving; and) filament production

Figure 2.1 - Preparing the filament from PLA debris

2.1.2 Sieving of shredded polylactide waste

Shredded real waste was sorted according to particle size using an electric sieve (Fritsch, Idar-Oberstein, Germany) with square section holes of 5, 2.5, 1.25, 0.63, 0.32, 0.16, and 0.080 mm. The particle size distribution showed 65 % of the sieved PLA in the 1.25 mm fraction, so this fraction was used for filament production.

2.1.3 Filament making in single-screw extruder

Likewise, both virgin and recycled PLA were dried in a vacuum oven, VACUtherm VT 6025 from Thermo Scientific (Waltham, MA, USA), at 50 °C overnight before extrusion to avoid the hydrolysing effect of absorbed water. Different proportions of virgin and recycled PLA pellets were introduced in a laboratory-sized co-rotating single-screw extruder, Noztek Pro Filament Extruder (Shoreham, West Sussex, UK), with one controllable heating zone for melt mixing and filament extrusion.

2.1.4 Fused filament fabrication of samples for testing

For thermal and hydrothermal ageing regular dog-bone (type A2) specimens were printed using a Witbox 2 printer (BQ) with optimum operating temperatures of 200 °C and a printing glass table without heater.

For manufacturing samples from virgin PLA and real waste regular dog-bone (type 1BA) specimens from each PLA blend were printed using an Anycubic Kossel Delta Rostock Die kit 3D printer (Shenzhen, China), with a platform temperature of 60 °C.

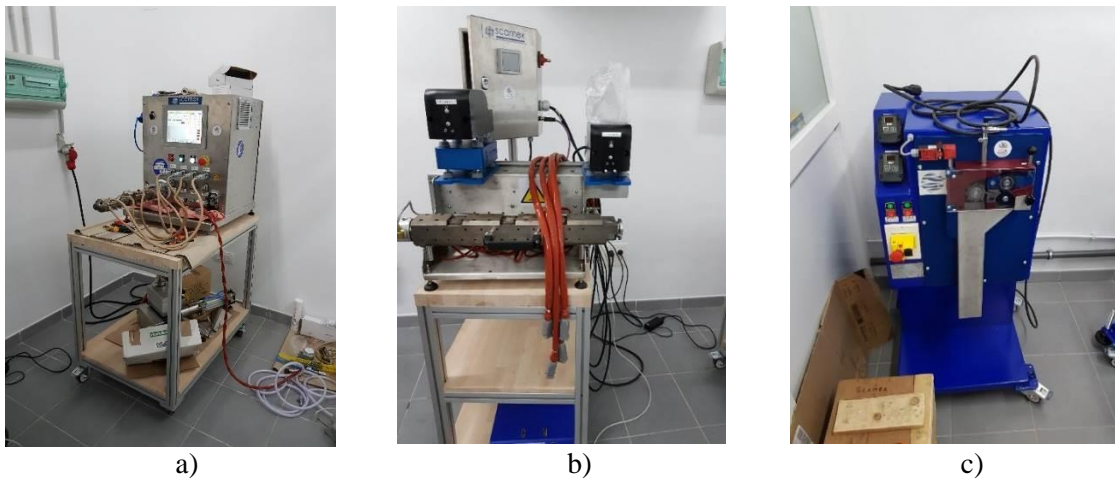
All specimens were printed considering the ISO 20753 standard [97] with a 100 % infill, horizontal pattern orientation of 0/90 (i.e., alternating layers with orientations at 0° and 90°), and a layer height of 0.2 mm. Each specimen was printed with a skirt of two extruded perimeters that composed the outermost edge (Figure 2.2). The selected deposition pattern orientations and layer height offered better quasi-isotropic mechanical properties for PLA parts manufactured by FFF compared with 45/45 orientation [98,99]. Likewise, the Ultimaker Cura 4.1.0. (Ultimaker B.V.) software was used for slicing the STL files into machine-readable G-code. All specimens were printed indoors in a temperature-controlled environment (23 ± 2 °C and 50 ± 5 % R.H., as defined in Ref. [100]).



Figure 2.2 - FFF printed samples for ageing tests

2.1.5 Reprocessing of polylactide granules to receive an imitation of polylactide waste

Recycled PLA for FGF were produced by reprocessing of PLA in twin-screw modular extruder system by Scamex (France) one time. The units of this extruder is shown in 2.3. Figure 2.3a illustrates the central unit where temperatures, screw speed, and work pressure can be established. The modular extruder from this study has five heater zones, starting from the first one which is the closest to the central unit until the last one, which is on the right in the nozzle area. Then, it has two electronic dosimeters with some different blades, the first one at the beginning is designed for pellets, and the second one for powder. The twin-screw with the dosimeters is presented in Figure 2.3b. The machine where the filament is cut off into small pieces is shown in Figure 2.3c.



a) central unit, b) twin-screw extruder, c) filament cutting machine

Figure 2.3 - Modular twin-screw extruder system by Scamex, installed in the central services at UCA

Raw PLA were dried overnight at 50 °C to remove any residual moisture. Then, this material was processed in the extruder system. A continuous filament with a diameter of 1.75 mm was produced due to the winder that has an optical reader that automatically adjusts the diameter of the filament. This filament was cut again in small pieces and used as recycle part in composites.

2.1.6 Nanocomposites fabrication

Blend pellets of nano-TiO₂ particles and PLA, both reprocessed and virgin, were produced with different %wt of TiO₂. After determining the quantity of each material, PLA has been introduced in the first dosimeter and the additive in the second dosimeter of twin-screw modular extruder system by Scamex (Figure 2.3). The pictures of produced pellets can be seen at Figure 2.4.



Figure 2.4 - Pellets from different composites produced for this thesis. The letter V stands for virgin polylactide, R - for polylactide debris, and A for titanium dioxide nanoparticles. The number to the right of the letter indicates the percentage of each material in the mixture

2.1.7 Fused granular fabrication of samples from nanocomposites

Specimens were printed using direct pellet extrusion technology with the Discovery 3D Granza printer from Bárcenas CNC (Spain) shown in Figure 2.5, whose printing volume is 1100x800x500mm.



Figure 2.5 - Discovery 3D Granza printer (right) and Piovan dehumidifying dryer (left)

The slicer software Simplify3D was used to prepare the print files of the specimens in a g-code format, the principles parameters used are shown in the Table 2.1. For horizontal specimens a 100 % linear infill at 0° (XY orientation) was used and for vertical specimens (XZ orientation) was used an unique contour (nomenclature according to AM standards [101]). All compositions processed with FGF were dried for 4 hours at 60°C in a Piovan (Group Piovan) dehumidifying dryer to avoid possible defects due to humidity.

Table 2.1 - 3D printing parameters

Nozzle diameter (mm)	Bead width (mm)	Layer height (mm)	Print speed horizontal specimen (mm/s)	Print speed vertical specimen (mm/s)
2	2	2	50	25

Screenshots of the Simplify3D slicer for horizontal and vertical printed samples are shown in Figure 2.6 and its result printed in FGF can be seen in Figure 2.7.

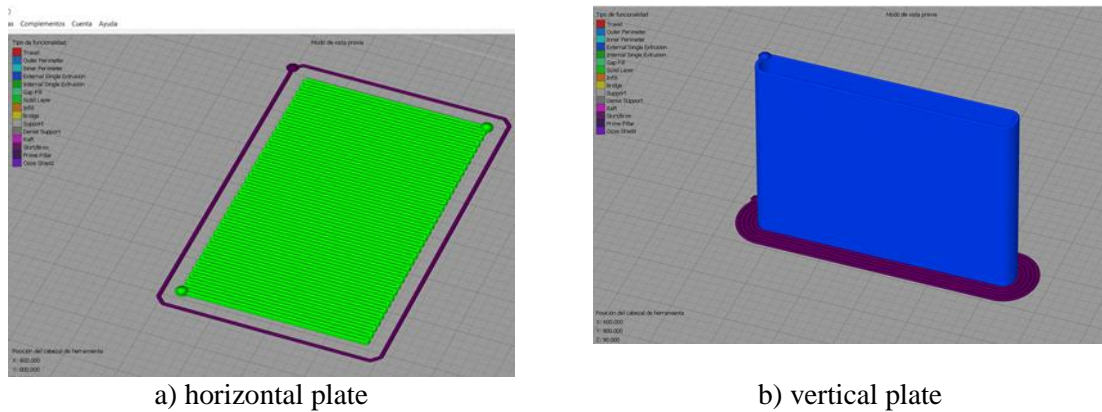


Figure 2.6 - Screenshots of the Simplify3D slicer



Figure 2.7 - Horizontal and vertical plates of size 150x90x2 mm (first two on the right, respectively), and examples of specimens for tensile test in the XY orientation and XZ orientation (last two on the left, respectively)

Temperature of extruder (considering the three heating zones of the extruder, the last one the closest to the nozzle), temperature of the bed, the printing speed for horizontal and vertical plates were constant. But multiplier, which is a parameter to control the amount of extruded material, were chosen for every mixture experimentally to receive specimens with good quality and control the bead width.

The specimens were cut from printed sheets because the bead width and dimensional accuracy made it impossible to produce them directly in FGF. At least 5 specimens type 1BA according ISO 527-2 [102] normalized tensile specimens have been milled with a LEKN(C1) 3020 CNC Router Machine Kit (Nanjing City, CHINA) shown in Figure 2.8, using a 2 mm diameter flat milling cutter with two cutting edges, 1 mm each one. The machine works to a speed 5000 rpm and advance 350 mm/min for the both horizontal and vertical printed plates. Before milling the surfaces of the plates were taped to avoid overcasting of the plate and the chips from adhering to it.

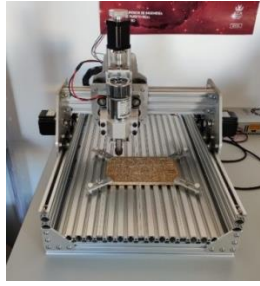


Figure 2.8 - LEKN(C1) 3020 CNC Router Machine Kit cnc machine.

2.2 Controlled degradation process

This practice is intended to define the exposure conditions for testing the resistance of plastics to oxidation or other degradation when exposed to controlled ambient conditions for extended periods of time. The effect of heat and/or humidity on any particular property will be determined by selection of the appropriate test method and specimens [103].

2.2.1 Thermal ageing according to ISO 188-2023

Accelerated thermal ageing of 3D printed specimens from PLA filament was carried out in a laboratory Selecta (Spain) oven at $50\pm 2^\circ\text{C}$ (Figure 2.9). This ageing temperature was chosen to be under the glass transition temperature (T_g) of PLA to prevent interphase transition. [104] Samples were removed at different time intervals (8, 16, 24, 48, 72, 168, 672, 1344 h) following ISO 188 [105].



Figure 2.9 - Laboratory oven Selecta (Spain) with aged samples

The simplified protocol for accelerated ageing states that service time of one month at room temperature can be simulated by an ageing time of 72 h at 50°C with thermo-oxidative degradation [106,107]. According to this protocol, Table 2.2 includes the correlation between ageing and service time for the intervals selected for this experiment. The maximum thermal ageing time in this experiment is 1344 h, corresponding to about 1.5–2.5 years of real service time.

Temperature stability was controlled during ageing at three points by electronic thermocouples Testo (Germany), with a constant temperature recording with intervals of 30 s. The points were as follows: in the laboratory air, on the surface of one of the specimens, and in the central point of the oven air without touching any surfaces.

Table 2.2 - Correlation between ageing and service time as per the simplified protocol for accelerated ageing

Ageing time at 50±2°C (h)	Approximate time (days)
0	0
8	2.5-5
16	5-10
24	10-16
48	16-24
72	24-56
168	56-112
672	224-448
1344	448-896

2.2.2 Hydrothermal ageing according to St JSC 002-2023

There is no international standard that regulates the conditions of hydrothermal ageing tests for plastic materials. After studying the most important works on the hydrothermal ageing of PLA [106,108–115], St JSC 002-2023 “Polylactide for additive manufacturing. Accelerated hydrothermal ageing test”, presented in appendix C, was offered. The test was conducted in a climatic chamber shown in Figure 2.10 (Dycometal 21CK-1000, Spain), at a temperature of 50±2 °C and humidity of 70±5 %. Ageing for 8 and 16 h corresponds to a short use period in real life, i.e., only 1-2 weeks, so these time intervals are not included in the hydrothermal ageing experiment. Specimens were aged 24, 48, 72, 168, 672, and 1344 h.



Figure 2.10 - Climatic chamber used in this doctoral thesis thanks to the collaboration of ‘Catedra Acerinox-UCA’

2.3 Characterization

2.3.1 Conditioning

After 3D printing, test specimens were conditioned before testing them for more than 88 h at 23 ± 1 °C air temperature and 50 ± 5 % relative humidity, according to ISO 291 [116]. All experiments were conducted in a standard atmosphere.

2.3.2 Dimensional measurements

Thickness, width and length of each specimen were measured with a micrometer, as per ISO 16012 – Plastics - Determination of linear dimensions of test specimens [117] with ± 0.02 mm accuracy.

2.3.3 Structural analysis

To provide detailed information on polymer structure scanning electron microscopy (SEM) will reveal the depth to which serious degradation has penetrated. During the test the electron beam interacts with the specimen and produce information about surface.

The fractured surface was characterized via SEM (Figure 2.11). SEM measurements were carried out at FEI Nova NanoSEM 450 (Waltham, MA, USA) microscope equipped with a field-emission gun for high-resolution analyses. In order to protect the samples during the analysis, they were covered by a 10 nm layer of gold using a Balzers SCD 004 Sputter Coater (Balzers, Liechtenstein). SEM images were analyzed and processed using ImageJ software.

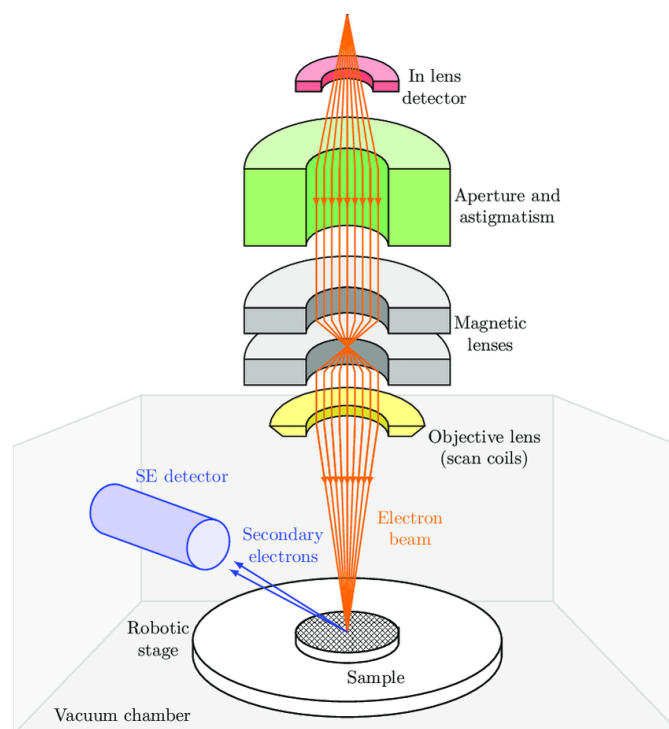
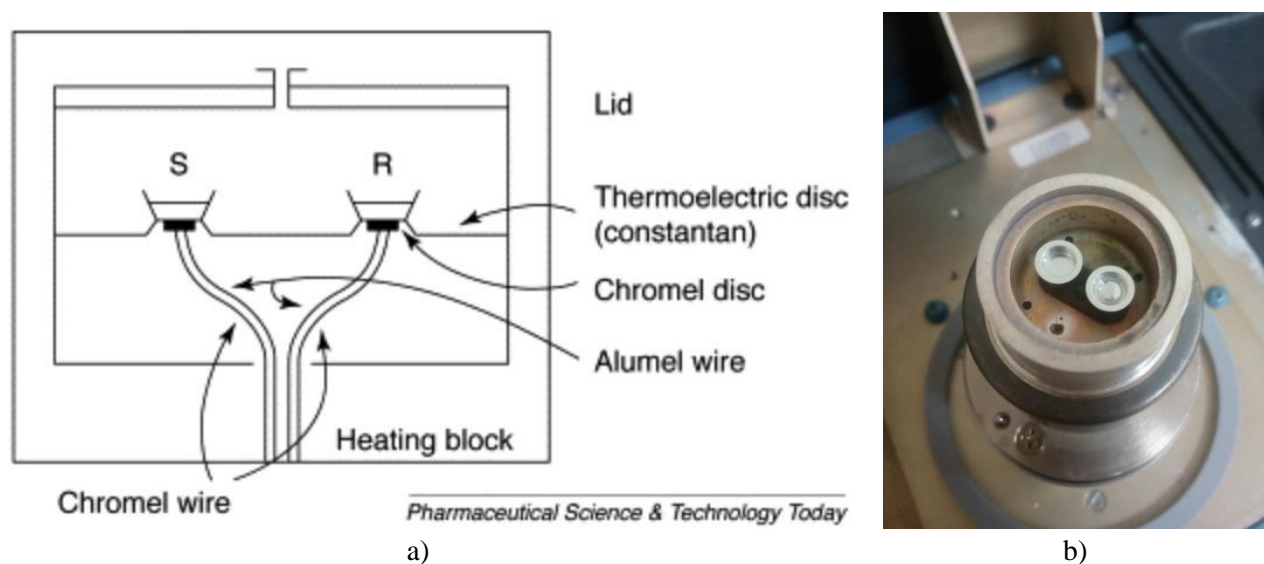


Figure 2.11 - Internal structure of SEM. Scale of elements is not respected [118]

2.3.4 Differential scanning calorimetry

Differential scanning calorimetry (DSC) measures some thermal properties of the material like glass transition temperature, melting temperature, crystallization temperature, heat capacity, etc. This technique in which the difference between the rate of flow of heat into a specimen crucible containing the specimen and that into a reference crucible (Figure 2.12) is derived as a function of temperature and/or time while the specimen and reference are subjected to the same controlled temperature program in an inert atmosphere using a symmetrical measurement system [119].



a) Scheme of differential scanning calorimeter [120]; b) Reference and examined samples in differential scanning calorimeter

Figure 2.12 - Differential scanning calorimetry

A Q20 differential scanning calorimeter from TA Instruments Inc. (New Castle, DE, USA) was used to measure the thermal properties of potential PLA waste following ISO 11357-1 [119]. Measurements were carried out using nitrogen purge gas of purity 99.99 % to avoid oxidative or hydrolytic degradation while testing at the 10 mL/min flow rate with heating run at a rate of 10 °C/min and cooled at 2 °C/min under a nitrogen flow of 10 mL/min. Specimens were cut with a razor blade from 3D printed aged pieces, from 5 mg to 10 mg for measurements. Moreover, they were weighed together with aluminum crucibles with an oxidized surface and their lids with a resolution of ± 0.01 mg and an accuracy of ± 0.1 mg. Data were taken during the first heating cycle to evaluate the properties of especially pre-conditioned (aged for 8, 16, 24, 48, 72, 168, 672, 1334 h) without erasing the material's previous history for aged samples. And the results were taken from the second heating cycle for samples from virgin and recycled PLA. The thermal properties of the specimens, i.e., the glass transition temperature (T_g), crystalline melting point (T_m), and crystallization point (T_c), were determined. The enthalpy of crystallization and fusion (ΔH_c and ΔH_m , respectively) were counted using TA Universal Analysis software

from TA Instruments Inc. (New Castle, DE, USA). All data are reported to the nearest 1°C according to ISO 11357-1.

2.3.5 Thermogravimetric analysis

Additionally, thermogravimetric analysis (TGA) was done to identify the temperature at which chemical degradation of the material commences. It indicates the thermal stability of material [121]. With TGA the mass of the sample is recorded continuously while the temperature is increased at a constant rate and in appropriate environment. Weight losses occur when volatiles absorbed by the polymer are driven off. The scheme of thermogravimetric analyser is presented in Figure 2.13.

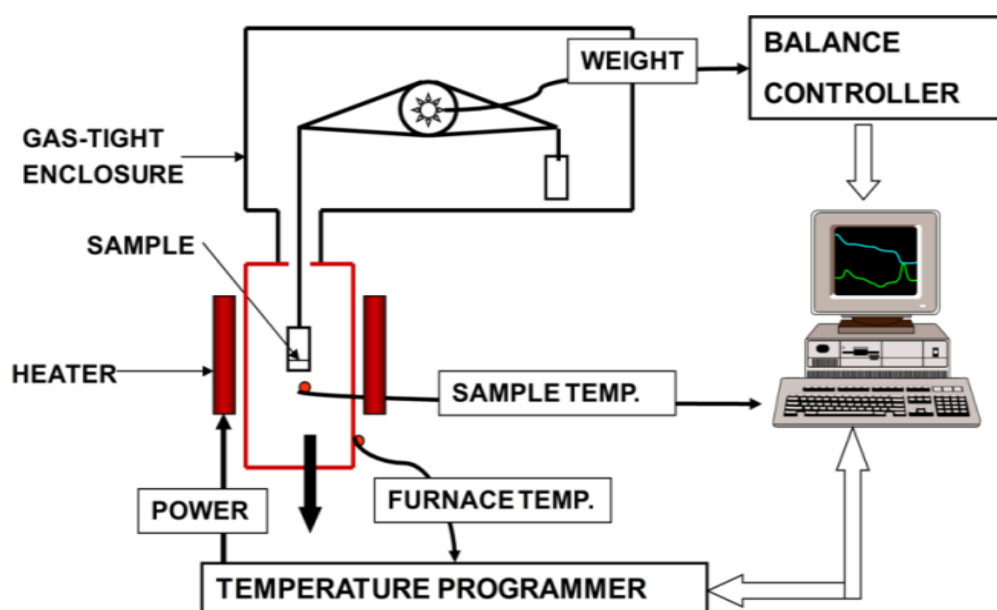


Figure 2.13 - Schematic representation of components of thermogravimetric analysis [122]

TGA was carried out in a Q50 (T&A Instruments, USA). Approximately 15 mg of polymer were heated from 30 to 430°C at 10 °C/min, under N₂ flow at 10 mL/min. The temperature of 5 % wt. mass loss ($T_{\text{loss}5\%}$) and initial and final degradation temperatures (T_i and T_f) were determined from the received TGA curves and according to ISO11358-1 [123].

2.3.6 Determination of mechanical properties

Tensile testing is based on stretching the specimen along its main longitudinal axis at a constant speed until failure or until the voltage (load) or deformation (elongation) reaches a certain, previously set value. When tested using this method, the load which the specimen withstands and elongation are measured [124]. From these, a stress-strain curve is drawn, which mechanical properties such as Young's modulus, elastic limit, ultimate strength and ductility are calculated.

The tensile test was performed using a universal testing machine, the Shimadzu AG-X series (Kyoto, Japan) presented in Figure 2.14. Five dog-bone 3D-printed specimens from every PLA blend were tested. The width and thickness were measured using a digital micrometre, with an accuracy of 0.01 mm at multiple points [124]. The averaged mean of three cross-section measurements was taken as the measurement result. Speed was at a constant rate of 1 mm/min for samples type 1BA, and 2 mm/min for samples type A2 according to ISO 527-2 [102] in a standard atmosphere (the temperature was $23\pm 2^{\circ}\text{C}$ and the relative humidity $50\pm 5\%$). During this procedure, both the load sustained by the specimens and elongation were measured. Likewise, an extensometer with a nominal length of 50 mm was used for aged samples and 20 mm for PLA blends, but many specimens broke outside of the gage length due to assumed stress concentrations in the regions changing geometry as was also seen by other authors [99]. Data were included in this study for specimens that broke out of the gage length but displayed a distinct maximum stress before failure. The results of the tensile test for the 3D-printed materials were transmitted using Trapezium software version 1.5.1. Tensile strength and ductility were also calculated [124].



Figure 2.14 - Tensile testing machine

Young's modulus was calculated as the slope between 0.05 % and 0.25 % strain on a stress-strain plot. Yield strength was obtained as the stress value where an increase in strain does not increase stress (maximum value on the Y-axis). Elongation at break was obtained as the strain value in the rupture point (maximum value on the X-axis). Results were averaged and standard deviations were presented as error bars. The repeatability of the individual measurements is calculated as the difference between the maximum and minimum values among five samples.

2.4 Standardization of nanocomposite from recycled polymer

To create a standard of organization the following methods will be used:

- 1 Unification.
- 2 Encoding
- 3 Ordering of objects of standardization.
- 4 Advanced standardization.

To exclude the unjustified variety of products by the method of unification, the number of standardized nanocomposites will be reduced to a sufficient minimum number required for most main consumers. During the unification procedure, only the compositions of those nanocomposites that are suitable for further production or use will be selected.

To replace the long name of the resulting nanocomposite, a coding method will be used that allows several characters to replace the name of the standardization object.

The ordering of the standardization object will be carried out by optimizing the quality indicators of standardization objects. As a result of optimizing the quality indicators of the standardized objects, the best (optimal) values of the quality parameters from the possible ones will be selected.

Because the creation of an organization standard for improved recycled polylactide is in the area of advanced standards development, during the work on the standard the advanced standardization method will be used. Therefore, the standard will establish higher norms and requirements for the object of standardization compared to the level already achieved in practice, which will be optimal in the future.

Conclusions to chapter

Mechanical recycling of plastic waste is planned to be carried out using a single-screw and twin-screw extruders. Samples for mechanical testing will be printed using FFF and FGF methods.

Morphological, thermal and mechanical properties of the materials will be determined at each stage of the study using scanning electron microscopy, differential scanning calorimetry, thermogravimetric analysis and tensile testing of samples.

3 EFFECT OF THERMAL AND HYDROTHERMAL ACCELERATED AGEING ON 3D PRINTED POLYLACTIDE

3.1 Materials used during the experiment

Commercially available PLA filament of 1.75 mm width was purchased from BQ (Madrid, Spain) with the printing temperature range of 200/220 °C, optimum printing temperature of 205 °C, bending temperature under load of 56 °C (ISO 75/2B), melting temperature of 145/160 °C (ASTM D3418), and glass transition temperature of 56/64 °C (ASTM D3418). This filament was used to 3D print samples using the methodology described in section 3.1.1-3.1.3. A total of 90 regular dog-bone (type A2) specimens for thermal and hydrothermal ageing were printed in batches of 5 considering the ISO 20753 standard [97] using a Witbox 2 printer (BQ) with optimum operating temperatures of 200 °C and a printing glass table without heater. Five specimens are used for every ageing cycle, and one extra specimen for contingency. All specimens were printed indoors in a temperature-controlled environment (23 ± 2 °C and 50 ± 5 % R.H., as defined in Ref. [100]) with 100 % infill, horizontal pattern orientation 0/90 (i.e., alternating layers with orientations at 0° and 90°), and layer height 0.2 mm.

3.2 Results of experiment

3.2.1 Dimensional stability

Table 3.1 and Figure 3.1 shows the results of three perpendicular dimensions of the specimens before and after thermal and hydrothermal ageing.

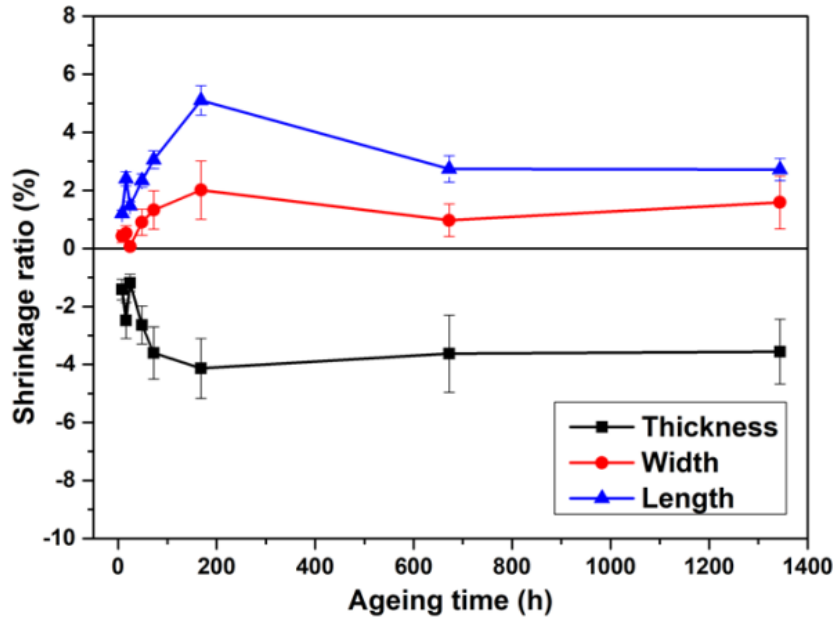
Table 3.1 - Dimensional changes (shrinkage ratios) versus ageing time

	Ageing time	Thickness			Width			Length		
		Before	After	Shrinkage ratio	Before	After	Shrinkage ratio	Before	After	Shrinkage ratio
	h	mm	mm	%	mm	mm	%	mm	mm	%
Thermal ageing	8	3.852	3.907	-1.41	10.162	10.119	0.42	149.800	148.000	1.20
	16	3.853	3.949	-2.48	10.194	10.141	0.52	150.000	146.400	2.40
	24	3.883	3.929	-1.18	10.070	10.063	0.07	149.600	147.400	1.47
	48	3.835	3.936	-2.64	10.209	10.117	0.90	149.800	146.300	2.34
	72	3.825	3.963	-3.61	10.227	10.092	1.32	150.300	145.700	3.06
	168	3.806	3.963	-4.14	10.292	10.085	2.01	153.000	145.200	5.10
	672	3.880	4.021	-3.63	10,052	9.955	0.97	150.170	145.906	2.74
	1344	3.973	4.081	-3,56	10,101	9.948	1.59	150.067	145.989	2.72
Hydrothermal ageing	24	3.836	4.002	-4.33	10.186	10.002	1.81	150.100	145.175	3.28
	48	3.836	3,997	-4.20	10.186	9.991	1.91	150.100	145.117	3.32
	72	3.836	4.000	-4.28	10.186	10.015	1.68	150.100	144.773	3.55
	168	3.836	4.015	-4.67	10.186	10.061	1.23	150.100	144.500	3.73
	672	3.836	4.044	-5.42	10.186	9.950	2.32	150.100	142.533	5.92
	1344	3.836	4.128	-7.61	10.186	9.873	3.07	150.100	139.883	6.81

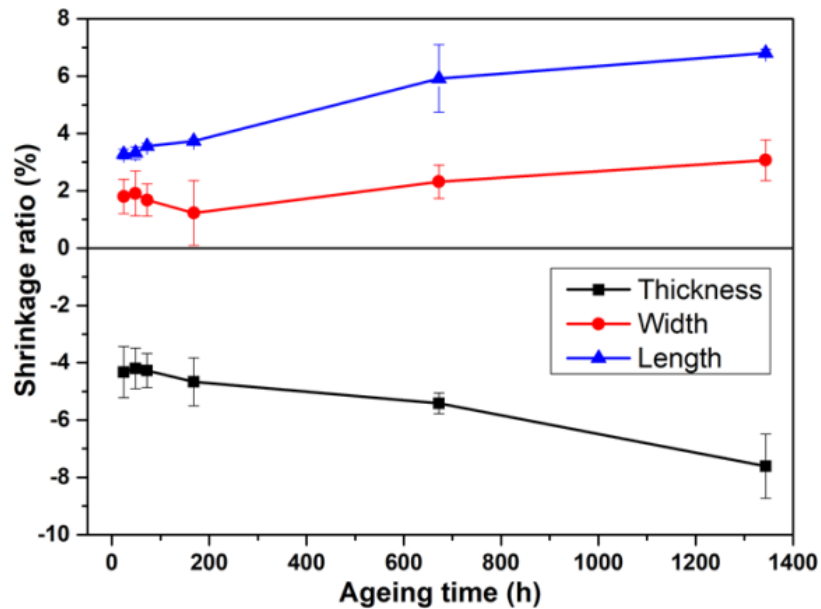
The shrinkage ratio of length is calculated using the following equation:

$$R = \frac{100(L_0 - L_a)}{L_0}, \quad (1)$$

where R is the shrinkage ratio, L_0 is the whole length of the specimen before ageing, and L_a is the entire length of the aged specimens [125]. To calculate the shrinkage ratio of width and thickness, equation (1) is used too.



a)



b)

Figure 3.1 - Shrinkage ratios in width, length, and thickness directions versus ageing time for thermal ageing (a) and hydrothermal (b) ageing. Error bars are inserted considering standard deviations for six calculated shrinkage ratios

Results of dimensional measurements show that the mobility of the PLA molecules occurs during ageing. Refs. [125] and [126] mentioned this molecular .

According to the data in Table 3.1 and Figure 3.1 the shrinkage ratio in width direction for most thermal ageing periods, except 72 and 168 h, doesn't exceed 1 %. On the other hand, the shrinkage ratio in width direction for hydrothermally aged specimens until 168 h stays approximately the same between 1-2 % and, after 672 h, grows constantly and reaches 3.14 % after 1344 h of hydrothermal treatment. Water and temperature significantly influenced PLA molecular mobility is higher.

The shrinkage ratios in the length and thickness directions, as shown in Table 3.1 and Figure 3.1, have approximately the same values with opposite signs after each ageing period. Also, it must be mentioned that the values of shrinkage ratios in the length and thickness directions of specimens influenced only by temperature are lower than the ones treated by temperature and humidity. In addition, there is no constant tendency in numeral values of shrinkage ratios for thermal aged-PLA. But for hydrothermal samples, there is a rising trend. Finally, it can be supposed that printing the skirt in FFF doesn't let the width change. Even though shrinkage during ageing is not substantial, this fact must be considered during designing the goods manufactured through FFF, where high accuracy is needed.

Accelerated ageing for 8 h of PLA specimens, which simulates using 3D printed PLA goods during 2.5-5 days in real service conditions, shows that even a short period of use leads to a change in geometric dimensions. As shown in Ref. [127], the physical ageing rate is very fast initially and decreases as time increases. Thus, it can be concluded that any PLA product manufactured through FFF will change its geometric dimensions during the early days after printing. After this initial change, the sizes will stay approximately the same for 1-2 years, with a maximum shrinkage ratio of 8 % after water and temperature influences.

3.2.2 Calorimetry

Figure 3.2 shows the DSC results. The preliminary DCS results of thermally aged samples have been published in [128]. The first shift of the curves down corresponds to T_g , for unaged polymer $T_g=58$ °C. The next rising maximum is due to the crystallisation process (T_c , crystallisation temperature) in which the polymer gives off heat. Unaged PLA reaches this point at 117 °C. The third peak shows that the polymer achieves its melting point ($T_m=151$ °C for unaged PLA). Figure 3.2 shows that all curves correspond to semicrystalline PLA, showing both glass transition and melting peaks [129]. Likewise, T_g , T_c , and T_m of unaged PLA specimens are marked with a vertical thin continuous line to compare the unaged sample and each aged one easily.

As Table 3.2 summarises (third column), T_g fluctuates slightly along ageing within a range of 4 °C (between 58 and 62 °C), and it doesn't follow any constant tendency. Nevertheless, results show that the T_g of aged PLA is higher than the one declared for PLA filament by supplier $T_g=56$ °C, meaning that the aged material is somewhat stiffer.

Also, it must be pointed out that T_g affects how easily the material will be extruded, how the parts will shrink during the cooling process, and the thermostability of the printed part [130]. Considering the numeral value of T_g and its influence on the 3D printing process, the re-extrusion of the PLA used in this experiment doesn't have shrinkage problems during printing.

From Table 3.2, it can be noticed that melting temperature (T_m) fluctuates from 149 to 155 °C. T_m is rising and decreasing tendency during thermal treatment could be due to molecular rearrangements with ageing [7]. Dimensional measurements of the specimens prove the mobility of the PLA molecules before and after ageing. So, shorter polymer chains effectively reorganise themselves into more ordered crystals, hence increasing the relevance of the high-temperature melting peak [131].

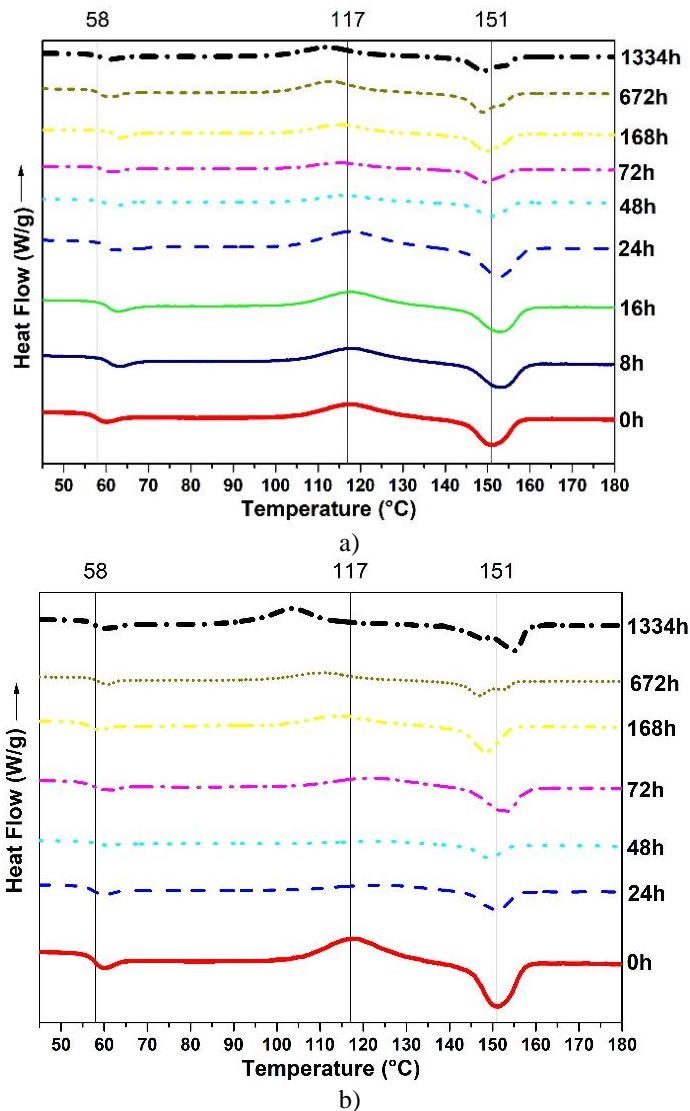


Figure 3.2 - DSC test of PLA specimens after thermal ageing (a) and hydrothermal ageing (b). The lines at 58, 117 and 151 °C correspond to T_g , T_c , and T_m of unaged PLA specimens, respectively. The graphs are shifted in the Y-axis axis to compare the peak temperatures better. Measurement error 0.0010 °C. Measurement uncertainty 0.0003 °C

DSC thermograms of thermal and hydrothermal ageing have two melting peaks after 672 and 1344 h of treatment. This can be because of the annealing during the DSC scans; some material regions recrystallise and remelt [8]. When the scan rate is low, i.e., 10°C/min, there is enough time for the thinner crystals to melt and recrystallise before a second endotherm at a higher temperature occurs [132].

The degree of crystallinity X_c was quantified according to [39] as

$$X_c = \frac{\Delta H_m - \Delta H_c}{\Delta H^*} * 100 \%, \quad (2)$$

where $\Delta H^*=93$ J/g denotes the heat of melting for an infinitely large crystal [7]. The degree of crystallinity for thermally aged specimens stays constant at about 1-3 %. But for hydrothermally aged PLA, the degree of crystallinity rises from 4.3 % after 24 h of hydrothermal influence to 8.6 % after 1344 h. It can be because linear macromolecules do not typically crystallise completely; they are semicrystalline, as previously mentioned. The restriction to crystallisation is caused by a kinetic hindrance to the full extension of the molecular chains, which, in the amorphous phase, are randomly coiled and entangled [133].

Table 3.2 - Results of thermal analysis of specimens after ageing

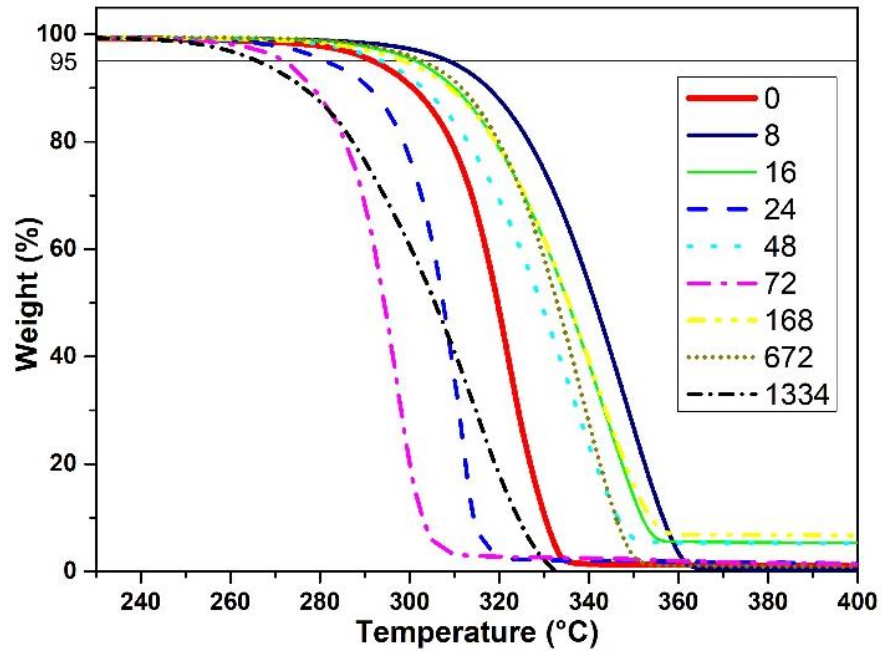
	Ageing time	T_g	T_c	ΔH_c	T_m	ΔH_m	X_c	$T_{loss5\%}$
	h	°C	°C	J/g	°C	J/g	%	°C
Unaged	0	58	118	27	151	28	1.1	292
Thermal ageing	8	61	118	27	153	28	-	309
	16	61	118	30	153	28	-	301
	24	60	118	29	153	28	-	281
	48	59	117	32	149	27	-	294
	72	60	115	32	149	29	2.2	272
	168	62	115	26	150	28	0	298
	672	59	113	29	149	29	1.1	303
	1344	59	112	27	149	28	3.2	266
Hydrothermal ageing	24	58	125	15	151	18	4.3	311
	48	59	123	11	149	20	4.3	305
	72	58	123	16	153	20	4.3	278
	168	57	115	23	149	27	4.3	287
	672	59	111	27	147	31	4.3	303
	1344	58	104	31	155	39	8.6	264

As crystallinity is an important characteristic affecting mechanical properties [134], its influence on mechanical properties will be shown in 3.2.4. So, for thermally aged PLA, T_g , T_m , and X_c do not change; for hydrothermally aged, T_g and T_m stay the same, but X_c increases.

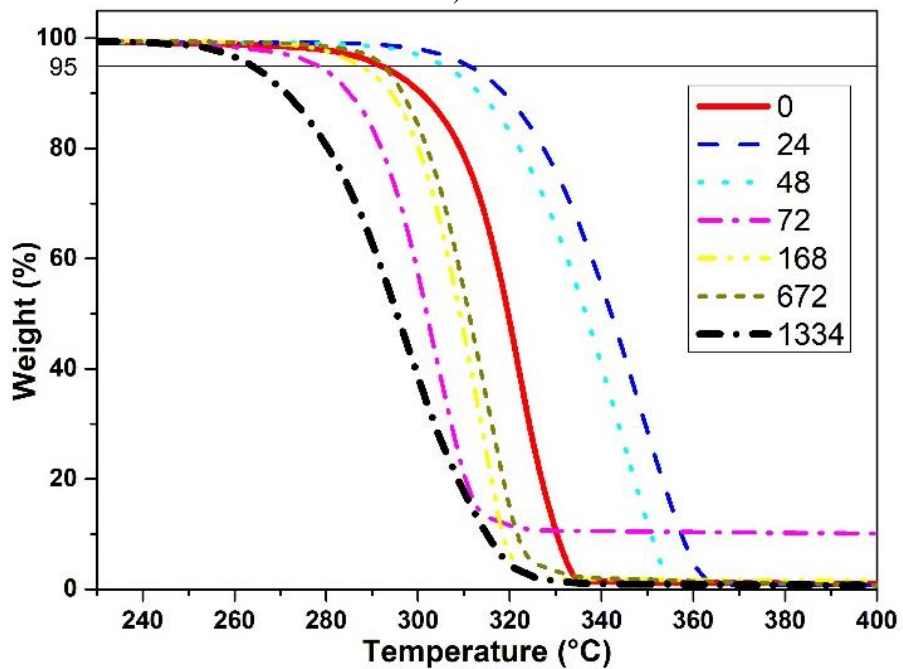
3.2.3 Thermogravimetry

The thermal decomposition properties of PLA were studied by TG from room temperature up to 430 °C in nitrogen. Figure 3.3 shows the parts of TG curves from

230 to 400 °C for all specimens. Virgin PLA is very stable, up to around 300 °C. The fact that there is very little change in mass from room temperature up to 300 °C indicates that the PLA is pure with no contaminants, is very dry with no solvent, and is very stable. The sharp drop in mass around 300 °C shows relatively complete decomposition and that the samples were pure with no contaminants [129]. Additionally, all samples show only one single degradation peak, indicating the presence of only one type of polymer (PLA).



a)



b)

Figure 3.3 - TG curves of PLA specimens after thermal (a) and hydrothermal (b) ageing. Measurement error 0.0010 °C. Measurement uncertainty 0.0003 °C

Values of $T_{\text{loss}5\%}$ indicate that the thermal stability of aged PLA generally has no constant rising or decreasing tendency. It can be conducted that the ageing process does not influence the values of $T_{\text{loss}5\%}$. So, 3D printed PLA goods during their life cycle do not have permanent thermal behaviour because of the unstable thermal nature of PLA.

3.2.4 Tensile testing

Table 3.3 and Figure 3.4 shows the results of the tensile test with the 95 % confidence intervals of the values counted by the procedure given in ISO 2602 [135]. It is discernible that tensile properties gradually increase up to 24 h of ageing then decrease to 31.126 MPa for thermal aged and to 20.890 MPa for hydrothermally aged specimens after 1344 h.

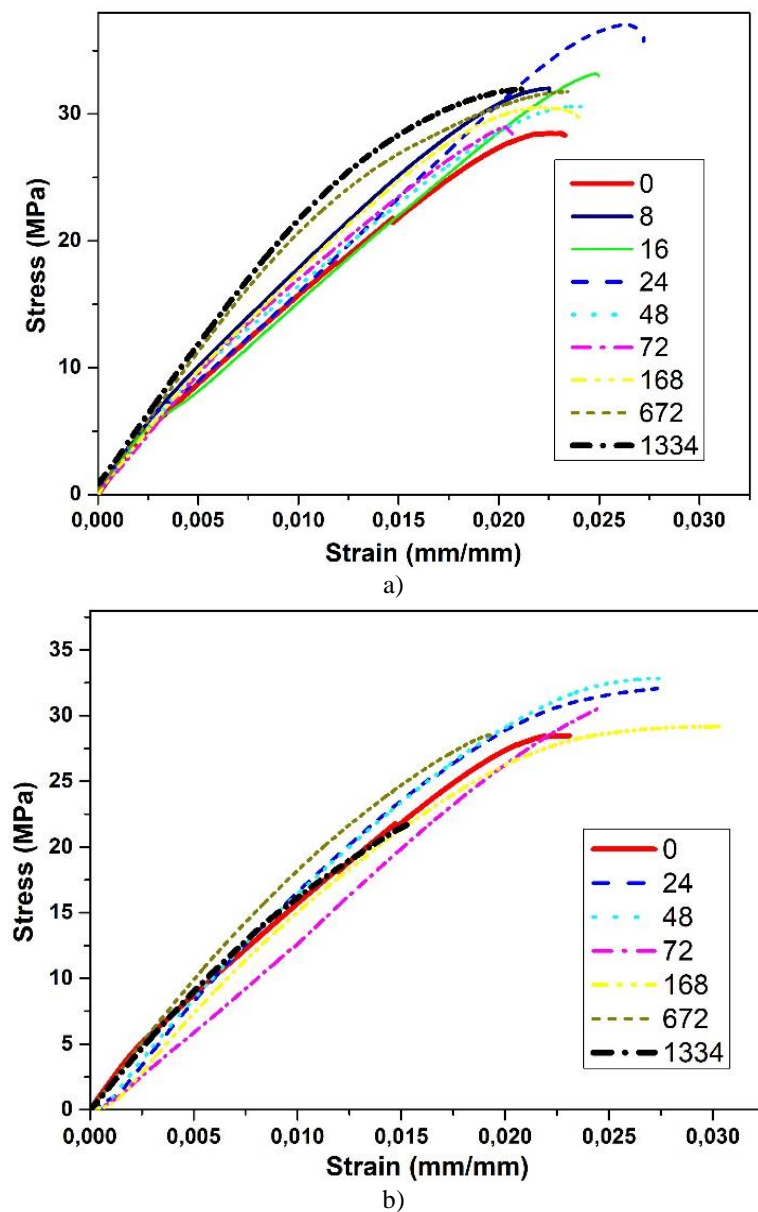


Figure 3.4 - Tensile strength after thermal (a) and hydrothermal (b) ageing

The average tensile strength for thermally aged specimens after 1344 h of ageing is about 31.126 MPa. This value is a little bit higher than the value of non-aged polymer. It can be explained that water absorption of PLA is 1-4 % and during the first 8 h the process of evaporation occurred. As water disappeared between the PLA molecules, they became closer to each other which is a reason for improving the tensile property.

Table 3.3 - Tensile properties of 3D printed thermally aged specimens

	Ageing time	Tensile Yield Strength		Young's Modulus		Elongation	
		Average	Standard deviation	Average	Standard deviation	Average	Standard deviation
	h	MPa	MPa	MPa	MPa	%	%
Virgin	0	28.746	0.607	1800.208	150.395	2.34	0.19
Thermal ageing	8	31.189	1.322	2158.489	117.927	2.19	0.14
	16	33.164	1.129	2115.412	157.063	2.39	0.16
	24	36.799	1.154	2134.546	286.843	2.53	0.21
	48	29.135	1.681	1612.385	312.078	2.49	0.22
	72	29.721	1.551	1875.389	71.578	2.28	0.21
	168	29.516	0.495	1968.879	102.064	2.05	0.23
	672	32.602	0.477	2141.455	48.957	2.06	0.46
	1344	31.126	2.851	2077.937	186.864	2.00	0.46
Hydrothermal ageing	24	33.454	1.238	1552.181	74.724	3.16	0.15
	48	32.672	2.040	1652.115	243.715	2.94	0.43
	72	32.530	1.218	1340.578	322.173	3.05	0.29
	168	29.613	1.259	1664.317	144.847	2.81	0.49
	672	29.816	3.097	1962.120	94.488	2.40	0.57
	1344	20.890	4.240	1598.108	383.587	1.74	0.19

Variations in the tensile strength after ageing processes are similar to the changes in T_g and have the same explanation as the temporary rising trend in T_m . It should be noted that after 1344 h in the climatic chamber, the tensile strength drops to 20.890 MPa. Comparing the results of thermal and tensile testing, at the crystallinity of about 1-3 %, the tensile strength remains unchanged, however, at a crystallinity of 8.6 %, the tensile stress decreases. This could be affected by the anisotropy of the crystalline part of the polymer.

Conclusions to chapter

The results of this experiment is presented in [136].

Lab-controlled ageing of PLA has been considered for the prediction of their long-term behaviour for future recycling. The degradation process under thermal and hydrothermal ageing is observed up to 1334 h (1-1.5 years of real service life cycle) from results of dimensional measurements, DSC, TG and tensile tests.

After ageing, PLA parts experience a shrinkage ratio from 1 to 8 %, depending on the printing pattern (actual material density in the measured dimension), the ageing time and the nature of ageing (thermal or hydrothermal). The shrinkage ratio for hydrothermal aged specimens is higher.

Calorimetry test shows that the T_g and T_m stay approximately the same for both types of ageing, with a maximum shift of 6 °C, that could be due to molecular rearrangements also observed by the dimensional measurements. The degree of crystallinity for thermal aged specimens stays constant at about 1-3 %, while for hydrothermal aged PLA it continuously rises up to 8.6 %.

The results of the TGA test confirm the unstable thermal nature of PLA. The TGA curves of aged samples change their shape from sharp drop curves to slopes with lower angles.

In general, the mechanical properties of PLA show stable conditions. But after 1344 h of hydrothermal treatment, when crystallinity is 8.6 %, tensile strength decreases to 20.890 MPa (33 % reduction).

In general conclusions, the PLA specimens can be recycled but the crystallinity of PLA debris must be considered to predict future mechanical properties. According to the received data, it can be assumed that PLA waste before 1-year-old can be mechanically recycled, without risk of substantial loss of properties of the virgin material. It is also worth noting that PLA waste mixture has the same thermo-mechanical properties before reaching 1-year-old, so it can be mixed together for recycling. Finally, during designing and printing the goods through FFF future dimensional changes must be considered.

The first statement for defense: Standardized process of accelerated hydrothermal ageing in standard of organization St JSC 002-2023 “Polylactide for additive manufacturing. Accelerated hydrothermal ageing test” of 3D printed polylactide samples at 50 °C and 70 % humidity for 1344 hours results in a 33 % reduction in tensile strength.

4 MANUFACTURE AND CHARACTERIZATION OF POLYLACTIDE FILAMENTS RECYCLED FROM REAL WASTE FOR 3D PRINTING

4.1 Materials used during the experiment

Commercially available PLA pellets, Smartfil®PLA3D850, from SmartMaterials 3D (Jaen, Spain) and with a 1240 kg/m³ density and printing temperature of 210 ± 10 °C [137] were used as primary PLA. Filament for FFF were produced in single-screw extruder as described in section 2.1.3. Four blends were produced from virgin and recycled PLA. Blend of compositions and sample codes are presented in Table 4.1.

Table 4.1 - Blend of compositions and sample codes

Sample Code	Weight Ratio (%)	
	Virgin PLA	Recycled PLA
V100R0	100	0
V75R25	75	25
V50R50	50	50
V25R75	25	75

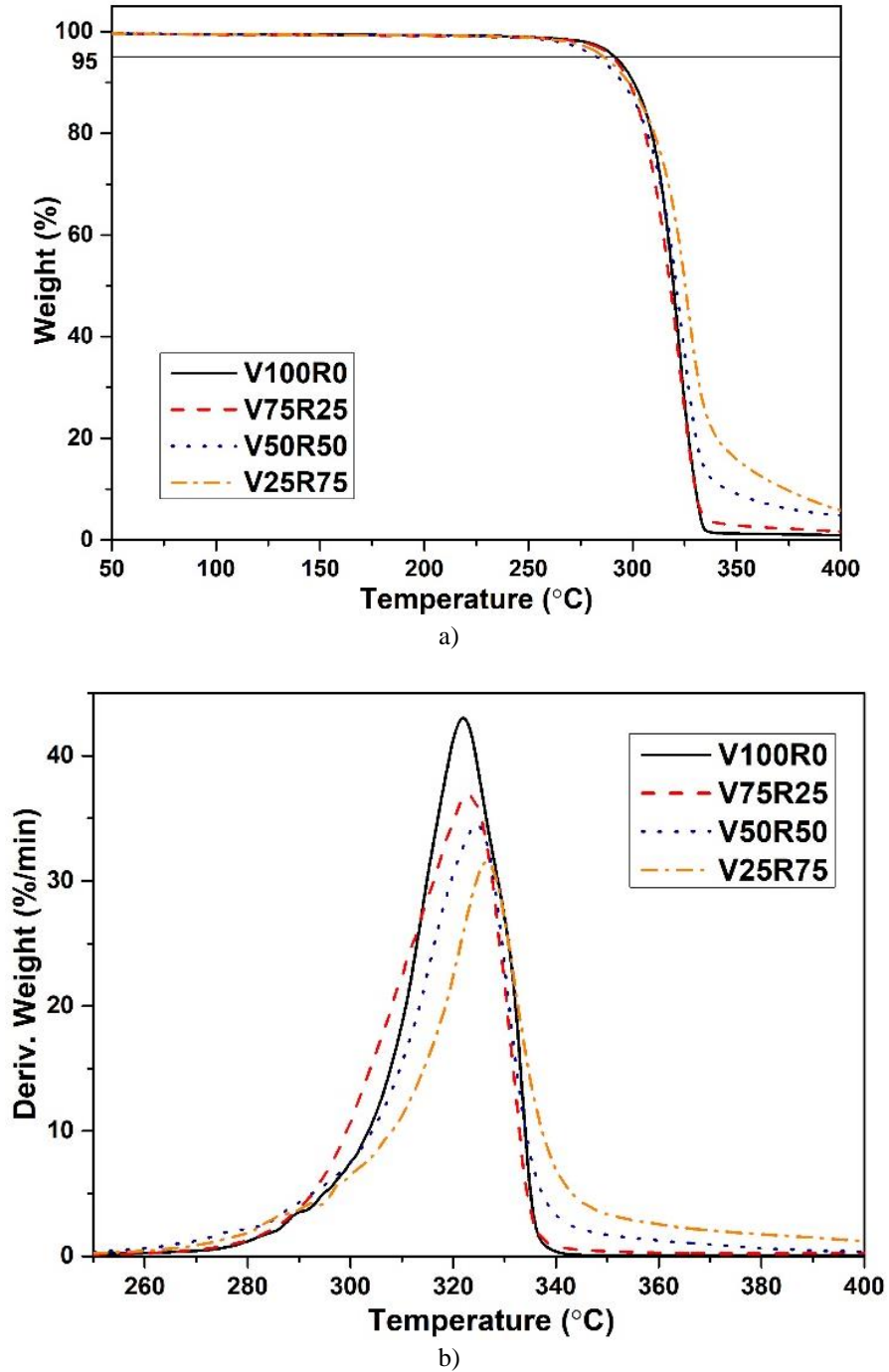
The temperature of the mixing zone in the extruder was different for various filaments. The temperature of the mixing zone in the extruder was 225 °C to produce V100R0 and V75R25 filaments, and it was reduced to 205 °C to produce V50R50 and V25R75 filaments. The temperature was changed to process V50R50 and V25R75 blends better. During filament manufacturing, the produced filament had high fluidity to form a filament with a constant diameter. The temperature was reduced as regards the greater recycled PLA content due to the chain scission in post-consumer polymer structures. The Noztek extrudes to a speed of 40 rpm. Likewise, a fan was placed near the extrusion nozzle to rapidly cool the material when it came out of the nozzle. This was turned on to ensure that the filament diameter remained as close as possible to the desired diameter of 1.75 mm. The produced filament showed a constant diameter, and its surface finish was comparable to the virgin PLA filament. About 30 m of filament was produced from 0.1 kg of the PLA blends, with an average diameter of 1.7 mm.

4.2 Results of experiment

4.2.1 Thermogravimetric analysis

The averaged thermograms, depicting the evolution of the weight versus the temperature of the 3D-printed specimens, are shown in Figure 4.1a. All the samples had a curve shape with single-stage mass reduction. In addition, V100R0 sharply dropped in mass at the end of the graph (320–350 °C section), unlike the recycled PLA blends. As the percentage of PLA waste increased, the slope of this part of the graph became more gradual. The reason could be the presence of dust and/or contaminants that could occasionally be mixed in the blends during the filament

preparation process [129]. Another reason could be that the PLA filament for FFF has special additives and/or fillers used by manufacturers to improve the 3D-printed parts' quality, so their degradation could influence the decomposition of the PLA blend. This degradation behaviour could, therefore, be the result of various chain end structures, which initiate different degradation reactions [138].



a) The evolution of the weight versus the temperature; b) The derivative curve

Figure 4.1 - TGA curves of the PLA blends with different waste content. Measurement error 0.0010 °C. Measurement uncertainty 0.0003 °C

Table 4.2 summarizes the TGA data analysis of the PLA blends: $T_{5\%loss}$, T_i , T_f , the difference between T_f and T_i (T_f-T_i), and the maximum temperature of polymer degradation (T_{max}) computed according to ISO 11358-1:2014 [123]. As a result, the 5 % mass of the recycled blends was reduced at a slightly lower temperature compared with V100R0; therefore, adding debris did not significantly influence the thermal stability of the PLA blends. The accurate temperature at which degradation occurs cannot be defined from the averaged thermograms' weight and temperature (Figure 4.1a). The derivative curve is, therefore, presented in Figure 4.1b.

Table 4.2 - Thermogravimetric analysis results of the samples: the temperature of the 5 % wt. mass loss ($T_{loss5\%}$), initial and final degradation temperatures and the difference between them, and the maximum temperature of polymer degradation (T_i , T_f , (T_f-T_i), T_{max} , respectively) computed according to ISO 11358-1:2014 [123] are shown. All values are given in °C.

Sample Code	$T_{5\%loss}$	T_i	T_f	T_f-T_i	T_{max}
V100R0	292	306	334	28	322
V75R25	290	304	332	28	323
V50R50	283	305	335	30	325
V25R75	286	308	340	32	327

Table 4.2 and Figure 4.1b show that the T_{max} of the PLA blends slightly increased, and the lost weight rate was reduced when the waste content increased. The reason could be the presence of polymers with different thermal histories in the structure of the PLA blends. Additionally, PLA and its blends degraded in a narrow temperature range of about 30 °C. The results of the TGA, therefore, indicated that adding PLA debris to the virgin material did not significantly impact the thermal stability of the 3D-printed sample.

4.2.2 Differential scanning calorimetry

All of the figures in Table 4.3 and Figure 4.2 present the results of the DSC test. Analysing the evolution of the thermal properties with increasing recycled content, it is observed that the T_g of the PLA blends slightly varied between 58 and 61 °C for the first heating and between 60 and 64 °C for the second heating. Likewise, the T_m fluctuated between 173 and 177 °C, which can be attributed to the melting peak of α crystals, normally observed around 180 °C [139]. In addition, as the T_m depends on the flexibility of the polymer chain, no greater mobility of the macromolecular chain could be supposed [39].

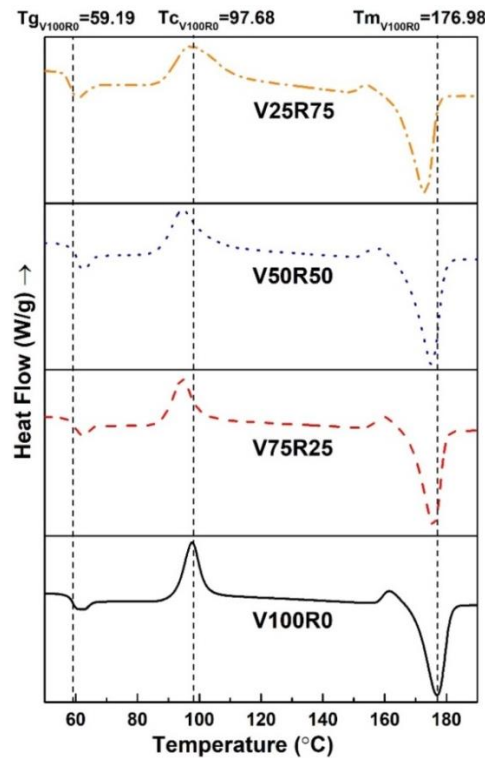
Regarding the measured enthalpies, reductions were observed in both the ΔH_c and ΔH_m with increasing recycled content. However, the ΔH_c was not revealed during the second heating because the cooling rate for PLA 3D-printed specimens at 2 °C/min was too slow. The magnitude of the crystallisation exotherm decreased when the sample was more slowly cooled, and it vanished at scan rates equal to or lower

than 10 °C/min [132]. The cooling of the 3D-printed specimens at an ambient temperature had, therefore, slow crystallisation kinetics.

Table 4.3 - Results of DSC tests: glass transition, crystallisation, and melting temperatures (T_g , T_c , and T_m , respectively) are shown, as well as the enthalpy of crystallisation and fusion (ΔH_c and ΔH_m) and the calculated degree of crystallinity (X_c). Measurement error 0.0010 °C. Measurement uncertainty 0.0003 °C

Sample Code	First Heating					Second Heating			X_c
	T_g	T_c	ΔH_c	T_m	ΔH_m	T_g	T_m	ΔH_m	
	°C	°C	J/g	°C	J/g	°C	°C	J/g	%
V100R0	59.19	97.68	45.41	176.98	57.24	64.20	177.60	50.86	48
V75R25	59.84	94.45	37.34	175.80	50.25	63.20	173.50	49.91	47
V50R50	60.71	94.63	27.38	175.01	36.21	60.98	176.82	38.24	36
V25R75	58.43	97.87	24.85	173.25	28.51	60.12	174.31	31.62	30

The V25R75 and V50R50 DSC thermograms in Figure 4.2b, after the second heating, had two melting peaks. A double melting peak is a common phenomenon for polymers such as poly (ethylene terephthalate), isotactic polystyrene, poly (ether ether ketone), and poly (ether imide). The reason could be the presence of two different crystal or morphological structures in the initial sample, but it is generally the result of annealing during the DSC scans whereby crystals of a low perfection melt have time to recrystallise a few degrees above and to remelt [132]. When the scan rate is low, i.e., 10 °C/min, there is enough time for the thinner crystals to melt and recrystallise before giving a second endotherm at a higher temperature [132].



a)

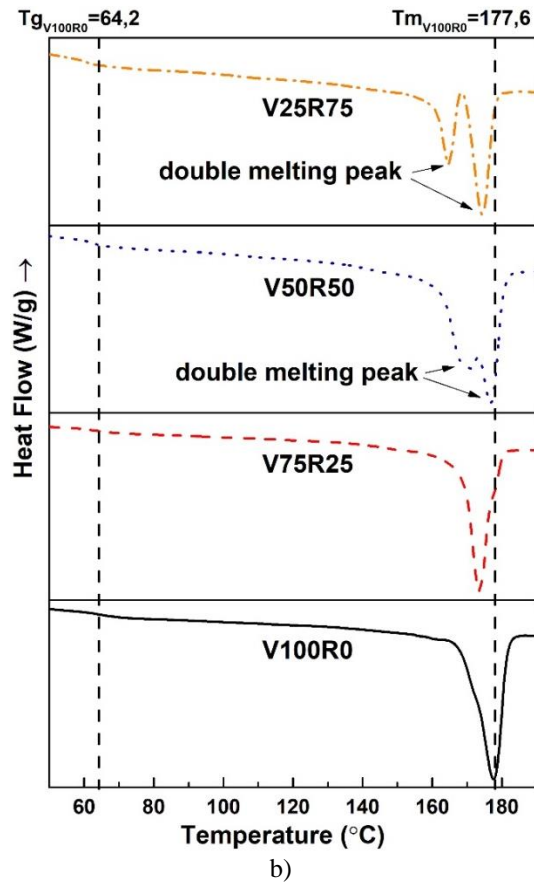


Figure 4.2 - DSC curves of the PLA blends with various waste content at first heating (a) and second heating (b) after a 2 °C/min cooling step. Measurement error 0.0010 °C. Measurement uncertainty 0.0003 °C

Degree of crystallinity, X_c , was defined according to [131,140–142] as:

$$X_c = \frac{\Delta H_m}{\Delta H^*} * 100 \%, \quad (3)$$

Table 4.3 shows that the degree of crystallinity was reduced from 48 % for neat PLA 3D-printed specimens to 30 % for specimens with 75 % of waste. These values had a linear tendency, with a regression of $R^2 = 0.92$, thus reducing the crystallinity by 0.26 % per percentage of the recycled PLA added. As the crystallisation process depends on the molecular weight of PLA [143–147], the PLA waste used in this experiment had low crystallisation kinetics.

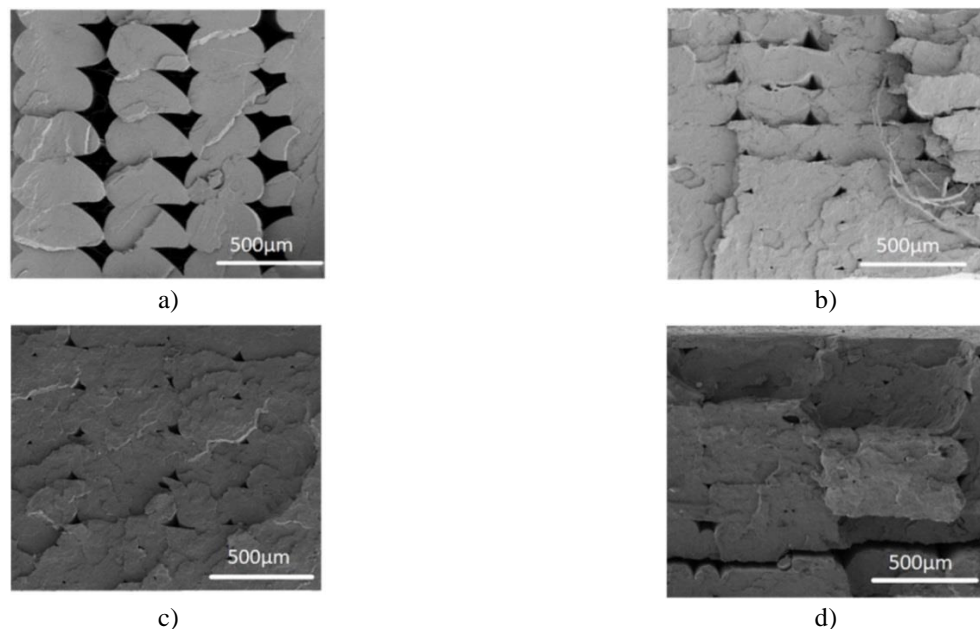
It is worth stressing that T_m , T_c , and T_g of V25R75 were almost the same for the pure PLA specimens. However, the V25R75 PLA blend had a more amorphous nature because the crystallisation exotherm and melting endotherm had identical energy content (the same area). The fracture mechanism and the behaviour of the 3D-printed specimens were, therefore, influenced during the tensile test. Nevertheless, the DSC curves of the PLA blends had several degradation peaks, thus confirming

the presence of additives in the PLA filament that the manufacturers use to improve the PLA's quality.

Despite the fact that the filament from 100 % of PLA waste was not suitable for 3D printing, the DSC results show that the T_g and T_m are 59.36 °C and 174.99 °C after the second heating, respectively. These characteristics are in the same numerical range as the T_g and T_m of V100R0, V75R25, V50R50, and V25R75. Decreasing tendency for both the ΔH_c and ΔH_m is preserved. Taking into account that PLA degrades during thermal processing, rapidly reducing the molecular weight [148], it can be predicted that the T_g , T_m , ΔH_c , and ΔH_m of the 3D-printed samples from 100 % waste could be lower.

4.2.3 Scanning electron microscopy

The fracture surfaces of the V100R0, V75R25, V50R50, and V25R75 PLA blend specimens were studied in the post-tensile test condition through SEM to characterize the fracture surface. The SEM images of the samples are shown in Figures 4.3 and 4.4 shows that the fracture surface (the cross-section view) significantly changed from one sample to another. First, the 3D-printed beads were visible in the pure PLA and were gradually softened as the recycled content increased, thus showing the V75R25 as a more continuous matter. Second, the roughness also changed: V100R0 depicted a brittle fracture crack with clean and sudden surfaces, while in the remaining samples, there was a rougher surface with features of a more ductile rupture where the material underwent slight plastic deformation.



a) V100R0; b) V75R25; c) V50R50; and d) V25R75

Figure 4.3 - SEM secondary electron micrographs of the fracture surface of the PLA blends. Scale bar: 500 µm

Figure 4.4 presents the micrographs acquired at a higher magnification to analyse and determine structural changes in the blends. All of the micrographs showed materials with similar characteristics: a porous matrix with homogeneous SEM secondary electron contrasts, which means that the PLA blends were not exposed to any other material content when preparing the FFF filaments, and some strands of fibres protruded from inside of some of the holes. The strands seemed to be greater when the recycled content increased. The holes between these fibres and their surrounding matrix are shown. The micro-pores' density, which was measured from high magnification SEM images such as those in Figure 5.4, was gradually reduced from $6.4 \cdot 10^9 \text{ cm}^{-2}$ in V75R25 to $2.5 \cdot 10^9 \text{ cm}^{-2}$ in V25R75.

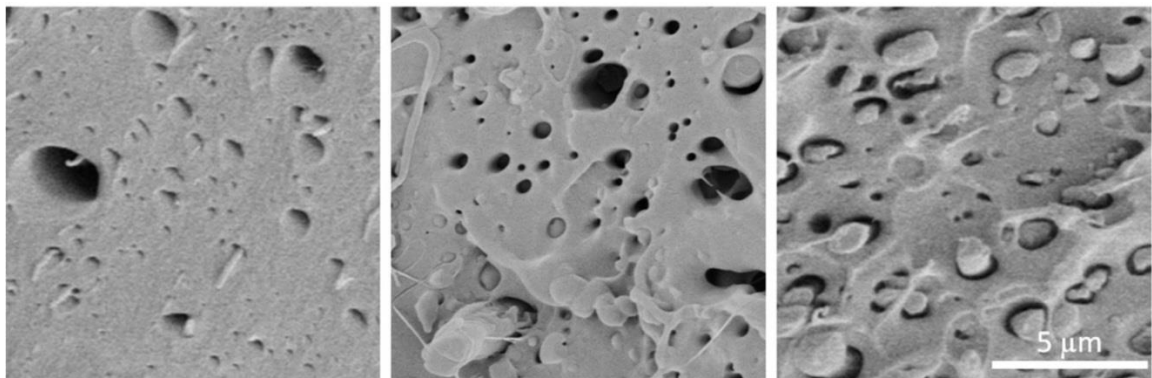


Figure 4.4 - SEM images from $12 \times 12 \mu\text{m}$ fracture regions of samples V75R25 (left), V50R50 (middle), and V25R75 (right)

4.2.4 Mechanical properties

Figure 4.5 shows the results of the tensile tests. The maximum strength values of all of the samples were within 95 % confidence intervals of the values counted, according to ISO 2602 [135]. The tensile strength increased with the increasing percentage of recycled material, from $44.2 \pm 2.18 \text{ MPa}$ for pure PLA to $52.61 \pm 2.28 \text{ MPa}$ for 75 % of recycled PLA loading.

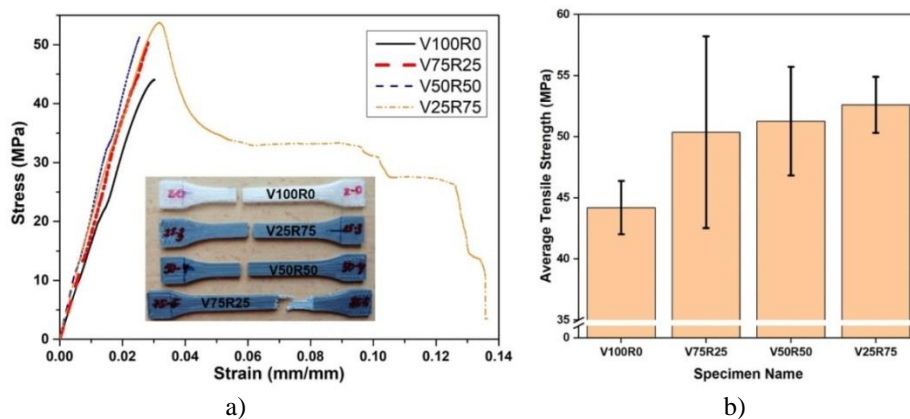


Figure 4.5 - a) Tensile stress–strain curves of the PLA blends. The inset picture shows the samples after the tensile test. b) Resultant tensile strengths

Figure 4.5a shows the tensile stress–strain graphs of the 3D-printed specimens from the PLA blends with different levels of PLA waste. Only one of the five specimens per blend, which represented the overall behaviour, is shown here for comparison. According to ISO 527 [124], the curves of V100R0, V75R25, and V50R50 corresponded to brittle materials with no yield point. Samples from the V25R75 PLA blend showed a much more ductile behaviour, with a ductility higher than 13 % (measured as the percentage of elongation), with 3 % being the average value for the other three PLA blends. Moreover, the inset in Figure 4.5a shows that the specimens from the PLA blends without waste and with 25 and 50 % of post-consumer polymer experienced a brittle fracture. In these cases, the neck was not formed, so there was neither fluidity nor hardening of the material.

The mechanical properties of polylactides beyond the elastic region are dependent on the amount and type of crystalline regions developed during processing [139]. In addition, a greater degree of crystallisation in semicrystalline thermoplastics means a lower content of the free volume, and the stiffness generally increases [139]. The DSC test revealed that the V25R75 PLA blend was more amorphous than the other mixtures. Hence, this could be the reason for the strong increase in ductility. Additionally, the slight reduction in the T_g when the PLA recycled content increased could also influence this fact.

The rising trend of tensile strength with increasing recycled content can be explained by the micrographs of the SEM depicted in Figure 4.3. In Figure 4.3a, bigger voids between the 3D-printed layers of the V100R0 sample are clearly seen than they are for V25R75, V50R50, and V75R25. Therefore, the higher value of tensile strength could be due to better inter-layer bonding for the samples with the recycled PLA. It is a well-known fact that the melt flow index increases for recycled PLA [74,140], which means that recycled PLA filament tends to flow better. Therefore, it can be supposed that the tensile strength continues to increase with a larger content of waste because the number and size of the voids decrease.

Conclusions to chapter

The results of this experiment is presented in [149].

In this study, we evaluated the recyclability of PLA FFF-printed parts. Hence, FFF filaments from recycled PLA feedstock from real waste mixed with virgin PLA pellets in three different proportions (25 %, 50 %, and 75 %) were produced with a constant cross-section and good flowability.

Based on the results of the thermal, morphological, and mechanical tests of 3D-printed specimens, the following conclusions have been drawn:

- The crystallinity degree dropped when the percentage of post-consumer PLA increased from 48 % in V100R0 to 30 % in V25R75. The reason could be the fact that the molecular chains of the secondary PLA were too short to organize the crystals;

- SEM micrographs of the fracture surface showed that virgin PLA specimens were more brittle and less dense than recycled PLA blends, thus significantly reducing both the millimetre- and micrometre-sized holes;
- The mechanical test showed that 3D printing with recycled PLA was a viable option; the tensile strength increased with the recycled content by 19 % compared with the PLA samples.

It must be mentioned that all three blends showed good FFF processability, and there was not any clogging during printing. It is worth stressing that there was a detriment in the processability during the production of the filaments obtained from 100 % recycled sources. Another problem during the conduction of this experiment was that the filament from the blend with the 75 % content of PLA waste was brittle, although its printed samples had the highest tensile strength. However, this study indicates that the mechanical properties of the reprocessed parts and their basic association are better than those made up of virgin material. Further studies should, therefore, focus on solving the filament embrittlement problem by finding suitable additives or proposing a different AM method, such as fused granulated fabrication, where the material is applied directly in the form of granules.

The second statement for defense: Increasing the proportion of secondary polylactide from 0 to 75 % in a mixture with pure polylactide increases the tensile strength of FFF printed samples from 44.20 ± 2.18 MPa to 52.61 ± 2.28 MPa.

5 IMPROVING THE THERMAL AND MECHANICAL QUALITY INDICATORS OF RECYCLED POLYLACTIC ACID USING NANO ADDITIVES

5.1 Materials used during the experiment

Six mixtures from neat PLA pellets with or without adding rPLA and/or nanoparticles of titanium dioxide were produced for investigation and comparison. Proportions of PLA and rPLA pellets and nanoTiO₂ are presented in Table 5.1. The codes of the composites consist of letters and numbers. Letter V stands for virgin PLA, R for one-time reprocessed PLA, A for additives, which in this study titanium dioxide nanoparticles. The number to the left of the letter indicates the percentage of each material in the mixture.

Table 5.1 - Sample Name and Its Composition

Sample code	Weight ratio (%)		
	Virgin PLA	Reprocessed PLA	Titanium dioxide
V100	100	0	0
V97A3	97	0	3
V93A7	93	0	7
V25R75	25	75	0
V22R75A3	22	75	3
V18R75A7	18	75	7

PLA granules named NatureWorks 3D850, purchased from NatureWorks LLC (Plymouth, Minnesota, USA) were used as virgin PLA, with relative viscosity 4.0, peak melt temperature 165-180 °C, 55-60 °C glass transition temperature, as reported in the technical data and security sheet [150]. Additive nanopowder of titanium (IV) oxide with particles size of approximately 10-20 nm was purchased from ALDRICH Chemistry (Germany). The TiO₂ was used as received.

The technical data used to process the rPLA are collected in Table 5.2.

Table 5.2 - Technical data to process the materials

Sample code	Central Unit						Dehumidifier	Dosimeter		Winder	Pelletizing machine		Work pressure (bar)
	Screw Speed (rep)	T1 (°C)	T2 (°C)	T3 (°C)	T4 (°C)	T5 (°C)	Initial Material temperature (°C)	D1 (rpm)	D2 (rpm)	Winder Speed (m/min)	Cutting	Pull	
rPLA	126.1	180	180	190	200	200	60	2.5	-	2.3	44	32	3
V97A3	130.3	185	190	190	180	175	60	1.5	3	1.75	27	20	7
V93A7	130.3	185	190	190	180	175	60	0.5	6	1.75	27	20	7
V25R75	130.3	185	190	190	180	175	60	1.5	3	1.75	27	20	8
V22R75A3	100	185	190	190	180	185	60	1.5	5	1.20	27	20	7
V18R75A7	100	185	190	190	180	185	60	1.5	5	1.20	48	18	8

All the parameters used for the manufacture of the plates are shown in Table 5.3.

Table 5.3 - FGF printing parameters.

Composite	Multiplier horizontal specimens	Multiplier vertical specimens	Temperature of extruder (°C)	Temperature of the bed (°C)	Horizontal plate (mm/s)	Vertical plate (mm/s)
V100	0.16	0.16	205/210/215	50	50	23
V97A3	0.22	0.22				
V93R7	0.18	0.20				
V25R75	0.26	0.27				
V22R75A3	0.22	0.22				
V18R75A7	0.23	0.24				

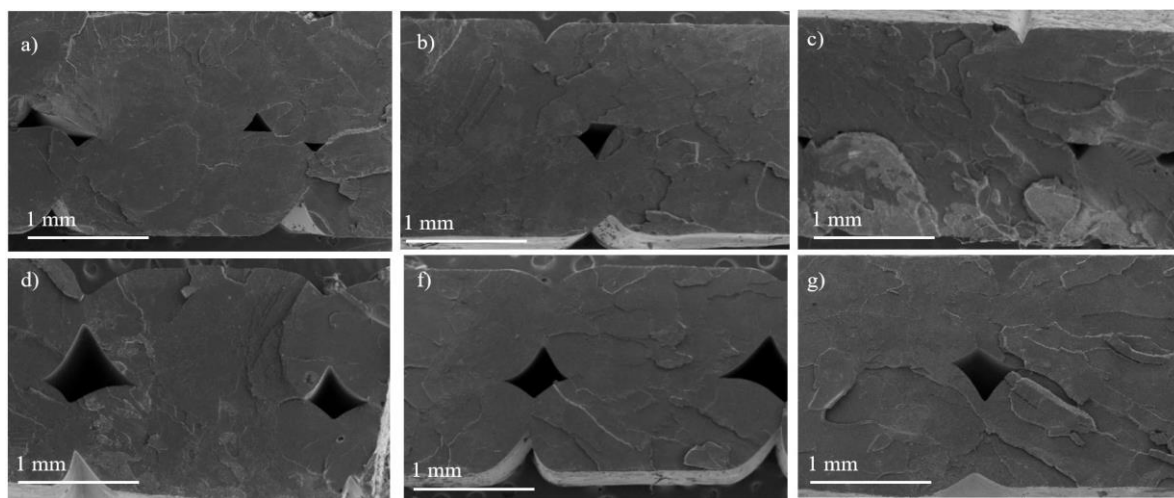
Considering the multiplier for a PLA material of 0.2, the V18R75A7 the flow is moderately controllable, somewhat better than the V100, V97A3 and V22R75A3. So the plate comes out quite well filled. In the case of horizontal and vertical plates from V22R75A3 it was only necessary to increase the multiplier to 0.22 in order to cover well the plate. The V93R7 is a compound that needed the least multiplier of 0.18, due to the high fluidity that it presented at the used temperature range. Although, there is a problem with some flow control which were also experienced in other compounds. In contrast, the V25R75 compound requires much more extrusion than the rest, because of the 75 % presence of incorporated rPLA, considering the parameters used in the rest of the materials, raising the multiplier up to 0.26. Finally, the V100 compound performs very well in printing, as it is the untreated and pure base, avoiding excess material and flow variations during printing. On the vertical plate, excellent wall stability is observed, as expected. It must be mentioned that warping, cracking, delamination problems or nozzle clogging during the 3D printing process were not detected for any sample.

5.2 Results of experiment

5.2.1 Scanning electron microscopy

The dispersion of nanoparticles in the polymer matrix is the key factor influencing the physical properties of the nanocomposites. Therefore, the SEM analysis of the FGF printed PLA and PLA/TiO₂ and PLA/rPLA/TiO₂ nanocomposites fracture surfaces was performed to investigate the dispersion and distribution of TiO₂ nanoparticles within the biodegradable matrix. Figure 5.1 shows the SEM images with magnification 40k of the fracture surfaces of the samples V100, V97A3, V93A7, V25R75, V22R75A3 and V18R75A7. No significant differences between V100 and V25R75, V97A3 and V22R75A3, and V93A7 and V18R75A7 are found at this magnification. The surfaces are quite flat and smooth, indicating a brittle nature,

which is consistent with the break without necking observed in the tensile tests (see section 5.2.4) and reported in [151].



a) V100; b) V97A3; c) V93A7; d) V25R75; e) V22R75A3; f) V18R75A7

Figure 5.1 - SEM images from fracture surfaces of the FGF printed samples

The SEM analysis has been also carried out at higher magnifications to study the integration of the nanoparticles in the polymer. As it can be seen in Figure 5.2, the TiO_2 nanoparticles are revealed with a higher intensity in the secondary electrons' micrographs, being clearly differentiated from the PLA matrix. To corroborate the composition of the TiO_2 nanoparticles, EDX analysis were carried out. Figure 5.2d) shows the Ti peak corroborating the presence of TiO_2 . The Au peak is due to the gold coating necessary for SEM analysis of organic samples (see section 2.3.3).

Images in Figure 5.2 show a homogeneous distribution and adequate integration of the TiO_2 in all samples. Nevertheless, Figure 5.2c, e and f depict clearly that nanoparticles gathered in agglomerations in V93A7, V22R75A3 and V18R75A7. To know the equivalent diameters of nanoparticles agglomerations, the areas corresponding to TiO_2 were measured in the high magnification images. The histogram of aggregates' equivalent diameter is presented in Figure 5.3. The areas of agglomerations are from $0.0003 \mu\text{m}^2$ to $0.2180 \mu\text{m}^2$. According to manufacture the average size of TiO_2 nanoparticles is between 10-20 nm. Considering this information, the equivalent diameter of the smallest agglomeration with area $0.0003 \mu\text{m}^2$ is around 20 nm. It means that the smallest circle in received micrographs consist of one TiO_2 nanoparticle. The separate nanoparticles can be seen in all samples, but their density is low for all samples ($<7 \cdot 10^6 \text{ cm}^{-2}$). Otherwise, the percentage of 2-nanoparticles-aggregates is higher than the one for separate particles and is 14, 14, 13 and 10 % in V97A3, V93A7, V22R75A3, and V18R75A7, respectively. The biggest agglomeration was revealed in V93A7, with an area of $0.2180 \mu\text{m}^2$ which corresponds to the union of 26 nanoparticles of 20 nm diameter. The results of measured equivalent diameters were statistically normalized in

OriginPro 2018 64-bit software and presented in Figure 5.3. The highest content of agglomerations is $0.003 \mu\text{m}^2$ and $0.005 \mu\text{m}^2$ (about 3-4 nanoparticles with size 20 nm) for V97A3, $0.01 \mu\text{m}^2$ (about 5-6 nanoparticles with size 20 nm) for V93A7 and V22R75A3, $0.005 \mu\text{m}^2$ (4 nanoparticles with size 20 nm) for V18R75A7. From this data it can be supposed that the highest content of agglomerations consists of 3-6 nanoparticles in all samples. Figure 5.3 illustrates that V18R75A7 has lower agglomerations size than V93A7 and V22R75A3.

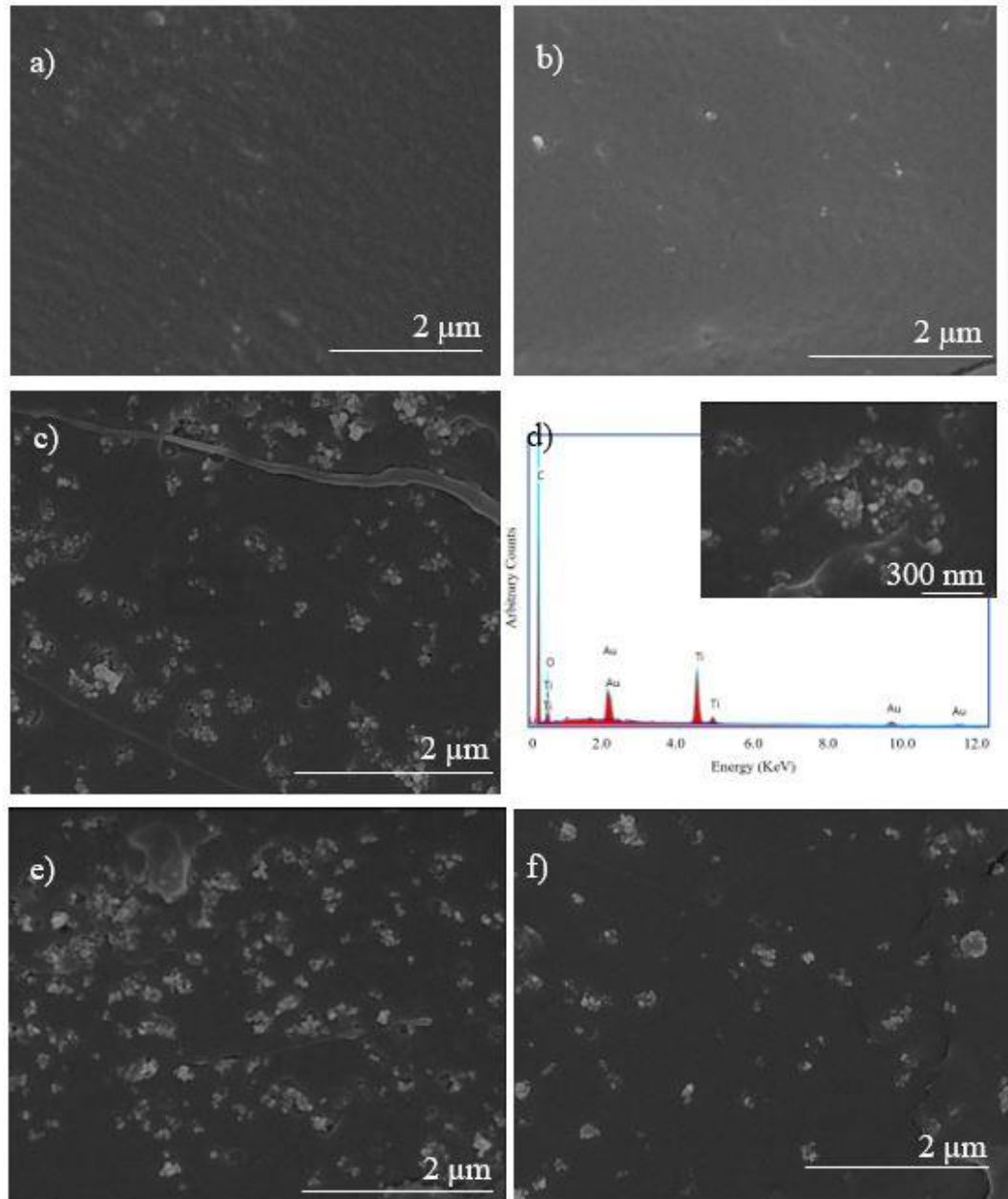


Figure 5.2 - a) SEM image of V100 sample and its respective EDX spectra; b) SEM images of V97A3 sample; c) SEM image of V93A7 sample; d) EDX spectra of one of the V93A7 zones with TiO_2 particles (the inset is an image of the region of the sample where EDX was taken); e) SEM image of V22R75A3 sample; f) SEM image of V18R75A7 sample

The tendency to aggregation can be explained by the fact that no surface treatment was performed on the oxide particles as in study [152]. Severe aggregation of TiO₂ nanoparticles could be reduced by surface modification [153]. The gathering of nanoparticles in agglomerations may be due to the hydrogen bonds on the surface of the TiO₂ particles. P. Dubois et al. [154] and W. Zhuang et al. [48] state that because of the special surface properties of the nanoparticles, they easily formed agglomeration, which can be divided into soft and hard agglomeration. Soft agglomeration is mainly caused by electrostatic force and van de Waals force. These forces are weak, and this kind of agglomeration can be eliminated through chemical or mechanical process. By contrast, hard agglomeration is caused by many kinds of forces including van der Waals force, Coulomb force, and chemical bonding. As a result, the particles are closely combined, and it is not easy to eliminate this kind of agglomeration.

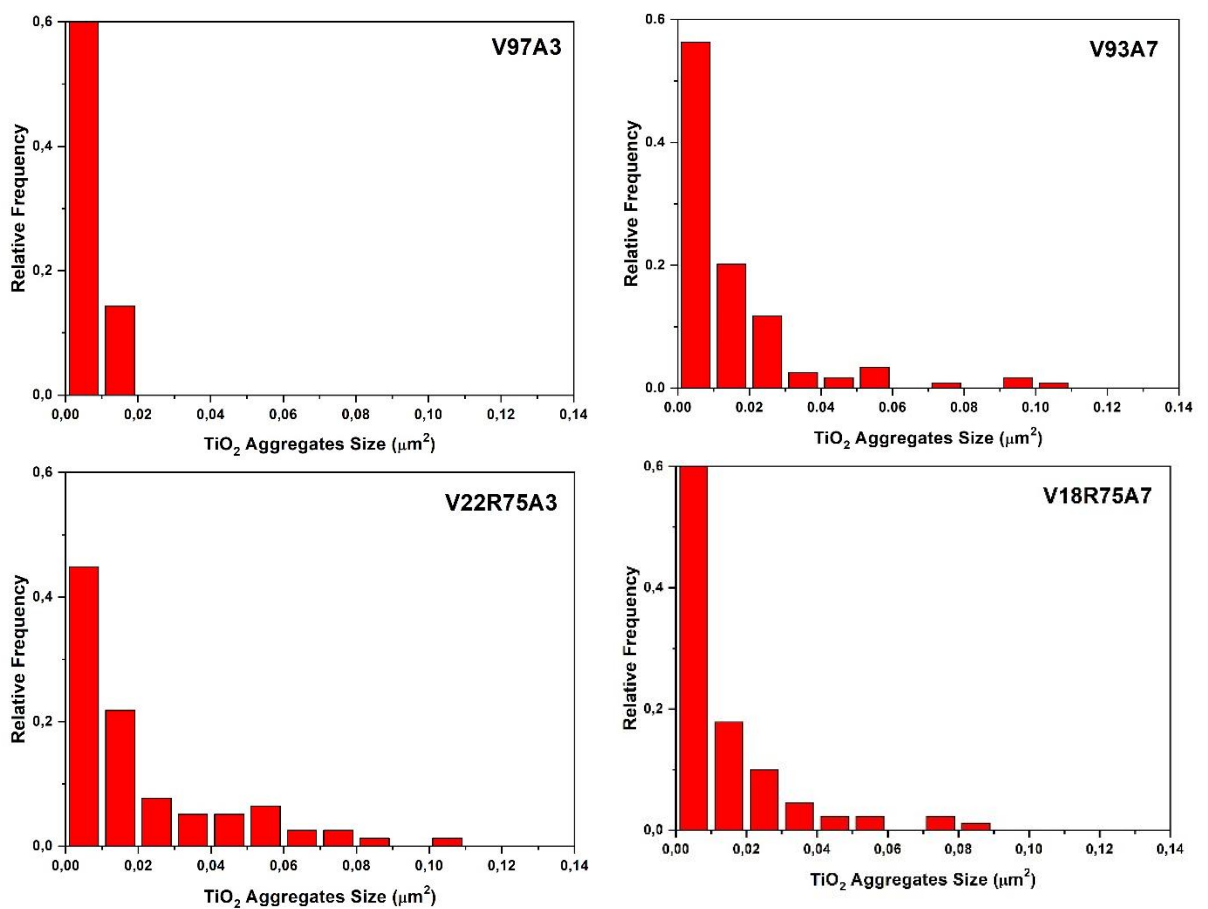


Figure 5.3 - Normalized frequencies of TiO₂ aggregates

So, SEM micrographs clearly revealed good dispersion of nano-TiO₂ aggregates in the matrix at the low nano-TiO₂ content, while higher content contributed to easy aggregation within the matrix, which was consistent with the results of mechanical properties and thermal properties. The same results were received by Q. Zhang et al. [59].

5.2.2 Thermogravimetric analysis

The effect of nano-TiO₂ addition on thermal stability of PLA nanocomposites was evaluated by thermogravimetry (TG). Figure 5.4a illustrates the TG curves and Figure 5.4b presents their respective derivative thermograms (DTG) of pure PLA, mixture of pure and rPLA and their nanocomposites. TGA curves of PLA nanocomposites have single-stage sample weight reduction with a maximum decomposition temperature (T_{max}) around 350 °C. T_{max} is listed in last row of Table 5.4 (extracted from DTG in Figure 5.4b), evidencing that the composites degrade similarly to PLA.

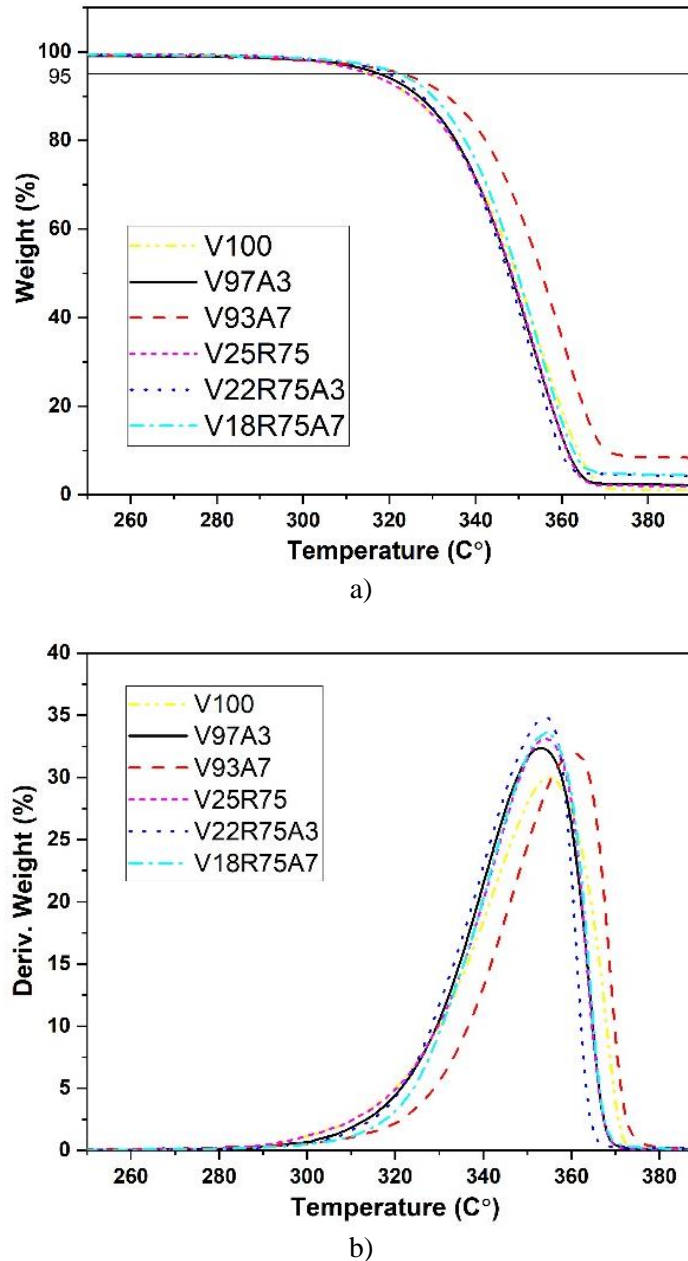


Figure 5.4 - a) thermogravimetric curve of PLA and its nanocomposites; b) respective derivative thermograms curves. Measurement error 0.0010 °C. Measurement uncertainty 0.0003 °C

V100 has the smallest decomposition temperature at 5 % weight loss ($T_{5\%loss}$) among all samples. This temperature rises with the addition of rPLA, V25R75 experiencing an increase on almost 3 °C. This effect is also observed after the addition of nano-TiO₂, so $T_{5\%loss}$ of PLA/TiO₂ and PLA/rPLA/TiO₂ nanocomposites shifted to a higher value compared with that of the reference samples without TiO₂. This fact indicated that the addition of nano-TiO₂ improved the thermal stability of nanocomposites. Generally, the particles can enhance the thermal stability of a polymer because the presence of nano-TiO₂ particles constrains the mobility of PLA molecular chains [48].

Table 5.4 - The results of thermogravimetric analysis: decomposition temperature at 5 % weight sample loss and maximum decomposition temperature ($T_{5\%loss}$ and T_{max} , respectively). All values are given in °C. Measurement error 0.0010 °C. Measurement uncertainty 0.0003 °C

Sample code	V100	V97A3	V93A7	V25R75	V22R75A3	V18R75A7
$T_{5\%loss}$	312.000	317.803	322.191	315.117	319.000	322.000
T_{max}	355.114	352.859	361.042	354.037	353.930	354.227

The temperature T_{max} shows the maximum degradation temperature. According to the results presented in Figure 5.4 and Table 5.4 most of the samples, except V93A7, reached maximum degradation condition at the same temperature range about 353-355 °C. For polymers without nanoparticles, complete degradation occurs at about 400 °C. With nanoparticles, zero residue weight was not reached when the samples were heated up to 600 °C. Hence, the particles are stable in the considered temperature range. TGA results show that the introduction of TiO₂ has rising tendency of the thermal stability for both nanocomposites PLA/TiO₂ and PLA/rPLA/TiO₂ with increasing of nanoparticle concentration. The same results were obtained by H. Zhang et al. [155].

5.2.3 Differential scanning calorimetry

Table 5.5 and Figure 5.5 illustrate the results of DSC test. They show that T_g appears between 60-62 °C and doesn't changes much from sample to sample, as T_m does. Otherwise, T_c is higher for samples with virgin PLA than for samples with rPLA. The reduction of T_c can be explained by the higher mobility of polymer chain, as consequence of reduced molecular weight in V25R75 and their nanocomposites because of the addition of recycled polymer [131].

The degree of crystallinity X_c was quantified according to formula (2). Comparing the crystallinity degree X_c of V100 and V25R75 it can be noticed that crystallinity of PLA mixture is higher. It can be because recycled part of V25R75 has molecules with shortened molecular chains, as was mentioned earlier, that can organize crystals easier. For both groups of nanocomposites, PLA and rPLA, there is a clear trend: the reduction in crystallinity when increasing the nanoparticles concentration. As previously mentioned in section SEM, nanoparticles form

agglomerations, and they can restrict the mobility of PLA macromolecules and the formation of crystals. In this study the TiO₂ nano filler has no significant influence on the T_g and T_m temperature, but have an effect on the mobility of macromolecular chains in all investigated samples. Similar results were observed by Refs. [152,155] [156].

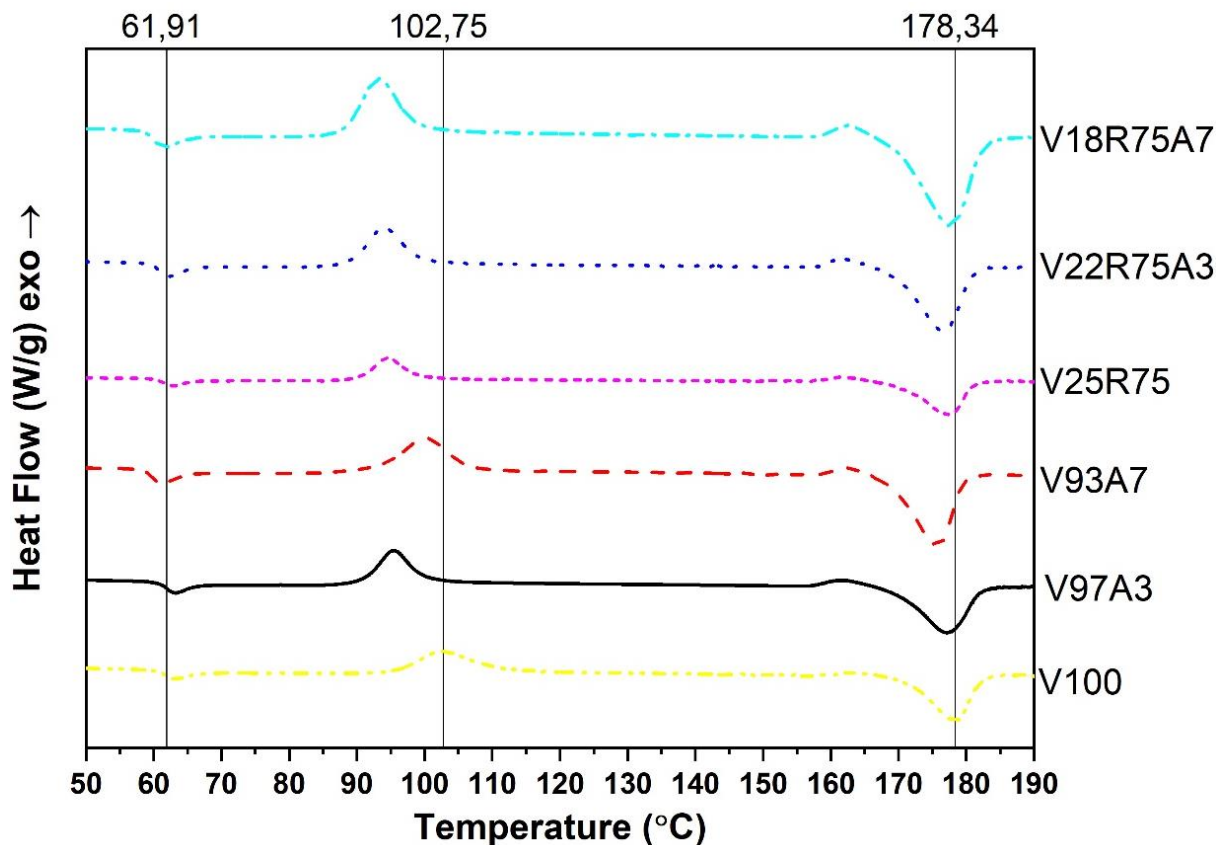


Figure 5.5 Differential scanning calorimetry curves. Measurement error 0.0010 °C. Measurement uncertainty 0.0003 °C

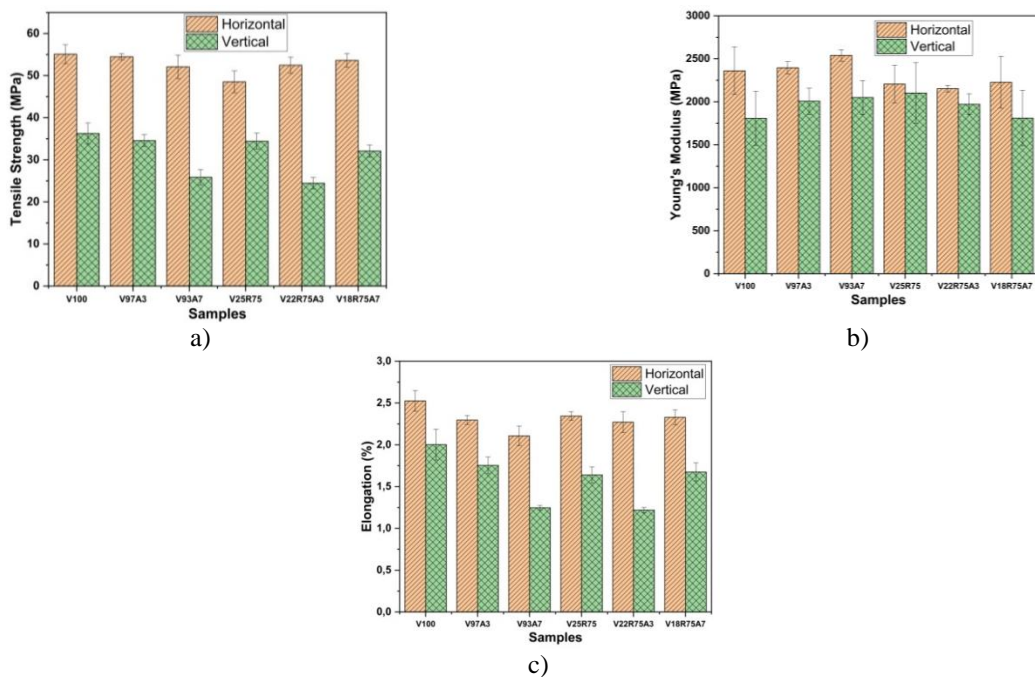
Table 5.5 - Results of DSC tests: glass transition, crystallisation, and melting temperatures (T_g, T_c, and T_m, respectively) are shown, as well as the enthalpy of crystallisation and fusion (ΔH_c and ΔH_m) and the calculated degree of crystallinity (X_c). Measurement error 0.0010 °C. Measurement uncertainty 0.0003 °C

Sample code	T _g	T _c	ΔH _c	T _m	ΔH _m	X _c
	°C	°C	J/g	°C	J/g	%
V100	61.91	102.75	31.83	178.34	46.08	15.323
V97A3	62.16	95.57	31.25	177.18	41.62	11.151
V93A7	60.19	99.97	37.34	175.66	46.03	9.344
V25R75	62.57	94.69	26.61	177.29	45.02	19.796
V22R75A3	60.86	93.96	29.15	176.54	43.22	15.129
V18R75A7	60.25	93.09	36.43	177.67	44.66	9.581

5.2.4 Tensile testing

In this study all samples were printed in horizontal and vertical printing orientation. Tensile strength of V100 is 55.100 ± 2.243 MPa and is higher than tensile strengths of V25R75 which is 48.535 ± 2.590 MPa in horizontal printed samples. It can be explained by the tendency of PLA to undergo degradation during thermal processing from the molten state, giving rapid reduction of molecular weight [157], that was seen in DSC section results. Reduction in tensile strength after 3D printing reprocessing were also observed by Anderson [38] and Cruz Sanchez *et al.* [74].

Nanocomposites from 100 % rPLA weren't produced because previous experiments conducted with 100 % rPLA samples (not considered in this study) resulted in a drastic drop in the vertical tensile strength of almost the half of that for V100, from 36.242 ± 2.512 MPa to 18.675 ± 0.711 MPa, while tensile strength in vertical direction of V25R75 stayed almost the same as V100. This was the reason of considering the TiO₂ nanocomposites with a maximum content of 75 % rPLA in this work. This difference in the tensile strength of rPLA and V25R75 can be explained by the fact that the strength acquired by the vertical specimen can be considered to be due to the adhesion strength between layers [158]. As the strength of printed parts depends on the strength of the used thermoplastic filament and the bond strength between layers [159]. Thus, it can be concluded that short molecular chains in rPLA cannot form strong interlayer adhesion during printing compared to V25R75 with long and short flexible molecular chains which have stronger molecular entanglement. The results presented in Figure 5.6 show that the addition of nanoparticles to pure PLA reduces the tensile strength in both printing directions.



a) tensile strength; b) Young's modulus; c) elongation

Figure 5.6 - Results of tensile strength test

Zhang *et al.* [155] revealed that adding nano TiO₂ to injection molded samples up to 2 wt % slightly shifts tensile strength to a higher value as compared with pure PLA. But when the TiO₂ content is more than or equal to 2 wt %, the nanocomposites showed a lower tensile strength than neat PLA. At high loading, the lack of strong interaction between polymer and particles due to filler aggregation resulted in debonding of the particles at lower tensile stress and a subsequent premature yielding [60]. So, it can be said that adding 3-7 % of nanoparticles to pure 3D printed PLA is too much to enhance the mechanical properties of nanocomposite because of nano TiO₂ agglomerations, which were seen in SEM part, that restrict the movement of polymer chain in the composites.

On the other hand, positive dynamics can be observed due to the addition of nanoparticles to a mixture of pure and reprocessed polymer. The tensile strength of V22R75A3 and V18R75A7 grow from 48.535±2.590 MPa to 52.470±1.916 and 53.622±1.651 MPa in horizontal printing direction, respectively. These results show that tensile strength in XY orientation of nanocomposites from the mixture of virgin and rPLA reach the same value as V100. In the vertical direction, tensile strength of V18R75A7 is almost the same as V25R75 considering the standard deviation. Hence, nanocomposite from PLA and rPLA with 7 % of TiO₂ has almost the same tensile strength as specimens manufactured through FGF from 100 % PLA. It can be explained by the formation of two new bonds. First, according to the published research, there are a lot of hydroxyl groups (Ti–OH) covering the surface region of TiO₂ nanoparticles which could form a strong interfacial bond Ti–O–C with carbonyl groups of PLA [155]. In this sense, compared with V100, V25R75 would have increased the concentration of carboxylic acid end groups in the degradation medium because of chain scission in recycled PLA [157]. Secondly, Zhang [59] reported the increasing amount of hydrogen bonds being formed between the titanium hydroxyl and hydroxyl groups of the PLA matrix. That is why, it can be concluded that the molecular chains of the mixture with rPLA have more hydroxyl and carbonyl end groups that can form strong internal friction (interaction) between nanoparticles in the matrix of V18R75A7 hence enhancing tensile strength. Also, it was mentioned in section 5.2.1 that V18R75A7 has a lower agglomeration size than V93A7 and V22R75A3, which may be the reason for its slightly higher strength.

According to the Figure 5.6b Young's Modulus of V97A3 and V93A7 rises when increasing the TiO₂ content in both printing directions, while this effect is not observed in nanocomposites with rPLA. Young's Modulus of nanocomposites from neat and rPLA is approximately the same as reference sample in both XY and XZ orientations considering standard deviation. It must be mentioned that V93A7 has the highest value of Young's Modulus among all studied samples.

The values of elongation presented in Figure 5.6c follows similar tendency as tensile strength for all the samples, with the only exception of the horizontal rPLA samples series, which ductility does not vary with the addition of TiO₂. Therefore, in general, ductility is reduced when adding nanoparticles, hence becoming more brittle.

Conclusions to chapter

The results of this experiment is presented in [160].

This study comprises the processing, thermal-mechanical and structural characterization of six polymer blends for FGF additive manufacturing: from pure PLA, from a mixture of 25 % of pure and 75 % of reprocessed PLA, and from their nanocomposites with 3 and 7 % of TiO₂. To manufacture the granules, the extruder's technical data varies for every type of granules and is established experimentally. The same was with the printing parameters. Whatever, all granules showed good flowability and printable quality.

Even though the nanoparticles are collected in agglomeration in some blends, they are uniformly distributed. The thermal stability has rising tendency with increasing the additive's content. Crystallization temperature and degree of crystallinity of nanocomposites fell with TiO₂ addition. Tensile testing showed that the addition of nanoparticles to pure PLA reduces the tensile strength and increases the Young's Modulus in both printing directions. However, this effect is not observed in nanocomposites with rPLA. Nanocomposite from primary and secondary PLA with 7 % of nano-TiO₂ has almost the same mechanical characteristics as V100, taking into account the standard deviation. In summary, FGF nanocomposites samples based on virgin and recycled PLA with the addition of titanium dioxide are a good option for improving the tensile strength and thermal stability of recycled PLA.

The third statement for defense: Adding 18 % of pure polymer and 7 % of titanium dioxide nanoparticles to secondary polylactide increases the tensile strength and fluidity of FGF samples to match those of a standard sample during 3D printing.

6 STANDARDIZATION OF RECYCLED POLYLACTIDE FOR ADDITIVE MANUFACTURING

Establishing a standard for improved polymer is an integral part of material development leading to improved quality and competitiveness. Compliance with the requirements of the standard makes it possible to correctly compare the properties of the same product obtained by different manufacturers. In this work, the object of standardization is a nanocomposite based on a virgin and recycled polymer with the addition of titanium dioxide nanoparticles, further nanocomposite.

To control the quality of nanocomposite from recycled polymer the main quality characteristics will be listed in the standard of organization. The standardized quality control methods will be proposed there too.

It is still possible for multiple manufacturers trying to manufacture a similar product with the same design characteristics to have different products based on different mechanical properties, surface finish, and dimensions and tolerances. Therefore, establishing process-structure-property-performance relationships for polymer AM materials and parts is the central factor that must be addressed as the efforts for standards development move forward. In the early phases of technology implementation, the industry relies exclusively on internal proprietary materials and process specifications for internal qualification work and certification by regulatory agencies. According to the regulatory framework of Spain and the Republic of Kazakhstan, standards of ISO can be adopted directly. However, there is no international standard for PLA, much less for a recycled one. Therefore, this part describes the standard developing process for recycled PLA used in AM.

The regulatory document for recycled PLA used in AM and recycled with AM will be called “Nanocomposites based on virgin polylactide and its waste with titanium dioxide nanoparticles for additive manufacturing. Technical specifications” and will consist of the following parts:

- title page;
- preface;
- name of the standard;
- scope;
- normative references;
- terms and definitions;
- classification;
- technical requirements;
- safety requirements
- acceptance rules;
- control methods;
- transportation and storage;
- manufacturer's warranties.

This standard defines specific and unambiguous provisions regarding the object of standardization. The object of standardization is a nanocomposite obtained from virgin PLA and PLA waste with titanium dioxide nanopowder. Waste PLA was

obtained after 3D printing from polylactide (prototypes, defects, and support structures of 3D printing). These wastes were not exposed to direct sunlight and did not come into direct contact with food or other aggressive chemical media.

The requirements established in this standard are based on the results of scientific research and the provisions of international and national standards of Spain and the Republic of Kazakhstan. While developing this standard, some requirements established in the international and national standards of Spain and the Republic of Kazakhstan are not repeated, since the corresponding references to the sections in these standards are made. The standard's presentation, design, and content comply with the Republic of Kazakhstan StRK 1.5 standard. The choice of quality and safety indicators is carried out considering the study's complexity.

The title page of the draft standard of organization contains the following data:

- status of the standard;
- the name of the standard;
- designation of the standard;
- output data.

The preface is placed on the second page of the title page of the standard. The word "Foreword" shall be written with a capital letter in the middle of the page and highlighted in bold. The general information given in the preface shall be written in bold, numbered in Arabic numerals without a dot at the end, and arranged in the following sequence:

- information about the developer;
- information on the approval and enactment of the standard;
- information about the first and subsequent revisions of the standard;
- information on the novelty of the standard.

The name of the standard unambiguously defines the object of standardization without a detailed analysis of the content of the standard. This name helps to distinguish the standard from other similar standards. The name of the standard consists of two elements: the title (the central element of the name) and the subheading (additional element). The title of the standard is printed in capital letters.

The element "Scope" specifies the purpose of the standard and the scope of its distribution (the object of standardization). In one sentence, the specification of the standardization object and the standard's scope are combined. The last paragraph indicates information about the rights to publish and distribute the standard. Element "Scope of application" is placed on the first page of the standard and is drawn in the form of section 1, highlighted in bold.

The structural element "Normative references" contains a list of normative documents to which mandatory references are given in the text of the standard and which establish normative provisions, without compliance with which the norms of the standard cannot be fulfilled.

The list of normative references includes complete designations and names of normative documents in ascending order of registration numbers of designations as follows:

- technical regulations;
- national standards of the RK;
- interstate standards;
- international standards.

The section “Terms and definitions” is provided to ensure terminological understanding between the various users of this standard by defining terms not standardized at the state or interstate level, as well as by clarifying standardized terms since these measures are used in this standard in a narrower sense and do not meet the requirements of international standards. A term and its definition are written with a capital letter, separated by a colon, and highlighted in bold. Terminological articles are arranged in alphabetical order.

The product can be produced in two forms: filament and pellets.

Depending on the percentage of reagents (raw materials) is classified into the following three types:

Type one (I) 25 percent virgin substance, 75 percent waste substance (V75R25A0);

Type Two (II) 22 percent virgin substance, 75 percent waste substance, 3 percent titanium dioxide nanoparticles (V22R75A3);

Type Three (III) 18 percent virgin substance, 75 percent waste substance, 7 percent titanium dioxide nanoparticles (V18R75A7).

The chapter “Technical requirements” on the organization's standard describes the product's characteristics by organoleptic and thermo-mechanical properties. Also, requirements for packaging and labeling are given.

As for the success of any other recycling process, the correct consumer behavior and attitude towards waste management is not questioned, but specific policies or incentives might be proposed for material disposal in the 3D printing sector. Material traceability and the possibility of including specific markings in the design of 3D printed parts is still an open question. The best way to impose it could be by including an automatic marking function in the 3D printer software. The software should automatically add the mark to the part during the computation of the printing path, i.e., during the slicing operation. The area selection for marking should be left up to the user to maintain the aesthetics of the part relatively. Nonetheless, in open 3D printers the identification of the right material is not provided, because the software cannot automatically identify the filament material [161]. The software cannot automatically identify the filament and pellet material, so the used material must be identified.

All product safety requirements are spelled out in the chapter “Safety requirements”.

However, the rule-level certification requirements often do not define the specific acceptable testing procedures or compliance methods. This level of detail needs to be defined by an applicant.

One of the elements toward establishing confidence in components fabricated using AM is to employ recognized standardized tests to measure the key mechanical

properties, including tensile strength and fatigue resistance. Any change in part geometry, the number of builds per plate, and design parameters (printing patterns, layer orientation, support structure) can significantly affect the thermal history, ultimately altering microstructural details and defect-type statistics. This, in turn, can significantly affect mechanical properties, especially the fatigue behavior of AM parts. [84].

The tensile test is the most common or basic mechanical test to obtain maximum strength values for the materials considered [90]. ISO 17296-3:2014 recommended ISO 527 for tensile testing. UNE 116005:2012 is fully oriented to the performance of mechanical tests, specifically tensile testing for polymeric materials. ISO 527 is also the standard that identifies the UNE 116005:2012 as a reference for tensile testing. So, ISO 527, which is oriented to the determination of tensile properties in plastic materials, is also considered for additive manufacturing. In turn, this standard has five different parts. The first one addresses the general principles [124], and the following four establish the conditions to determine the tensile properties in molding and extrusion plastics, films and sheets, and isotropic and orthotropic fiber-reinforced plastic composites, respectively [102]. Thus, the second part, ISO 527-2:2012, is oriented to the testing of plastics for molding and extrusion, and that case is understood as the one closer to FFF and FGF manufacturing process.

Developed standard of organization St JSC 001-2023 “Nanocomposites based on virgin polylactide and its waste with titanium dioxide nanoparticles for additive manufacturing. Technical specifications” is presented in appendix D.

Conclusions to chapter

The forth statement for defense: Advanced standardization of the percentage of pure and recycled polylactide and titanium dioxide nanoparticles in proportions 25/75/0, 22/75/3, 18/75/7 in the modernized nanocomposite can ensure the competitiveness of this nanomaterial for the 3D printing process through further certification. The Certificate of Implementation is presented in appendix E.

CONCLUSIONS

In this work, printable quality FFF filaments, FGF pellets, and samples for mechanical testing were produced and characterized from primary processed PLA (virgin), secondary processed PLA (recycled), as well as from the mixture of virgin and recycled PLA, and with the addition of titanium dioxide nanoparticles. The obtained results allowed us to come to the following conclusions.

1. Regarding the ageing process of FFF-printed PLA samples:
 - a. 3D printed samples change their geometric dimensions during the entire period of hydrothermal ageing in the range from 1 to 8 %.
 - b. During 1344 h of hydrothermal ageing, the crystallization temperature decreases from 125 to 104 °C, the percentage of crystallinity increases from 3.2 to 8.6 %, and the tensile strength drops by 33 %.
 - c. After 1.5 years of real-life operation in 3D-printed polylactide samples, thermal and mechanical quality indicators drop significantly.
2. Regarding the recyclability of FFF-processed PLA:
 - d. The addition of 25 % virgin polymer to the polylactide debris leads to an increase in the tensile strength of 3D-printed FFF samples.
 - e. It is possible to produce FFF printable quality wires based on a mixture of real recycled polylactide and virgin polylactide, up to maximum of 75 % of recycled content.
3. Regarding the synthesis of a hybrid material made of virgin PLA, recycled PLA, and nano-TiO₂:
 - f. It is possible to produce printable quality pellets for FGF based on a mixture of virgin PLA with nanoparticles of titanium dioxide in the following proportions 97/3, 93/7, respectively
 - g. Recycled polylactide and its mixtures with virgin polylactide and titanium dioxide nanoparticles are printable materials for additive manufacturing based on FGF in the following proportions 25/75/0, 22/75/3, 18/75/7, respectively.
 - h. Nanocomposites based on 75 % recycled and 18 % virgin polylactide with the addition of 7 % titanium dioxide nanoparticles can have thermal and mechanical properties like those of a standard sample.
4. Advanced standardization of the percentage of pure and recycled polylactide and titanium dioxide nanoparticles in proportions 25/75/0, 22/75/3, 18/75/7 in the modernized nanocomposite can ensure the competitiveness of this nanomaterial for the 3D printing process through further certification.
 - i. Standardization of the received nanocomposite can ensure the competitiveness of the created nanomaterial through further certification.

Evaluation of the complete solution of the assigned tasks. In the thesis all the goals and objectives are fully resolved. During the study, the consistency of the results obtained was proven, the results were discussed and analyzed by domestic and foreign scientific consultants, as well as members of the INNANOMAT scientific research group (Spain).

Assessment of the scientific level of the dissertation work. The research was carried out at the Department of Thermophysics and Technical Physics of the Faculty of Physics and Technology of al-Farabi KazNU and University of Cadiz, the reliability of the results obtained is confirmed on the basis of published scientific data based on the results of the research work. The results obtained during the research work were published in foreign and domestic scientific publications with a high impact factor, and discussed at international conferences.

REFERENCES

1. Chua C.K., Wong C.H., Yeong W.Y. Standards, Quality Control, and Measurement Sciences in 3D printing and additive manufacturing. Elsevier Ltd, 2017. 209 p.
2. Gibson I., Rosen D.W., Stucker B. Additive Manufacturing Technologies. Springer-Verlag, 2015.
3. Singh S., Prakash C., Ramakrishna S. 3D Printing of Polyether-etherketone for Biomedical Applications // Eur. Polym. J. Elsevier Ltd, 2019. № February.
4. Wohlers Associates. Additive manufacturing and 3D printing: State of the industry // Wohlers Rep. 2013. P. 14.
5. Hague R., Mansour S., Saleh N. Material and design considerations for Rapid Manufacturing // Int. J. Prod. Res. 2004. Vol. 42, № 22. P. 4691–4708.
6. Bogers M., Hadar R., Bilberg A. Additive manufacturing for consumer-centric business models: Implications for supply chains in consumer goods manufacturing // Technol. Forecast. Soc. Change. Elsevier Inc., 2016. Vol. 102. P. 225–239.
7. Tofail S.A.M. et al. Additive manufacturing: scientific and technological challenges, market uptake and opportunities // Mater. Today. Elsevier Ltd., 2018. Vol. 21, № 1. P. 22–37.
8. Wohlers Associates. Wohlers Report 2023 [Electronic resource]. 2023. URL: <https://wohlersassociates.com/product/wr2023/>.
9. Ullah A.M.M.S. et al. Sustainability analysis of rapid prototyping: material / resource and process perspectives Hiroyuki Hashimoto Akihiko Kubo and Jun ' ichi Tamaki // Int. J. Sustain. Manuf. 2013. Vol. 3, № 1. P. 20–36.
10. Rejeski D., Zhao F., Huang Y. Research needs and recommendations on environmental implications of additive manufacturing // Additive Manufacturing. Elsevier B.V., 2018. Vol. 19. 21–28 p.
11. Cruz Sanchez F.A. et al. Plastic recycling in additive manufacturing: A systematic literature review and opportunities for the circular economy // J. Clean. Prod. Elsevier Ltd, 2020. Vol. 264. P. 121602.
12. Brenken B. et al. Fused filament fabrication of fiber-reinforced polymers: A review // Addit. Manuf. Elsevier, 2018. Vol. 21, № October 2017. P. 1–16.
13. Gebler M., Schoot Uiterkamp A.J.M., Visser C. A global sustainability perspective on 3D printing technologies // Energy Policy. Elsevier, 2014. Vol. 74, № C. P. 158–167.
14. Sasse J. et al. Investigation of Recycled and Coextruded PLA Filament for Additive Manufacturing // Polymers (Basel). 2022. Vol. 14, № 12.
15. Wittbrodt B.T. et al. Life-cycle economic analysis of distributed manufacturing with open-source 3-D printers // Mechatronics. Elsevier Ltd, 2013. Vol. 23, № 6. P. 713–726.
16. Wohlers associates. Wohlers Report 2019 3D Printing and Additive

Manufacturing State of the Industry. 2019.

17. J'son & Partners Consulting. 3D printing market in Russia and the world (Additive Manufacturing, AM), 2018 [Electronic resource]. 2019. URL: http://json.tv/ict_telecom_analytics_view/rynok-3d-pechati-v-rossii-i-mire-additivnoe-proizvodstvo-ap-additive-manufacturing-am-2018-g-20190117060056.

18. Peng T. et al. Sustainability of additive manufacturing: An overview on its energy demand and environmental impact // *Addit. Manuf.* Elsevier, 2018. Vol. 21, № April. P. 694–704.

19. ASTM-F42.91. Standard terminology for additive manufacturing technologies. 2015.

20. Tolcha S.D. Additive manufacturing technologies // *BEST Int. J. Manag. Inf. Technol. Eng. (BEST IJMITE)*. 2016. Vol. 4, № 7. P. 89–112.

21. ISO/TC 261 Additive manufacturing. ISO/ASTM 52900:2015 Additive manufacturing — General principles — Terminology. Geneva, Switzerland, 2021. P. 19.

22. Breški T. et al. Suitability of Recycled PLA Filament Application in Fused Filament Fabrication Process // *Teh. Glas.* 2021. Vol. 15, № 4. P. 491–497.

23. Gardan J. Additive manufacturing technologies: State of the art and trends // *Addit. Manuf. Handb. Prod. Dev. Def. Ind.* 2017. Vol. 7543, № November. P. 149–168.

24. Marchewka J., Laska J. Processing of poly-l-lactide and poly(l-lactide-co-trimethylene carbonate) blends by fused filament fabrication and fused granulate fabrication using RepRap 3D printer // *Int. J. Adv. Manuf. Technol. The International Journal of Advanced Manufacturing Technology*, 2020. Vol. 106, № 11–12. P. 4933–4944.

25. Gupta A.K., Taufik M. Improvement of part strength prediction modelling by artificial neural networks for filament and pellet based additively manufactured parts // *Aust. J. Mech. Eng. Taylor & Francis*, 2022. Vol. 00, № 00. P. 1–18.

26. Patel A., Taufik M. Extrusion-Based Technology in Additive Manufacturing: A Comprehensive Review // *Arab. J. Sci. Eng. Springer Berlin Heidelberg*, 2022.

27. Hanon M.M., Marczis R., Zsidai L. Influence of the 3D printing process settings on tensile strength of PLA and HT-PLA // *Period. Polytech. Mech. Eng.* 2021. Vol. 65, № 1. P. 38–46.

28. Sukindar N.A. et al. Effects of nozzle die angle on extruding polymethylmethacrylate in open-source 3D printing // *J. Comput. Theor. Nanosci.* 2018. Vol. 15, № 2. P. 663–665.

29. Taufik M., Jain P.K. Role of build orientation in layered manufacturing: A review // *Int. J. Manuf. Technol. Manag.* 2013. Vol. 27, № 1–3. P. 47–73.

30. Ahn S.H. et al. Anisotropic material properties of fused deposition modeling ABS // *Rapid Prototyping Journal*. 2002. Vol. 8, № 4. 248–257 p.

31. Yang L. et al. Experimental Investigations for Optimizing the Extrusion

Parameters on FDM PLA Printed Parts // *J. Mater. Eng. Perform.* Springer US, 2019. Vol. 28, № 1. P. 169–182.

32. Gao G. et al. A Survey of the Influence of Process Parameters on Mechanical Properties of Fused Deposition Modeling Parts // *Micromachines*. 2022. Vol. 13, № 4. P. 1–28.

33. Bellini A., Shor L., Guceri S.I. New developments in fused deposition modeling of ceramics // *Rapid Prototyp. J.* 2005. Vol. 11, № 4. P. 214–220.

34. Duty C.E. et al. Structure and mechanical behavior of Big Area Additive Manufacturing (BAAM) materials // *Rapid Prototyp. J.* 2017. Vol. 23, № 1. P. 181–189.

35. Moreno Nieto D., Casal López V., Molina S.I. Large-format polymeric pellet-based additive manufacturing for the naval industry // *Addit. Manuf.* Elsevier, 2018. Vol. 23, № March. P. 79–85.

36. Kumar N. et al. Extrusion-based additive manufacturing process for producing flexible parts // *J. Brazilian Soc. Mech. Sci. Eng.* Springer Berlin Heidelberg, 2018. Vol. 40, № 3.

37. Yakdoui F.Z., Hadj-Hamou A.S. Effectiveness assessment of TiO₂-Al₂O₃ nano-mixture as a filler material for improvement of packaging performance of PLA nanocomposite films // *J. Polym. Eng.* 2020. Vol. 40, № 10. P. 848–858.

38. Anderson I. Mechanical Properties of Specimens 3D Printed with Virgin and Recycled Polylactic Acid // *3D Print. Addit. Manuf.* 2017. Vol. 4, № 2. P. 110–115.

39. Pillin I. et al. Effect of thermo-mechanical cycles on the physico-chemical properties of poly(lactic acid) // *Polym. Degrad. Stab.* 2008. Vol. 93, № 2. P. 321–328.

40. Sangeetha V.H. et al. State of the Art and Future Prospectives of Poly(Lactic Acid) Based Blends and Composites // *Polym. Compos.* 2018. Vol. 39, № 1. P. 81–101.

41. Kuo C.F.J. et al. Property modification and process parameter optimization design of polylactic acid composite materials. Part I: Polylactic acid toughening and photo-degradation modification and optimized parameter design // *Text. Res. J.* 2015. Vol. 85, № 1. P. 13–25.

42. Farah S., Anderson D.G., Langer R. Physical and mechanical properties of PLA, and their functions in widespread applications — A comprehensive review // *Adv. Drug Deliv. Rev.* Elsevier B.V., 2016. Vol. 107. P. 367–392.

43. Tanikella N.G., Wittbrodt B., Pearce J.M. Tensile strength of commercial polymer materials for fused filament fabrication 3D printing // *Addit. Manuf.* Elsevier B.V., 2017. Vol. 15, № 2010. P. 40–47.

44. Ngaowthong C. et al. Recycling of sisal fiber reinforced polypropylene and polylactic acid composites : Thermo-mechanical properties , morphology , and water absorption behavior // *Waste Manag.* 2019. Vol. 97. P. 71–81.

45. Balla E. et al. Poly (lactic Acid): A Versatile Biobased Polymer for the Future with Multifunctional Properties — From Monomer Synthesis , Polymerization

Techniques and Molecular Weight Increase to PLA Applications // *Polymers* (Basel). 2021.

46. Sun C. et al. Progress in upcycling polylactic acid waste as an alternative carbon source : A review // *Chem. Eng. J. Elsevier B.V.*, 2022. Vol. 446, № P1. P. 136881.

47. Mofokeng J.P., Luyt A.S. Dynamic mechanical properties of PLA/PHBV, PLA/PCL, PHBV/PCL blends and their nanocomposites with TiO₂ as nanofiller // *Thermochim. Acta. Elsevier B.V.*, 2015. Vol. 613. P. 41–53.

48. Zhuang W. et al. Preparation, Characterization, and Properties of TiO₂/PLA Nanocomposites by In Situ Polymerization // *Polym. Compos.* 2009.

49. Beltran F.R. et al. Effect of Yerba Mate and Silk Fibroin Nanoparticles on the Migration Properties in Ethanolic Food Simulants and Composting Disintegrability of Recycled PLA Nanocomposites // *Polymers* (Basel). 2021. Vol. 13. P. 1925.

50. Fahim I.S., Chbib H., Mohamed H. The synthesis , production & economic feasibility of manufacturing PLA from agricultural waste // *Sustain. Chem. Pharm. Elsevier*, 2019. Vol. 12, № March. P. 100142.

51. Kolstad J.J. et al. Assessment of anaerobic degradation of Ingeo™ polylactides under accelerated landfill conditions // *Polym. Degrad. Stab.* 2012. Vol. 97. P. 1131–1141.

52. Jamshidian M. et al. Poly-Lactic Acid: Production, applications, nanocomposites, and release studies // *Compr. Rev. Food Sci. Food Saf.* 2010. Vol. 9, № 5. P. 552–571.

53. Fan Y. et al. Control of racemization for feedstock recycling of PLLA // *Green Chem.* 2003. Vol. 5, № 5. P. 575–579.

54. Lasprilla A.J.R. et al. Poly-lactic acid synthesis for application in biomedical devices - A review // *Biotechnol. Adv. Elsevier Inc.*, 2012. Vol. 30, № 1. P. 321–328.

55. Lim L.T., Auras R., Rubino M. Processing technologies for poly(lactic acid) // *Prog. Polym. Sci.* 2008. Vol. 33, № 8. P. 820–852.

56. Maga D., Hiebel M., Thonemann N. Life cycle assessment of recycling options for polylactic acid // *Resour. Conserv. Recycl. Elsevier*, 2019. Vol. 149, № October 2018. P. 86–96.

57. Tsukegi T. et al. Racemization behavior of L,L-lactide during heating // *Polym. Degrad. Stab.* 2007. Vol. 92, № 4. P. 552–559.

58. Ranakoti L. et al. Critical Review on Polylactic Acid: Properties, Structure, Processing, Biocomposites, and Nanocomposites // *Materials* (Basel). 2022. Vol. 15, № 12.

59. Zhang Q. et al. Preparation and properties of poly(lactic acid)/sesbania gum/nano-TiO₂ composites // *Polym. Bull. Springer Berlin Heidelberg*, 2018. Vol. 75, № 2. P. 623–635.

60. Meng B. et al. Toughening of polylactide with higher loading of nano-titania particles coated by poly(ε-caprolactone) // *Mater. Lett. Elsevier B.V.*, 2011.

Vol. 65, № 4. P. 729–732.

61. Peinado V. et al. Effect of extrusion on the mechanical and rheological properties of a reinforced poly(lactic acid): Reprocessing and recycling of biobased materials // *Materials (Basel)*. 2015. Vol. 8, № 10. P. 7106–7117.

62. Orellana-barrasa J. et al. Natural Ageing of PLA Filaments , Can It Be Frozen ? // *Polymers (Basel)*. 2022. Vol. 14. P. 3361.

63. Lee D. et al. Development and Evaluation of a Distributed Recycling System for Making Filaments Reused in Three-Dimensional Printers // *J. Manuf. Sci. Eng. Trans. ASME*. 2019. Vol. 141, № 2.

64. Tanney D., Meisel N.A., Moore J.P. Investigating Material Degradation through the Recycling of PLA in Additively Manufactured Parts // *Solid Freeform Fabrication Symposium*. 2017. P. 519–531.

65. Bergaliyeva S., Bolegenova S. Prospects for the processing of polymer waste // *International conference of students and young scientists “Farabi alemi”*. 2019. P. 298.

66. Baechler C., Devuono M., Pearce J.M. Distributed recycling of waste polymer into RepRap feedstock // *Rapid Prototyp. J.* 2013. Vol. 19, № 2. P. 118–125.

67. Woern A.L. et al. RepRapable Recyclebot: Open source 3-D printable extruder for converting plastic to 3-D printing filament // *HardwareX*. The Authors, 2018. Vol. 4. P. e00026.

68. Zhao X.G. et al. Enhanced mechanical properties of self-polymerized polydopamine-coated recycled PLA filament used in 3D printing // *Appl. Surf. Sci.* 2018. Vol. 441. P. 381–387.

69. Maga D., Hiebel M., Aryan V. A comparative life cycle assessment of meat trays made of various packaging materials // *Sustain*. 2019. Vol. 11, № 19.

70. Kreiger M.A. et al. Life cycle analysis of distributed recycling of post-consumer high density polyethylene for 3-D printing filament // *J. Clean. Prod.* 2014. Vol. 70. P. 90–96.

71. Zhong S., Pearce J.M. Tightening the loop on the circular economy: Coupled distributed recycling and manufacturing with recyclebot and RepRap 3-D printing // *Resour. Conserv. Recycl. Elsevier*, 2018. Vol. 128, № July 2017. P. 48–58.

72. Zander N.E., Gillan M., Lambeth R.H. Recycled polyethylene terephthalate as a new FFF feedstock material // *Addit. Manuf. Elsevier*, 2018. Vol. 21, № March. P. 174–182.

73. Zander N.E. et al. Recycled polypropylene blends as novel 3D printing materials // *Addit. Manuf. Elsevier B.V.*, 2019. Vol. 25. P. 122–130.

74. Cruz Sanchez F.A. et al. Polymer recycling in an open-source additive manufacturing context: Mechanical issues // *Addit. Manuf. Elsevier B.V.*, 2017. Vol. 17. P. 87–105.

75. Hart K.R., Frketic J.B., Brown J.R. Recycling meal-ready-to-eat (MRE) pouches into polymer filament for material extrusion additive manufacturing // *Addit. Manuf. Elsevier*, 2018. Vol. 21, № February. P. 536–543.

76. Chong S. et al. Physical Characterization and Pre-assessment of

Recycled High-Density Polyethylene as 3D Printing Material // *J. Polym. Environ.* Springer US, 2017. Vol. 25, № 2. P. 136–145.

77. Sam-Daliri O. et al. Recovery of Particle Reinforced Composite 3D Printing Filament from Recycled Industrial Polypropylene and Glass Fibre Waste // *Proc. World Congr. Mech. Chem. Mater. Eng.* 2022. Vol. 177. P. 3–4.

78. Ghabezi P., Flanagan T., Harrison N. Short basalt fibre reinforced recycled polypropylene filaments for 3D printing // *Mater. Lett. Elsevier B.V.*, 2022. Vol. 326, № March. P. 132942.

79. Babagowda et al. Study of Effects on Mechanical Properties of PLA Filament which is blended with Recycled PLA Materials Study of Effects on Mechanical Properties of PLA Filament which is blended with Recycled PLA Materials . // *IOP Conf. Ser. Mater. Sci. Eng.* 2018.

80. Hassan T. et al. Functional nanocomposites and their potential applications: A review // *J. Polym. Res.* Springer Netherlands, 2021. Vol. 28, № 2. P. 1–22.

81. Roussenova M. et al. Free volume, molecular mobility and polymer structure: Towards the rational design of multi-functional materials // *Acta Phys. Pol. A.* 2014. Vol. 125, № 3. P. 801–805.

82. Ávila A.F., Duarte M. V. A mechanical analysis on recycled PET/HDPE composites // *Polym. Degrad. Stab.* 2003. Vol. 80, № 2. P. 373–382.

83. Goutham R. et al. Study on mechanical properties of recycled Acrylonitrile Butadiene Styrene (ABS) blended with virgin Acrylonitrile Butadiene Styrene (ABS) using Taguchi method // *Materials Today: Proceedings.* Elsevier Ltd, 2018. Vol. 5, № 11. P. 24836–24845.

84. Seifi M. et al. Progress Towards Metal Additive Manufacturing Standardization to Support Qualification and Certification // *Jom.* 2017. Vol. 69, № 3. P. 439–455.

85. Monzón M.D. et al. Standardization in additive manufacturing: activities carried out by international organizations and projects // *Int. J. Adv. Manuf. Technol.* 2014. Vol. 76, № 5–8. P. 1111–1121.

86. Kawalkar R., Dubey H.K., Lokhande S.P. A review for advancements in standardization for additive manufacturing // *Mater. Today Proc.* Elsevier Ltd, 2021. Vol. 50. P. 1983–1990.

87. Pei E. Standardisation efforts of ISO/TC 261 “Additive Manufacturing”: 17th plenary meeting of ISO/TC 261 “Additive Manufacturing” // *Prog. Addit. Manuf.* Springer International Publishing, 2022. Vol. 7, № 2. P. 433–434.

88. Xiao J. et al. Standardisation focus on process planning and operations management for additive manufacturing // *Lect. Notes Mech. Eng.* 2017. Vol. 0. P. 223–232.

89. Na J.K., Oneida E.K. Nondestructive evaluation method for standardization of fused filament fabrication based additive manufacturing // *Addit. Manuf.* Elsevier, 2018. Vol. 24, № September. P. 154–165.

90. Garcia-Dominguez A. et al. Analysis of General and Specific

Standardization Developments in Additive Manufacturing from a Materials and Technological Approach // IEEE Access. 2020. Vol. 8. P. 125056–125075.

91. Bergaliyeva S., Bolegenova S., Sales D.L. Standardization of additive manufacturing // Bull. KBTU. 2020. Vol. 4, № 55. P. 142–149.

92. ISO. ISO/TC 261 Additive manufacturing [Electronic resource]. URL: <https://www.iso.org/committee/629086.html>.

93. ASTM. Additive Manufacturing Standards [Electronic resource]. 2023. URL: <https://www.astm.org/products-services/standards-and-publications/standards/additive-manufacturing-standards.html>.

94. ISO/TC 261 Additive manufacturing. ISO 17296-2:2015 Additive manufacturing - General principles - Part 2: Overview of process categories and feedstock. Geneva, Switzerland: ISO, 2015. P. 8.

95. ISO/TC 261 Additive manufacturing. ISO 17296-3:2014 Additive manufacturing - General principles - Part 3: Main characteristics and corresponding test methods. Geneva, Switzerland: ISO, 2014. P. 14.

96. AENOR. Fabricación por adición de capas en materiales plásticos. Fabricación aditiva Preparación de probetas. 2012. P. 9.

97. ISO/TC 61/SC 2 Mechanical behavior. ISO 20753:2008 Plastics — Test specimens. 2008. P. 15.

98. Torres J. et al. An approach for mechanical property optimization of fused deposition modeling with polylactic acid via design of experiments // Rapid Prototyp. J. 2016. Vol. 22, № 2. P. 387–404.

99. Tymrak B.M., Kreiger M., Pearce J.M. Mechanical properties of components fabricated with open-source 3-D printers under realistic environmental conditions // Mater. Des. Elsevier Ltd, 2014. Vol. 58. P. 242–246.

100. ISO/TC 61/SC 6 Ageing chemical and environmental resistance. ISO 291: Plastics – Standard Atmospheres for Conditioning and Testing. 2008. P. 8.

101. AENOR. UNE-EN ISO/ASTM 52902:2020. Fabricación aditiva. Artefactos de ensayo. Evaluación de la capacidad geométrica de los sistemas de fabricación aditiva. 2020. P. 51.

102. ISO/TC 61/SC 2 Mechanical behavior. ISO 527-2:2012 Plastics — Determination of tensile properties — Part 2: Test conditions for moulding and extrusion plastics. 2012. P. 11.

103. Oven T., Ovens V. Standard Practice for Heat Aging of Oxidatively Degradable Plastics 1. 2001. Vol. 08, № Reapproved. P. 2–6.

104. Solarski S., Ferreira M., Devaux E. Ageing of polylactide and polylactide nanocomposite filaments // Polym. Degrad. Stab. 2008. Vol. 93, № 3. P. 707–713.

105. ISO/TC 45/SC 2 Testing and analysis. ISO 188:2011 Rubber, vulcanized or thermoplastic — Accelerated ageing and heat resistance tests. 2013. P. 20.

106. Yarahmadi N., Jakubowicz I., Enebro J. Polylactic acid and its blends with petroleum-based resins: Effects of reprocessing and recycling on properties // J. Appl. Polym. Sci. 2016. Vol. 133, № 36. P. 1–9.

107. Boldizar A., Möller K. Degradation of ABS during repeated processing and accelerated ageing // *Polym. Degrad. Stab.* 2003. Vol. 81, № 2. P. 359–366.
108. Beltrán F.R. et al. Valorization of poly(lactic acid) wastes via mechanical recycling: Improvement of the properties of the recycled polymer // *Waste Manag. Res.* 2019. Vol. 37, № 2. P. 135–141.
109. Porfyris A. et al. Accelerated ageing and hydrolytic stabilization of poly(lactic acid) (PLA) under humidity and temperature conditioning // *Polym. Test.* Elsevier, 2018. Vol. 68, № November 2017. P. 315–332.
110. Avolio R. et al. PLA-based plasticized nanocomposites: Effect of polymer/plasticizer/filler interactions on the time evolution of properties // *Compos. Part B Eng.* Elsevier Ltd, 2018. Vol. 152. P. 267–274.
111. Mangin R. et al. Improving the resistance to hydrothermal ageing of flame-retarded PLA by incorporating miscible PMMA // *Polym. Degrad. Stab.* Elsevier Ltd, 2018. Vol. 155. P. 52–66.
112. Islam M.S., Pickering K.L., Foreman N.J. Influence of accelerated ageing on the physico-mechanical properties of alkali-treated industrial hemp fibre reinforced poly(lactic acid) (PLA) composites // *Polym. Degrad. Stab.* Elsevier Ltd, 2010. Vol. 95, № 1. P. 59–65.
113. Lesaffre N. et al. Revealing the impact of ageing on a flame retarded PLA // *Polym. Degrad. Stab.* 2016. Vol. 127. P. 88–97.
114. Mary K. Mitchell, Hirt D.E. Degradation of PLA Fibers at Elevated Temperature and Humidity // *Polym. Eng. Sci.* 2015.
115. Acioli-Moura R., Sun X.S. Thermal Degradation and Physical Aging of Poly(lactic acid) and its Blends With Starch Ricardo // *Polym. Eng. Sci.* 2008.
116. ISO. ISO 291:2008 Plastics — Standard atmospheres for conditioning and testing. 2008. P. 8.
117. ISO/TC 61/SC 2 Mechanical behavior. ISO 16012:2015 Plastics — Determination of linear dimensions of test specimens. 2015. Vol. 2015. P. 9.
118. Université D. et al. Thèse de doctorat Thèse de doctorat. 2006. № Paris VI.
119. ISO/TC 61/SC 5 Physical-chemical properties. ISO 11357-1:2016 Plastics — Differential scanning calorimetry (DSC) — Part 1: General principles. 2016. P. 33.
120. Clas S.-D., Dalton C.R., Hancock B.C. Differential scanning calorimetry: applications in drug development // *Pharm. Sci. Technol. Today.* 1999. Vol. 2, № 8. P. 311–320.
121. Bergaliyeva S., Bolegenova S. Determination of the thermal stability of polymeric materials obtained through additive manufacturing // International conference of students and young scientists “Farabi Alemi”. 2020. P. 119.
122. Akash M.S.H., Rehman K. Essentials of pharmaceutical analysis // *Essentials of Pharmaceutical Analysis.* 2019. 1–222 p.
123. ISO/TC 61/SC 5 Physical-chemical properties. ISO 11358-1:2014 Plastics — Thermogravimetry (TG) of polymers — Part 1: General principles. 2014.

Vol. 1. P. 9.

124. ISO/TC 61/SC 2 Mechanical behavior. ISO 527-1:2019 Plastics — Determination of tensile properties — Part 1: General principles. 2019. P. 26.

125. Kim K.W. et al. Thermal and mechanical properties of cassava and pineapple flours-filled PLA bio-composites // *J. Therm. Anal. Calorim.* 2012. Vol. 108, № 3. P. 1131–1139.

126. Rocca-Smith J.R. et al. Beyond Biodegradability of Poly(lactic acid): Physical and Chemical Stability in Humid Environments // *ACS Sustain. Chem. Eng.* 2017. Vol. 5, № 3. P. 2751–2762.

127. Cai H. et al. Effects of physical aging, crystallinity, and orientation on the enzymatic degradation of poly(lactic acid) // *J. Polym. Sci. Part B Polym. Phys.* 1996. Vol. 34, № 16. P. 2701–2708.

128. Bergaliyeva S. et al. Thermal analysis of 3D printed polylactic acid after accelerated thermal ageing // *Alternative Energy Sources, Materials & Technologies (AESMT'20)*. 2020. P. 91–92.

129. Malmgren T., Mays J., Pyda M. Characterization of poly(lactic acid) by size exclusion chromatography, differential refractometry, light scattering and thermal analysis // *J. Therm. Anal. Calorim.* 2006. Vol. 83, № 1. P. 35–40.

130. Torrado Perez A.R., Roberson D.A., Wicker R.B. Fracture surface analysis of 3D-printed tensile specimens of novel ABS-based materials // *J. Fail. Anal. Prev.* 2014. Vol. 14, № 3. P. 343–353.

131. Beltrán F.R. et al. Effect of simulated mechanical recycling processes on the structure and properties of poly(lactic acid) // *J. Environ. Manage.* 2018. Vol. 216. P. 25–31.

132. Sarasua J.-R. et al. Crystallization and Melting Behavior of Polylactides // *Macromolecules*. 1998. Vol. 31, № 9. P. 3895–3905.

133. Gallagher P.K., Stephen Z. D. Cheng. *Handbook of Thermal Analysis and Calorimetry: Application to Polymers and Plastics* // Elsevier Science B. V. 2002. Vol. 3. 828 p.

134. Sin L.T., Tuen B.S. *Polylactic Acid A Practical Guide for the Processing, Manufacturing, and Applications of PLA*. second. Elsevier Inc., 2019. 405 p.

135. ISO/TC 69 Applications of statistical methods. ISO 2602:1980 Statistical interpretation of test results — Estimation of the mean — Confidence interval. 1980. P. 5.

136. Bergaliyeva S. et al. Effect of Thermal and Hydrothermal Accelerated Aging on 3D Printed Polylactic Acid // *Polymers (Basel)*. 2022. Vol. 14, № 23. P. 13.

137. Smart Materials 3D Printing S. PLA 3D870 SmartMaterials3D Filament Datasheet v1.2 [Electronic resource]. URL: https://www.smartmaterials3d.com/en/index.php?controller=attachment&id_attachment=190.

138. Fan Y. et al. Thermal degradation behaviour of poly(lactic acid) stereocomplex // *Polym. Degrad. Stab.* 2004. Vol. 86, № 2. P. 197–208.

139. Sarasua J.R. et al. Crystallinity and mechanical properties of optically pure polylactides and their blends // *Polym. Eng. Sci.* 2005. Vol. 45, № 5. P. 745–753.
140. Zenkiewicz M. et al. Characterisation of multi-extruded poly(lactic acid) // *Polym. Test.* 2009. Vol. 28, № 4. P. 412–418.
141. Pluta M. et al. Polylactide/montmorillonite nanocomposites and microcomposites prepared by melt blending: Structure and some physical properties // *J. Appl. Polym. Sci.* 2002. Vol. 86, № 6. P. 1497–1506.
142. Nam P.H. et al. A hierarchical structure and properties of intercalated polypropylene/clay nanocomposites // *Polymer (Guildf).* 2001. Vol. 42, № 23. P. 9633–9640.
143. Kulinski Z., Piorkowska E. Crystallization, structure and properties of plasticized poly(L-lactide) // *Polymer (Guildf).* 2005. Vol. 46, № 23. P. 10290–10300.
144. Di Lorenzo M.L. The crystallization and melting processes of poly(L-lactic acid) // *Macromol. Symp.* 2006. Vol. 234. P. 176–183.
145. Di Lorenzo M.L. Calorimetric analysis of the multiple melting behavior of poly(L-lactic acid) // *J. Appl. Polym. Sci.* 2006. Vol. 100, № 4. P. 3145–3151.
146. Sánchez M.S. et al. On the kinetics of melting and crystallization of poly(l-lactic acid) by TMDSC // *Thermochim. Acta.* 2005. Vol. 430, № 1–2. P. 201–210.
147. Sarasua J.R. et al. Crystallization and thermal behaviour of optically pure polylactides and their blends // *J. Mater. Sci.* 2005. Vol. 40, № 8. P. 1855–1862.
148. Signori F., Coltelli M., Bronco S. Thermal degradation of poly (lactic acid) (PLA) and poly (butylene adipate- co -terephthalate) (PBAT) and their blends upon melt processing // *Polym. Degrad. Stab.* Elsevier Ltd, 2009. Vol. 94, № 1. P. 74–82.
149. Bergaliyeva S. et al. Manufacture and Characterization of Polylactic Acid Filaments Recycled from Real Waste for 3D Printing // *Polymers (Basel).* 2023. Vol. 15, № 9.
150. NatureWorks. Ingeo™ Biopolymer 3D850 Technical Data Sheet 3D Printing Monofilament – General Purpose Grade [Electronic resource]. P. 1–4. URL: <https://www.unicgroup.com/wp-content/uploads/2019/12/3D850.pdf>.
151. Thumsorn S. et al. Rheological Behavior and Dynamic Mechanical Properties for Interpretation of Layer Adhesion in FDM 3D Printing // *Polymers (Basel).* 2022. Vol. 14, № 13. P. 1–22.
152. Buzarovska A., Grozdanov A. Biodegradable Poly (L -lactic acid)/ TiO₂ Nanocomposites : Thermal Properties and Degradation // *J. Appl. Polym. Sci.* 2011. Vol. 123. P. 2187–2193.
153. Nakayama N., Hayashi T. Preparation and characterization of poly(l-lactic acid)/TiO₂ nanoparticle nanocomposite films with high transparency and efficient photodegradability // *Polym. Degrad. Stab.* 2007. Vol. 92, № 7. P. 1255–1264.

154. Dubois P. et al. Macromolecular engineering of polylactones and polylactides: 13. Synthesis of telechelic polyesters by coupling reactions // *Polymer (Guildf)*. 1994. Vol. 35, № 23. P. 4998–5004.
155. Zhang H. et al. Preparation, characterization and properties of PLA/TiO₂ nanocomposites based on a novel vane extruder // *RSC Adv. Royal Society of Chemistry*, 2015. Vol. 5, № 6. P. 4639–4647.
156. Luo Y.B. et al. Preparation and properties of nanocomposites based on poly(lactic acid) and functionalized TiO₂ // *Acta Mater. Acta Materialia Inc.*, 2009. Vol. 57, № 11. P. 3182–3191.
157. Gorrasi G., Pantani R. Hydrolysis and Biodegradation of Poly (lactic acid) // *Adv. Polym. Sci.* 2018. Vol. 279. P. 119–152.
158. Prasong W. et al. Improvement of interlayer adhesion and heat resistance of biodegradable ternary blend composite 3D printing // *Polymers (Basel)*. 2021. Vol. 13, № 5. P. 1–20.
159. Wickramasinghe S., Do T., Tran P. FDM-Based 3D printing of polymer and associated composite: A review on mechanical properties, defects and treatments // *Polymers (Basel)*. 2020. Vol. 12, № 7. P. 1–42.
160. Bergaliyeva S. et al. Thermal and Mechanical Properties of Reprocessed Polylactide/Titanium Dioxide Nanocomposites for Material Extrusion Additive Manufacturing // *Polymers (Basel)*. 2023. Vol. 15, № 16.
161. Ortega Z. et al. Banana Fiber Processing for the Production of Technical. 2017. Vol. 3, № April. P. 11.
162. ISO. Standards by ISO/TC 261 [Electronic resource]. URL: <https://www.iso.org/committee/629086/x/catalogue/>.

APPENDIX A

Summary of officially published standards according to ISO/TC 261 official catalogue

Table A.1 - Summary of officially published standards according to ISO/TC 261 official catalogue [162]. M stands for metals, P - for polymers, C - for composites

General standards				
Standard	Description	M	P	C
ISO/ASTM 52942:2020	Additive manufacturing - Qualification principles - Qualifying machine operators of laser metal powder bed fusion machines and equipment used in aerospace applications	+		
ISO 17295:2023	Additive manufacturing — General principles — Part positioning, coordinates and orientation	+	+	+
ISO 17296-2:2015	Additive manufacturing - General principles - Part 2: Overview of process categories and feedstock	+	+	+
Standards applied to terms and definitions				
ISO/ASTM 52900:2021	Additive manufacturing — General principles — Fundamentals and vocabulary	+	+	+
Standards for processes				
Design standards				
ISO/ASTM 52910:2018	Additive manufacturing – Design - Requirements, guidelines, and recommendations	+	+	+
ISO/ASTM 52911-1:2019	Additive manufacturing – Design - Part 1: Laser-based powder bed fusion of metals	+		
ISO/ASTM 52911-2:2019	Additive manufacturing – Design - Part 2: Laser-based powder bed fusion of polymers		+	
ISO/ASTM 52911-3:2023	Additive manufacturing — Design — Part 3: PBF-EB of metallic materials	+	+	+
ISO/ASTM TR 52912:2020	Additive manufacturing - Design – Functionally graded additive manufacturing	+	+	+
ISO/ASTM 52915:2020	Specification for additive manufacturing file format (AMF). Version 1.2.	+	+	+
ISO/ASTM TR 52916:2022	Additive manufacturing for medical — Data — Optimized medical image data	+	+	+
ISO/ASTM 52950:2021	Additive manufacturing – General principles – Overview of data processing	+	+	+
F3413-19e1	Guide for Additive Manufacturing — Design — Directed Energy Deposition	+	+	+
F3530-22	Standard Guide for Additive Manufacturing — Design — Post-Processing for Metal PBF-LB	+		
F3529-21	Guide for Additive Manufacturing — Design — Material Extrusion of Polymers		+	
Processes regulations				
ASTM F3049:2014 (2021)	Standard guide for characterizing properties of metal powders used for the additive manufacturing processes	+		
ASTM F3187:2016	Standard guide for the directed energy deposition of metals	+		
ASTM F3434:2020	Guide for additive manufacturing - Installation/operation and performance qualification (IQ / OQ / PQ) of laser beam powder bed fusion equipment for production manufacturing	+		
ISO/ASTM 52901:2017	Additive manufacturing — General principles — Requirements for purchased AM parts	+	+	+

Continuation of Table A.1

ISO/ASTM 52904:2019	Additive manufacturing - Process characteristics and performance: Practice for metal powder bed fusion process to meet critical apps	+		
ISO/ASTM TS 52930:2021	Additive manufacturing — Qualification principles — Installation, operation and performance (IQ/OQ/PQ) of PBF-LB equipment			
ISO/ASTM 52931:2023	Additive manufacturing of metals — Environment, health and safety — General principles for use of metallic materials	+		
Product standards				
ISO/ASTM 52925:2022	Additive manufacturing of polymers — Feedstock materials — Qualification of materials for laser-based powder bed fusion of parts	+		
ASTM F2924:2014 (2021)	Standard specification for additive manufacturing titanium-6 aluminium-4 vanadium with powder bed fusion	+		
ASTM F3001:2014 (2021)	Standard specification for additive manufacturing titanium-6 aluminium-4 vanadium ELI (Extra Low Interstitial) with powder bed fusion	+		
ASTM F3055:2014a (2021)	Standard specification for additive manufacturing nickel alloy (UNS N07718) with powder bed fusion	+		
ASTM F3056:2014 (2021)	Standard specification for additive manufacturing nickel alloy (UNS N06625) with powder bed fusion	+		
ASTM F3091/F3091M:2014 (2021)	Standard specification for powder bed fusion of plastic materials		+	
ASTM F3184:2016	Standard specification for additive manufacturing stainless steel alloy (UNS S31603) with powder bed fusion	+		
ASTM F3213:2017	Standard for additive manufacturing – Finished part properties – Standard specification for cobalt-28, chromium-6 molybdenum via powder bed fusion	+		
ASTM F3301:2018a	Standard for additive manufacturing – Post processing methods – Standard specification for thermal post processing metal parts made via powder bed fusion 1, 2	+		
ASTM F3302:2018	Standard for additive manufacturing – Finished part properties – Standard specification for titanium alloys via powder bed fusion	+		
ASTM F3318:2018	Standard for additive manufacturing – Finished part properties - Specification for AlSi10Mg with powder bed fusion - Laser beam	+		
ISO/ASTM 52903-1:2020	Additive manufacturing – Material extrusion-based additive manufacturing of plastic materials. Part 1: Feedstock materials		+	
ISO/ASTM 52903-2:2020	Additive manufacturing – Material extrusion-based additive manufacturing of plastic materials. Part 2: Process equipment		+	
ISO/ASTM 52909:2022	Additive manufacturing of metals — Finished part properties — Orientation and location dependence of mechanical properties for metal powder bed fusion	+		
Standards applied to test methods				
ASTM F2971:2013 (2021)	Standard practice for reporting data for test specimens prepared by additive manufacturing	+	+	+
ISO 17296-3:2014	Additive manufacturing - General principles - Part 3: Main characteristics and corresponding test methods	+	+	+
ASTM 3122:2014 (2022)	Standard guide for evaluating mechanical properties of metal materials made via additive manufacturing processes	+		

Continuation of Table A.1

ISO/ASTM 52902:2019	Additive manufacturing - Test artifacts - Geometric capability assessment of additive manufacturing systems	+	+	+
ISO/ASTM TR 52906:2022	Additive manufacturing — Non-destructive testing — Intentionally seeding flaws in metallic parts	+		
ISO/ASTM 52907:2019	Additive manufacturing - Feedstock materials - Methods for characterize metal powders	+		
ISO/ASTM 52941:2020	Additive manufacturing - System performance and reliability - Acceptance test for laser metal powder-bed fusion machines for metallic materials for aerospace application	+		
ISO/ASTM TR 52917:2022	Additive manufacturing — Round robin testing — General guidelines	+	+	+
UNE 116005:2012	Additive manufacturing of plastic materials. Additive manufacturing. Specimen preparation		+	
ISO 27547:2010	Plastics - Preparation of test specimens of thermoplastic materials using mouldless technologies - Part 1: General principles, and laser sintering of test specimens		+	
F3571-22	Standard Guide for Additive Manufacturing – Feedstock – Particle Shape Image Analysis by Optical Photography to Identify and Quantify the Agglomerates/Satellites in Metal Powder Feedstock	+		
F3606-22	Standard Guide for Additive Manufacturing — Feedstock Materials — Testing Moisture Content in Powder Feedstock	+	+	+
F3522-22	Standard Guide for Additive Manufacturing of Metals — Feedstock Materials — Assessment of Powder Spreadability	+		
F3624-23	Standard Guide for Additive Manufacturing of Metals – Powder Bed Fusion – Measurement and Characterization of Surface Texture	+		
F3626-23	Standard Guide for Additive Manufacturing — Test Artifacts — Accelerated Build Quality Assurance for Laser Beam Powder Bed Fusion (PBF-LB)	+		
ISO/ASTM 52936-1:2023	Additive manufacturing of polymers — Qualification principles — Part 1: General principles and preparation of test specimens for PBF-LB	+		

APPENDIX B

List of standards which are under development according to ISO/TC 261 official catalogue

Table B.1 - List of standards which are under development according to ISO/TC 261 official catalogue [162]. M stands for metals, P - for polymers, C - for ceramics

Standard	Description	M	P	C
ISO/DIS 27548	Additive manufacturing of plastics — Environment, health, and safety — Test method for determination of particle and chemical emission rates from desktop material extrusion 3D printer	+	+	+
ISO/ASTM DIS 52904	Additive manufacturing of metals — Process characteristics and performance — Metal powder bed fusion process to meet critical applications	+		
ISO/ASTM TR 52905	Additive manufacturing of metals — Non-destructive testing and evaluation — Defect detection in parts	+	+	+
ISO/ASTM DIS 52908	Additive manufacturing of metals — Finished Part properties — Post-processing, inspection and testing of parts produced by powder bed fusion	+		
ISO/ASTM DTR 52913-1	Additive manufacturing — Feedstock materials — Part 1: Parameters for characterization of powder flow properties	+		
ISO/ASTM CD TR 52918	Additive manufacturing — Data formats — File format support, ecosystem and evolutions	+	+	+
ISO/ASTM CD 52919	Additive manufacturing — Qualification principles — Test method of sand moulds for metal casting	+		
ISO/ASTM FDIS 52920	Additive manufacturing — Qualification principles — Requirements for industrial additive manufacturing processes and production sites	+	+	+
ISO/ASTM FDIS 52924	Additive manufacturing of polymers — Qualification principles — Classification of part properties	+	+	+
ISO/ASTM DIS 52926-1	Additive Manufacturing of metals — Qualification principles — Part 1: General qualification of operators	+	+	+
ISO/ASTM DIS 52926-2	Additive Manufacturing of metals — Qualification principles — Part 2: Qualification of operators for PBF-LB	+		
ISO/ASTM DIS 52926-3	Additive Manufacturing of metals — Qualification principles — Part 3: Qualification of operators for PBF-EB	+		
ISO/ASTM DIS 52926-4	Additive Manufacturing of metals — Qualification principles — Part 4: Qualification of operators for DED-LB	+		
ISO/ASTM DIS 52926-5	Additive Manufacturing of metals — Qualification principles — Part 5: Qualification of operators for DED-Arc	+		
ISO/ASTM DIS 52927	Additive manufacturing — General principles — Main characteristics and corresponding test methods	+	+	+
ISO/ASTM DIS 52928	Additive manufacturing of metals— Feedstock materials — Powder life cycle management	+		
ISO/ASTM CD 52929	Additive manufacturing of metals — Powder bed fusion — Presentation of material properties in material data sheets	+		
ISO/ASTM DIS 52933	Additive manufacturing — Environment, health and safety — Test method for the hazardous substances emitted from material extrusion type 3D printers in the non-industrial places	+	+	+
ISO/ASTM DIS 52935	Additive manufacturing of metals – Qualification principles – Qualification of AM coordination personnel	+	+	+
ISO/ASTM DIS 52938-1	Additive manufacturing of metals — Environment, health and safety — Part 1: Safety requirements for PBF-LB machines	+	+	+

Continuation of Table B.1

ISO/ASTM DIS 52939	Additive Manufacturing for construction — Qualification principles — Structural and infrastructure elements	+	+	+
ISO/ASTM CD 52940	Additive manufacturing of ceramics — Feedstock materials — Characterization of ceramic slurry in vat photopolymerization			+
ISO/ASTM DIS 52943-2	Additive manufacturing for aerospace — Process characteristics and performance — Part 2: Directed energy deposition using wire and arc	+	+	+
ISO/ASTM DIS 52945	Additive manufacturing for automotive — Qualification principles — Generic machine evaluation and specification of key performance indicators for PBF-LB/M processes	+	+	+
ISO/ASTM AWI 52948	Additive manufacturing for metals — Non-destructive testing and evaluation — Imperfections classification in PBF parts	+		
ISO/ASTM TR 52952	Additive manufacturing of metals — Feedstock materials — Correlating of rotating drum measurement with powder spreadability in PBF-LB machines	+		
ISO/ASTM DIS 52953	Additive manufacturing for metals — General principles — Registration of geometric data acquired from process-monitoring and for quality control	+	+	+
ISO/ASTM CD 52957	Additive Manufacturing — Design — Parts using ceramic materials			+
ISO/ASTM CD 52958	Additive Manufacturing of Metals — Powder Bed Fusion (PBF) — Best Practice for In-Situ Flaw Detection and Analysis for Laser-based PBF	+		
ISO/ASTM CD 52959	Additive Manufacturing — Test Artifacts — Compression Validation Coupons for Lattice Designs	+	+	+
ISO/ASTM CD 52941	Additive manufacturing — System performance and reliability — Acceptance tests for laser metal powder-bed fusion machines for metallic materials for aerospace application	+		

APPENDIX C

Standard of organization St JSC 002-2023 “Polylactide for additive manufacturing. Accelerated hydrothermal ageing test”

STANDART OF ORGANIZATION
JSC “Ust-Kamenogorsk Machine-Building Plant of Industrial Fittings”

UNIVERSAL DECIMAL CODE 54.384.2
PRODUCT CODE BY EXTERNAL ECONOMIC ACTIVITY 20.16.40

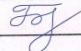
POLYLACTIDE FOR ADDITIVE MANUFACTURING. **Accelerated hydrothermal ageing test**

St JSC 002-2023
(the first edition)

Date of introduction: since 18.10.2023
Validity: until 17.10.2026

DEVELOPED


by Bergaliyeva S.A., doctoral student at
the Department of Thermal Physics and
Technical Physics, al-Farabi Kazakh
National University

 Bergaliyeva S.A.

APPROVED

by general manager of JSC “Ust-
Kamenogorsk Machine-Building Plant
of Industrial Fittings”



 Ashimov E.Zh.

Script holder JSC “Ust-Kamenogorsk Machine-Building Plant of Industrial
Fittings”

Almaty
2023

Preface

1 DEVELOPED by S.A. Bergalieva, doctoral student at the Department of Thermal Physics and Technical Physics, Faculty of Physics and Engineering, al-Farabi Kazakh National University.

2 APPROVED AND PUT INTO EFFECT JSC “Ust-Kamenogorsk Machine-Building Plant of Industrial Fittings”

3	TIMING OF THE FIRST REVIEW	2026
	PERIODICITY OF THE REVIEW	3 years

4 FIRST TIME INTRODUCED

POLYLACTIDE FOR ADDITIVE MANUFACTURING. Accelerated hydrothermal ageing test

Warning—Users of this standard of organization should be familiar with standard laboratory practices. This standard does not cover all safety issues associated with its use. The user of this standard is responsible for establishing appropriate safety and health regulations and determining the appropriateness of legal restrictions before using it.

1 Scope

This standard of organization applies to polylactide samples manufactured by additive manufacturing based on extrusion of materials, and establishes a method for testing them for accelerated ageing.

All requirements of this organization standard are mandatory.

This standard of organization is subject to copyright and may only be distributed with the permission of the organization that holds the original.

2 Normative references

The following reference normative documents are required for the application of this standard:

Technical regulation of the Customs Union "On safety of chemical products," approved by the Decision of the Council of the Eurasian Economic Commission of March 03, 2017 № 19

Technical Regulation of the Customs Union "On safety of packaging", approved by the Decision of the Commission of the Customs Union No. 769 of August 16, 2011.

Technical regulation "Requirements for product labeling", approved by Order No. 724 of the Minister of Investment and Development of the Republic of Kazakhstan on October 15, 2016.

Technical Regulation. "Conformity confirmation procedures," approved by the Decree of the Government of the Republic of Kazakhstan No. 90 dated 04.02.2008.

ST RK 1174-2003 Main types, placement and maintenance. Fire equipment for protection of objects.

ST RK GOST 12.4.026-2002 Signal colors, safety signs and signal labeling. General technical conditions and procedures for use.

GOST 8.579-2002 State system for ensuring uniformity of measurements. Requirements for the quantity of prepackaged goods in packages of any kind in their production, packaging, sale and import.

GOST 12.1.004-91 Occupational safety standards system. Fire safety. General requirements.

GOST 12.1.005-88 System of standards of labour safety. General sanitary and hygienic requirements for working area air.

GOST 12.1.044-2018 System of standards of labor safety. Fire and explosion hazards of substances and materials. Nomenclature of indicators and methods of their determination.

GOST 12.3.002-2014 System of labor safety standards. Processes manufacturing processes. General safety requirements.

GOST 12.4.021-75 Occupational safety standards system. Ventilation systems. General requirements.

GOST 12.4.028-76 Occupational safety standards system. Respirators SB-1 "Lepestok". Technical specifications.

GOST 12.4.103-83 Occupational safety standards system. Special protective clothing, individual protection means for feet and hands. Classification.

GOST 15.309-98 System for development and launching into manufacture. Testing and acceptance of output products. General provisions.

GOST 17.2.3.02-2014 Rules for establishing permissible emissions of pollutants by industrial enterprises.

GOST 14192-96 Labeling of goods.

GOST 24297-2013. Verification of purchased products. Organization and methods of control.

GOST R 54259-2010. Resources saving. Waste management. Standard guide for waste reduction, resource recovery and use of recycled polymeric materials and products.

ISO 11357-1:2016. Plastics. Differential scanning calorimetry (DSC). Part 1. General principles

ISO 11358-1:2016 Plastics. Thermogravimetry of polymers. Part 1. General principles.

ISO/TS 11937:2012 Nanotechnology. Nanoscale titanium dioxide in powder form. Characteristics and measurement.

ISO 291-2008 Plastics. Standard atmospheres for conditioning and testing.

ISO 527-1:20 Plastics. Determination of tensile properties. Part 1. General principles.

ISO 527-2:2019 Plastics. Determination of tensile mechanical properties. Part 2. Test conditions for molded and extruded plastics

ISO/ASTM 52900:2015 Additive manufacturing. General principles. Terminology.

Note: When using this standard, it is advisable for an organization to check the validity of reference standards and classifiers according to the information index "Normative documents on standardization" published annually for the current year and the corresponding monthly information indexes published in the current year. If the reference document is replaced (changed), the organization shall be guided by the replaced (changed) document when using this standard. If the reference document is repealed without a replacement, the provision in which the reference is made to it shall apply in part, not affecting this reference.

3. Essence of the method

Samples are subjected to controlled ageing in air at elevated temperatures and humidity in order to obtain the effect of natural ageing in a shortened time. The thermal properties of polylactide, tensile strength, stress at a given elongation, and elongation at break are then measured in accordance with ISO 527 and compared with the results of the same indicators for samples not subjected to ageing.

Samples are exposed to higher temperatures than when using polylactide products in order to obtain the effect of natural ageing in a shortened time.

4. Equipment

Climate chamber providing temperature (50.0 ± 2.0) °C and relative humidity (70.0 ± 5.0) %.

Means for measuring the dimensions of test samples with an error of ± 1.0 mm.

5. Test samples

Tests are carried out on at least five samples. For testing, samples according to ISO 527-1 are used. The samples are produced using the additive manufacturing method based on the extrusion of materials.

Conditioning of samples is carried out in accordance with ISO 23529.

Test specimens are measured before heating.

Marking for identification of samples should be applied to the non-critical part of the sample; it should not damage the polymer and be stable when heated.

6. Ageing conditions (duration and temperature)

Ageing duration intervals are selected according to ISO 23529, maximum ageing duration is 1344 hours.

Test temperature 50 ± 2 °C.

Test humidity 70 ± 5 %.

Ageing is carried out at atmospheric pressure.

7. Conducting the test

Operating temperature and humidity conditions are created in a climate chamber and samples are placed in it. The distance between suspended samples must be at least 10 mm, between samples and walls - at least 50 mm.

8. Presentation of results

The results of differential scanning calorimetry are formatted according to ISO 11357-1.

Thermogravimetry results are presented in accordance with ISO 11358-1.

The results of determining tensile mechanical properties are presented in accordance with ISO 527-1.

The test results of the samples before and after ageing are recorded.

9. Test report

The test report must contain:

- a) information about the sample:
 - 1) a complete description of the sample and its origin;
 - 2) sample preparation method.
- b) test method:
 - 1) designation of this standard;
 - 2) the indicators being determined and the type of sample used.
- c) test details:
 - 1) type of equipment used;
 - 2) the number of samples tested;
 - 3) duration and temperature of ageing;
 - 4) information about any procedures not specified in this standard.
- d) test results:
 - 1) separate values before and after ageing, expressed in accordance with the standards specified in clause 8 of this standard.
- e) date of testing.

APPENDIX D

Standard of organization St JSC 001-2023 “Nanocomposites based on virgin polylactide and its waste with titanium dioxide nanoparticles for additive manufacturing. Technical specifications”

STANDART OF ORGANIZATION
JSC “Ust-Kamenogorsk Machine-Building Plant of Industrial Fittings”

UNIVERSAL DECIMAL CODE 54.384.2
PRODUCT CODE BY EXTERNAL ECONOMIC ACTIVITY 20.16.40

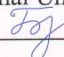
**NANOCOMPOSITES BASED ON VIRGIN POLYLACTIDE
AND ITS WASTE WITH
TITANIUM DIOXIDE NANOPARTICLES
FOR ADDITIVE MANUFACTURING.
Technical specifications**

**St JSC 001-2023
(the first edition)**

Date of introduction: since 18.10.2023
Validity: until 17.10.2026


DEVELOPED

by Bergaliyeva S.A., doctoral student of
the Department of Thermal Physics and
Technical Physics al-Farabi Kazakh
National University

 Bergaliyeva S.A.

APPROVED

by general manager of JSC “Ust-
Kamenogorsk Machine-Building Plant
of Industrial Fittings”

 Ashimov E.Zh.



Script holder JSC “Ust-Kamenogorsk Machine-Building Plant of Industrial
Fittings”

Almaty
2023

Preface

1 DEVELOPED by S.A. Bergalieva, doctoral student at the Department of Thermal Physics and Technical Physics, Faculty of Physics and Engineering, al-Farabi Kazakh National University.

2 APPROVED AND PUT INTO EFFECT

JSC “Ust-Kamenogorsk Machine-Building Plant of Industrial Fittings”

3	TIMING OF THE FIRST REVIEW	2026
	PERIODICITY OF THE REVIEW	3 years

4 FIRST TIME INTRODUCED

NANOCOMPOSITES BASED ON VIRGIN POLYLACTIDE AND ITS WASTE WITH TITANIUM DIOXIDE NANOPARTICLES FOR ADDITIVE MANUFACTURING. Technical specifications

1 Scope

This organization standard applies to nanocomposites based on virgin polylactide and its waste with titanium dioxide nanoparticles (hereinafter - the product), intended for manufacturing filaments or pellets for additive manufacturing.

All requirements of this standard of organization are mandatory.

This standard of organization can be used for conformity confirmation purposes.

This standard of organization is subjected to copyright and may be distributed only with the permission of the entity holding the original.

2 Normative references

The following reference normative documents are required for the application of this standard:

Technical regulation of the Customs Union "On safety of chemical products," approved by the Decision of the Council of the Eurasian Economic Commission of March 03, 2017 № 19

Technical Regulation of the Customs Union "On safety of packaging", approved by the Decision of the Commission of the Customs Union No. 769 of August 16, 2011.

Technical regulation "Requirements for product labeling", approved by Order No. 724 of the Minister of Investment and Development of the Republic of Kazakhstan on October 15, 2016.

Technical Regulation. "Conformity confirmation procedures," approved by the Decree of the Government of the Republic of Kazakhstan No. 90 dated 04.02.2008.

ST RK 1174-2003 Main types, placement and maintenance. Fire equipment for protection of objects.

ST RK GOST 12.4.026-2002 Signal colors, safety signs and signal labeling. General technical conditions and procedures for use.

GOST 8.579-2002 State system for ensuring uniformity of measurements. Requirements for the quantity of prepackaged goods in packages of any kind in their production, packaging, sale and import.

GOST 12.1.004-91 Occupational safety standards system. Fire safety. General requirements.

GOST 12.1.005-88 System of standards of labour safety. General sanitary and hygienic requirements for working area air.

GOST 12.1.044-2018 System of standards of labor safety. Fire and explosion hazards of substances and materials. Nomenclature of indicators and methods of their determination.

GOST 12.3.002-2014 System of labor safety standards. Processes manufacturing processes. General safety requirements.

GOST 12.4.021-75 Occupational safety standards system. Ventilation systems. General requirements.

GOST 12.4.028-76 Occupational safety standards system. Respirators SB-1 "Lepestok". Technical specifications.

GOST 12.4.103-83 Occupational safety standards system. Special protective clothing, individual protection means for feet and hands. Classification.

GOST 15.309-98 System for development and launching into manufacture. Testing and acceptance of output products. General provisions.

GOST 17.2.3.02-2014 Rules for establishing permissible emissions of pollutants by industrial enterprises.

GOST 14192-96 Labeling of goods.

GOST 24297-2013. Verification of purchased products. Organization and methods of control.

GOST R 54259-2010. Resources saving. Waste management. Standard guide for waste reduction, resource recovery and use of recycled polymeric materials and products.

ISO 11357-1:2016. Plastics. Differential scanning calorimetry (DSC). Part 1. General principles

ISO 11358-1:2016 Plastics. Thermogravimetry of polymers. Part 1. General principles.

ISO/TS 11937:2012 Nanotechnology. Nanoscale titanium dioxide in powder form. Characteristics and measurement.

ISO 291-2008 Plastics. Standard atmospheres for conditioning and testing.

ISO 527-1:20 Plastics. Determination of tensile properties. Part 1. General principles.

ISO 527-2:2019 Plastics. Determination of tensile mechanical properties. Part 2. Test conditions for molded and extruded plastics

ISO/ASTM 52900:2015 Additive manufacturing. General principles. Terminology.

Note: When using this standard, it is advisable for an organization to check the validity of reference standards and classifiers according to the information index "Normative documents on standardization" published annually for the current year and the corresponding monthly information indexes published in the current year. If the reference document is replaced (changed), the organization shall be guided by the replaced (changed) document when using this standard. If the reference document is repealed without a replacement, the provision in which the reference is made to it shall apply in part, not affecting this reference.

3 Terms and definitions

3.1 This standard uses the terms according to ISO/ASTM 52900:2015, GOST 54259-2010, as well as the following terms with corresponding definitions:

Poly lactide (polylactic acid, PLA) is a biodegradable, biocompatible, thermoplastic, aliphatic polyester with lactic acid monomer. The raw material used is a renewable resource, such as corn and sugarcane.

3.2 Designations and abbreviations

V

Virgin polylactide

R

3D-printed waste from polylactide

A

Titanium dioxide nanoparticles

The numbers to the right of the letters indicate the percentage of each component in the product.

4 Classification

4.1 The product is available in two forms:

- pellets with a size of (2.00 ± 0.05) mm.
- yarns with a diameter of (1.75 ± 0.05) mm.

4.2 The product, depending on the percentage of reagents (titanium dioxide nanoparticles) is classified into the following types:

Type one (I) 25 percent virgin substance, 75 percent waste substance (hereinafter referred to as V75R25A0);

Type Two (II) 22 percent virgin substance, 75 percent waste substance, 3 percent titanium dioxide nanoparticles (TiO_2) (hereinafter referred to as V22R75A3);

Type Three (III) 18 percent virgin substance, 75 percent waste substance, 7 percent titanium dioxide nanoparticles (TiO_2) (hereinafter referred to as -V18R75A7).

5. Technical requirements

5.1 The product must comply with the requirements of this standard of organization, taking into account the requirements of the Technical Regulations "On safety of chemical products," and manufactured according to the technological documentation, approved by the manufacturer in the prescribed manner.

5.2 Characteristics

5.2.1 By organoleptic characteristics, the ready-to-use product shall comply with the norms specified in Table 1.

Table 1

Indicator name	Standard value		
	Type I	Type II	Type III
1 Color	Color from colorless, transparent to light gray depending on the raw material, sheen in the product is allowed		
2 Product appearance	Filament and pellets		
3 Product dimensions	Diameter of the filament 1,75±0,05 Diameter of pellets 2MM ±0,05		

5.2.2 By thermo-mechanical properties, the product must meet the requirements and standards specified in Table 2.

Table 2

Indicator name	Standard value			Test method
	Type I	Type II	Type III	
Decomposition temperature at 5% weight loss, °C, no less	315.117	319.000	322.000	ISO 11358-1:2014
Glass transition temperature, °C, no less	62.57	60.86	60.25	ISO 11357-1:2016
Crystallization temperature, °C, no less	94.69	93.96	93.09	ISO 11357-1:2016
Melting temperature, °C, not more	177.29	176.54	177.67	ISO 11357-1:2016
For horizontally printed samples				
Tensile strength, MPa, not less	52,610±2,280	52.470±1.916	53.622±1.651	ISO 527-1
Modulus of elasticity, MPa, not less	2152,398±38,070	2227,127±302,270	2206.559±217,956	ISO 527-1
Elongation, %, no less	2,343±0,051	2,271±0,124	2,329±0,089	ISO 527-1
For vertically printed samples				
Tensile strength, MPa, not less	34.420±1.897	24.448±1.366	32.075±1.445	ISO 527-1
Modulus of elasticity, MPa, not less	2102,018±351,666	1971,235±122,129	1810,605±323,411	ISO 527-1
Elongation, %, no less	1,639±0,097	1,219±0,032	1,675±0,109	ISO527-1

5.3 Resistance to external influences, depending on the type of product, are shown in Table 3.

Table 3

Indicator name	Standard value		
	Type I	Type II	Type III
Temperature, °C	50	45	45
Chemical resistance	No contact with alkalis and acids		
Biological resistance	No contact with natural micro-organisms		

5.4 The provisions of the standard do not apply to polylactide waste that is exposed to direct sunlight, comes into direct contact with food products, and other aggressive chemical environments, before the recycling process, which had a service life of more than 1.5-2.5 years.

5.5 Requirements for virgin materials and supplies

5.5.1 Virgin materials and supplies shall comply with the requirements of technical regulations and current normative documents for them or, if necessary, be accompanied by certificates of conformity or declarations of conformity confirmation or by laboratory tests and authorized for use by the Sanitary and Epidemiological Control Committee of the Ministry of Health of the Republic of Kazakhstan and, in accordance with GOST 24297, be subject to verification of purchased products.

The manufacturer shall perform verification.

5.6 The following raw materials and supplies are used to manufacture the product:

Virgin polylactide - polylactide in accordance with the supplier's specifications*.

3D printed waste from polylactide - polylactide in accordance with the supplier's specifications*.

Titanium dioxide nanoparticles (TiO₂) по ISO/TS 11937:2012.

5.7 Packaging

5.7.1 Packaging for the products shall comply with the requirements of the Technical Regulations of the Customs Union "On safety of packaging.

5.7.2 Allowed negative deviations of the net weight of one packing unit from the nominal weight of the products shall comply with the requirements of GOST 8.579.

5.8 Labeling

5.8.1 Labeling shall comply with the requirements of the Technical Regulations "Requirements for Product Labeling".

5.8.2 A label with the following data shall accompany each set of the product:

- the name of the product;
- the name of the country of manufacture;
- name and location of the manufacturer (legal address including country and, if different from the legal address, enterprise address)
- the enterprise trademark (if any);
- bar code (if any);
- date of manufacture (month, year);

- expiration date;
- storage conditions;
- method of use (method of use may be indicated separately in the instructions for use);
- danger labels according to GOST 19433.3;
- information on conformity confirmation;
- designation of this standard of the organization.

5.8.3 Labeling shall be made by any method that provides clarity and safety of the inscription.

5.8.4 Transport marking shall be made in accordance with GOST 14192 with application of handling marks.

5.8.5 Labeling shall be made in the state and Russian languages.

5.8.6 Labeling may be fully or partially duplicated in foreign languages. When sending the product outside the Republic of Kazakhstan the marking may be made in the language of the country - importer.

6 Safety requirements

6.1 The product, ready for use, is fire and explosion-proof.

6.2 The product shall not emit harmful chemicals in contact with water. There are no flash, ignition and auto-ignition temperatures, temperature and concentration limits of flame propagation. The product, ready for use, is not capable of exploding and burning when interacting with water, air oxygen and other substances.

6.3 The product shall comply with the general safety requirements of GOST 12.3.005 during manufacturing, use and testing.

6.4 Maximum allowable concentrations (MAC) of harmful substances in the air of working area during manufacturing of the product shall comply with the requirements of GOST 12.1.005.

6.5 General requirements for occupational hazards during product manufacturing shall comply with the requirements of GOST 12.3.002.

6.6 Production areas where the product is manufactured shall be provided with effective exhaust and supply ventilation in accordance with GOST 12.4.021.

6.7 All sample preparation and testing operations shall be carried out in a fume hood.

6.8 Rubber boots, rubber gloves, protective clothing group K80 according to GOST 12.4.103, safety glasses according to the current regulatory documents, breathing apparatus "Lepestok" according to GOST 12.4.028 or other regulatory documents shall be worn when handling the product. Special clothing must be stored in special closed rooms.

6.9 Working conditions at working places shall meet the requirements of sanitary norms and rules, standards, rules and regulations on labor protection, operating on the territory of the Republic of Kazakhstan.

6.10. Methods of fire prevention systems and fire protection, as well as organizational and technical measures to prevent fire in product manufacturing shall be according to ST RK 1174, GOST 12.1.004.

Foam fire extinguishers OP-5 or carbon dioxide fire extinguishers OU-2, OU-5 according to the current regulatory documents shall be used as fire extinguishing means.

6.11. Hazardous areas in the enterprise, production facilities, workplaces (sites) must be marked with appropriate safety signs according to ST RK GOST 12.4.026.

6.12. Environmental protection

The environmental protection measures shall be performed in accordance with the applicable laws, standards, rules and regulations of the Republic of Kazakhstan.

Emissions and effluents of the enterprise producing the product shall not pollute the environment.

Permissible emissions of harmful substances at the enterprise should be established in accordance with the requirements of GOST 17.2.3.02.

7 Acceptance rules

7.1 The product shall be accepted in batches. Any quantity of the product, prepared during one shift or under one order, accompanied, according to GOST 15.309, by one bearer document, executed in accordance with the procedure accepted by the enterprise, is accepted as a batch.

7.2 Sampling of the product shall be carried out by random sampling from different places of the batch.

7.2.1 A sample of pure polylactide, waste 3D printing polylactide shall be not less than 0.05 kg. Nanoparticles of titanium dioxide (TiO₂) shall be not less than 0,005 kg.

7.3 To verify the quality of the product, acceptance, periodic and compliance testing shall be performed.

7.4 Product acceptance tests are performed by visual inspection according to 5.2.1.

7.5 Periodic product testing is carried out for all items of technical specifications at least once every 12 months. Fire and explosion safety data are checked when the product is put into production and at the request of the consumer.

7.6 Upon receipt of negative results at least for one indicator the repeated tests are carried out on doubled quantity of the product, selected from the same batch. The results of repeated tests are final and apply to the entire batch.

Tests for the purposes of confirmation of conformity of products shall be carried out in accordance with the regulatory documents of the State system of technical regulation of the Republic of Kazakhstan, including the Technical Regulations "Procedures for confirmation of conformity".

7.7 Raw materials used in manufacture of the product shall be checked during incoming inspection according to passports of suppliers and in accordance with GOST 10678, GOST 12601 and GOST 1307.

8 Control methods

8.1 Point samples are taken with a sampler, put together, thoroughly mixed, and an average sample of at least 0.1 kg is taken and placed in a clean, dry, tightly closed jar. The jar is labeled with the name of the manufacturer, the name and type of the product, batch number and date of sampling.

8.2 The color and appearance of the raw material of the product shall be determined visually.

8.3 The decomposition temperature at 5 % loss shall be determined according to ISO 11358-1:2014.

8.4 The glass transition temperature is determined according to ISO 11357-1:2016.

8.5 The crystallization temperature is determined according to ISO 11357-1:2016.

8.6 The melting point shall be determined according to ISO 11357-1:2016.

8.7 Tensile strength tests shall be carried out according to ISO 527-1. Uncertainty calculation in accordance with Appendix A to this standard.

8.8 The modulus of elasticity of specimens shall be determined according to ISO 527-1

8.9 Tensile elongation of specimens is determined according to ISO 527-1

8.10 The fire safety of the product is checked in accordance with GOST 12.1.044.

8.11 The harmful chemical substances shall be checked in accordance with the methods of the Committee for Sanitary and Epidemiological Control of the Ministry of Health of the Republic of Kazakhstan that have been approved in accordance with the established procedure.

8.12 Appearance, labeling shall be controlled by external inspection.

9 Transportation and storage

9.1 The product can be transported by any type of transport in accordance with the rules in force for this type of transport.

9.2 It is not allowed to transport the product together with flammable substances, acids and alkalis.

9.3 The product must be stored in closed rooms at a temperature of not less than 4 degrees Celsius.

9.4 The product must not be directly exposed to atmospheric precipitation.

10 Manufacturer's warranties

10.1 The manufacturer guarantees product conformity with the requirements of these specifications, provided that the consumer complies with the conditions of transportation and storage.

The warranty shelf life of the product is 12 months from the date of manufacture, provided it is stored in a cool dry place at a temperature of not less than 4 degrees Celsius.

Estimation of uncertainty of specimens in the tensile strength

A.1 Measurement task

The method is based on stretching the test sample at a certain strain rate until the sample breaks.

Double-blade specimens of type 1BA according to ISO 527-2 are used for testing.

Five samples are used for testing.

The thickness of each sample is measured in three places. From the obtained values, the arithmetic mean is calculated, from which the value of the initial cross section is calculated for each sample A_{0i} .

During testing, the load F_{ri} at which the samples rupture occurs is measured.

Tests are carried out at a temperature of (23 ± 2) °C and relative humidity (50 ± 5) %.

The following instruments are used during testing:

- 1) Tensile testing machine (load measurement error $\pm 1\%$);
- 2) Lever bracket SRP – 25 (graduation value 0.001 mm, error $\pm 0.7 \mu\text{m}$).

A.2 Mathematical measurement model

The tensile strength σ_r (MPa) measured during testing is determined by the following formula:

$$\sigma_r = \frac{F_r}{A_0} = \frac{\sum_{i=1}^{t=5} \sigma_i}{t} = \frac{\sum_{i=1}^{t=5} \frac{F_{ri}}{A_{0i}}}{t} = \frac{\sum_{i=1}^{t=5} \frac{F_{ri}}{b * d_i}}{t} \quad (\text{A.1})$$

where σ_i – tensile strength, MPa;

$\sigma_i = \frac{F_{ri}}{A_{0i}}$ – tensile strength for the i -th sample, MPa;

F_{ri} – tensile load at the moment of rupture for the i -th sample, N;

A_{0i} – initial cross section for the i -th sample, mm^2 ;

t – number of tested samples ($i=1, 2, \dots, t=5$);

$d_i = \frac{\sum_{k=1}^{n=3} d_{ki}}{n}$ – sample thickness, arithmetic mean of three measurements of the sample before testing, mm;

d_{ki} – the thickness in the k -th section of the i -th sample, mm;

n – number of thickness measurements for each sample ($k=1, 2, \dots, n=3$)

b – sample width, mm;

A.3 Analysis and quantification of input quantities and their uncertainties

A.3.1 Tensile load at the moment of rupture F_r

The uncertainty of the tensile load arises from the error in its measurement. In accordance with clause 5.1.4 of ISO 527-1, the force meter must indicate the load with an accuracy of at least 1 % of the actual value. Assuming a rectangular

distribution for the load error value in this interval ($\pm 1\%$), we will find a quantitative:

$$u(F_r)/F_r = 0,01/\sqrt{3} = 0,0058 \quad (\text{A.2})$$

A.3.2 Specimen thickness d

Contribution due to differences in sample thicknesses within samples $u(d_s)$, which is determined by the formula:

$$u(d_s) = \sqrt{\frac{1}{t(n-1)} \sum_{i=1}^5 \sum_{k=1}^3 (y_{ki} - \bar{y}_i)^2} \quad (\text{A.3})$$

A.3.3 Specimen width b

Contribution due to differences in sample width within samples $u(b_s)$, which is determined by the formula:

$$u(b_s) = \sqrt{\frac{1}{t(n-1)} \sum_{i=1}^5 \sum_{k=1}^3 (x_{ki} - \bar{x}_i)^2} \quad (\text{A.4})$$

A.3.4 Variability of the measured quantity from sample to sample

The relative uncertainty of tensile strength due to the variability of the measured value itself from sample to sample is determined by the formula:

$$\frac{u(\sigma_s)}{\sigma_r} = \sqrt{\frac{\sum_{i=1}^t (\sigma_i - \bar{\sigma})^2}{t(t-1)}} \quad (\text{A.5})$$

$$\text{Где } \sigma_i = \frac{F_i n}{\sum_{k=1}^n b \sum_{k=1}^n d_k} \quad (\text{A.6})$$

$$\bar{\sigma} = \frac{\sum_{i=1}^t \sigma_i}{t} \quad (\text{A.7})$$

A.4 Observation results

As a result of the test, the following results were obtained:

For each of the 5 samples ($t=5$), three thickness measurement results were obtained in different sections ($n=3$) and one measurement result of the applied tensile load at the moment of rupture. The results are presented in Table 1.

Table 1 – Measurement results during tensile testing

Sample No.	Thickness measurement results d_{ki} , mm	Average thickness d_i , mm	Results of tensile load measurements at the moment of rupture F_{ti} , N	Tensile strength σ_i , MPa
1	2.047	5.007	532.613	51.859
2	2.133	4.780	530.534	52.108
3	2.200	4.763	583.116	55.683
4	2.040	4.900	537.254	53.747
5	2.133	4.730	528.094	54.731

A.5 Calculation of the value of the measured quantity and its total standard uncertainty

The value of the measured quantity is found using formula (1): $\sigma_r=53.626$ MPa

The total relative standard uncertainty of tensile strength is determined by summing the relative standard uncertainties associated with all factors presented above using the formula:

$$\frac{u(\sigma_r)}{\sigma_r} = \sqrt{\left(\frac{u(F_r)}{F_r}\right)^2 + \left(\frac{u(d)}{d}\right)^2 + \left(\frac{u(b)}{b}\right)^2 + \left(\frac{u(\sigma_s)}{\sigma_r}\right)^2} \quad (\text{A.8})$$

The value of the standard uncertainty in units of the measured quantity is found using the formula:

$$u(\sigma_r) = \sigma_r \sqrt{\left(\frac{u(F_r)}{F_r}\right)^2 + \left(\frac{u(d)}{d}\right)^2 + \left(\frac{u(b)}{b}\right)^2 + \left(\frac{u(\sigma_s)}{\sigma_r}\right)^2} \quad (\text{A.9})$$

For the obtained measurement results:

$$\frac{u(\sigma_r)}{\sigma_r} = \sqrt{(0,0058)^2 + (0,1026)^2 + (0,0026)^2 + (0,0308)^2} = 0,1073 = 10,73 \%$$

$$u(\sigma_r) = 53.626 * 0,107 = 5.737 \approx 0,6 \text{ MPa}$$

A.6 Expanded uncertainty

The expanded uncertainty $U(\sigma_r)$ is obtained by multiplying the standard uncertainty of the measured tensile strength, coverage factor k equal to 2, for a 95 % confidence level:

$$U(\sigma_r) = k * u(\sigma_r) = 2 * u(\sigma_r) \quad (\text{A.10})$$

A.7 Complete measurement result

The complete measurement result, consisting of an estimate of the measured value of tensile strength σ_r and expanded uncertainty $U(\sigma_r)$, is presented in the following form:

“The tensile strength of the samples is (53.627 ± 1.200) MPa.

The specified expanded uncertainty is the product of the standard uncertainty and the coverage factor $k=2$, and under a normal distribution corresponds to a coverage probability of approximately 95%.”

APPENDIX E

Certificate of Implementation

APPROVED
by general manager of
JSC "Ust-Kamenogorsk
Machine-Building Plant
of Industrial Fittings"
Ashimov E.Zh.



» 10 2023

CERTIFICATE OF IMPLEMENTATION

of the thesis results of Bergaliyeva Saltanat on the topic "Standardization of Recycled Plastic Materials for Additive Manufacturing"


A commission consisting of: the chairman, the general manager of JSC "Ust-Kamenogorsk Machine-Building Plant of Industrial Fittings" Ashimov E.Zh.; members of the commission: the head of the department of quality control – Saibel O.V.; the head of the testing center – Sokolov E.Z., drew up this certificate stating that the thesis results of Bergaliyeva S.A. were implemented at JSC "Ust-Kamenogorsk Machine-Building Plant of Industrial Fittings".

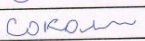
The commission found that the standards St JSC 001-2023 "Nanocomposites based on polylactide and its waste with titanium dioxide nanoparticles for additive manufacturing. Technical specifications" and St JSC 002-2023 "Polylactide for additive manufacturing. Accelerated hydrothermal ageing test" meet needs of JSC "Ust-Kamenogorsk Machine-Building Plant of Industrial Fittings" for future certification of products.

The commission decided:

The main statements of the thesis research by Bergaliyeva S.A. on the topic "Standardization of Recycled Plastic Materials for Additive Manufacturing" were implemented at JSC "Ust-Kamenogorsk Machine-Building Plant of Industrial Fittings".

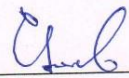
Members of the commission:





Saibel O.V.
Sokolov E.Z.

The chairman, the general manager of
JSC "Ust-Kamenogorsk Machine-
Building Plant of Industrial Fittings"



Ashimov E.Zh